UNIVERSITY OF KWAZULU-NATAL

GAS-PHASE ETHYLENE POLYMERIZATION STUDIES USING A MAGNESIUM CHLORIDE-SUPPORTED ZIEGLER-NATTA CATALYST

2006

OMASHA NAICKER

Gas-Phase Ethylene Polymerization Studies Using a Magnesium Chloride-Supported Ziegler-Natta Catalyst

Omasha Naicker
BScEng (Chemical)

A thesis submitted in fulfilment of the requirements for the degree MScEng in the School of Chemical Engineering at the University of KwaZulu-Natal

2006

Abstract

The gas phase polyethylene production process is the most recently developed and boasts many distinct advantages when compared with the commercial slurry and solution processes. However, in the public literature on ethylene polymerization with $MgCl_2$-supported Ziegler-Natta catalysts there is a general lack of kinetic data that can be used for reactor design and control of polymer properties. This is in spite of intensive research efforts and the successful application of these catalyst systems in industry. The reason is that olefin polymerization on a small scale is rather difficult to execute and the lack of fundamental kinetic models is therefore related to the difficulty in obtaining high-precision kinetic data. For kinetic studies, control of temperature and pressure is important and high precision in experiments demands close control of these parameters. In addressing the issues mentioned above, the solution lies in firstly designing and constructing competent reactor systems.

A 0.7 L stainless steel gas-phase semi-batch reactor system was therefore designed and constructed and was equipped with both temperature and pressure control systems. The reactor was also fitted with a specially designed catalyst injection system which was used to inject the solid catalyst and liquid co-catalyst into a porous catalyst basket. The catalyst remained in the basket where it catalyzed the formation of solid polymer from the gas phase monomer. The injection system safeguarded inert conditions and was essential since both the catalyst and co-catalyst were air and moisture sensitive. The catalyst basket was employed to provide gas and solid phase agitation while not mechanically destroying the catalyst and growing polymer, as would be the case if an impeller was used. Polymer melting and agglomeration was however observed and was attributed to inadequate agitation of the growing particles. With enough mixing energy the contents of the basket can be sufficiently mixed and it is therefore necessary that a higher power motor and magnetic drive replace the motor used in this work.

For the polymerization experiments, a spherical $MgCl_2$-supported Ziegler-Natta catalyst was synthesized. The re-crystallization method for active $MgCl_2$ preparation was preferred to the ball milling method and two of the three implementations of this method were tested. Both the quick cooling and the solvent evaporation techniques were unsuccessful and a variation of the latter was therefore proposed. In the original solvent evaporation method a magnetic stirrer was used and the ethanol was eliminated by evaporation under vacuum. In the method employed in this work, the reaction emulsion was more vigorously stirred with a mechanical stirrer and a vacuum was not required. Instead, the reaction emulsion was stirred under a high, continuous flow of nitrogen which together with the evaporated ethanol passed through an opening in the reaction flask. For polymerization reactions the final catalyst system was $MgCl_2/TiCl_4$/dibutyl phthalate, activated by the co-catalyst triethylaluminium. Scanning electron microscopy verified that the produced support and catalyst particles were both spherical. Further characterization of the catalyst by inductively coupled plasma analysis showed that the two catalysts prepared contained 3.69 wt% Ti and 6.48 wt% Ti, respectively.

The gas-phase ethylene polymerization experiments were aimed at determining the effect of the co-catalyst/catalyst (Al/Ti) molar ratio, the reaction pressure, and the reaction temperature on the product yield. To determine the effect of pressure, experiments were conducted at 1 and 2 barg, at 50°C, and with Al/Ti = 33 and 50. For Al/Ti = 33 an increase in the pressure from 1 to 2 barg led to an increase in the yield from 11.3 to 12 g PE/g cat. h. while for Al/Ti = 50, the same increase in the pressure led to an increase in the yield from 14.2 to 17 g PE/g cat. h. The effect of Al/Ti was determined at 10, 33, and 60 and the yields obtained were 0.8, 8.5, and 14.2 g PE/g cat. h., respectively. These runs were undertaken at 1 barg and 50°C. It was found that an increase in Al/Ti led to an increase in the yield while an optimum Al/Ti between 60 and 100 is generally observed in the literature. The effect of temperature was assessed at 50, 60 and 70°C and the yields obtained were 8.5, 24.4 and 8 g PE/g cat. h., respectively. A pressure of 1 barg and Al/Ti = 33 was used. The yield was found to increase as the temperature was increased from 50 to 60°C, but decreased when the temperature was further increased to 70°C. This optimum temperature is generally observed in the literature but is different for different types of catalyst systems.

The molar masses of the products of two experiments, carried out at 1 bar and 50°C, were determined by gel permeation chromatography. For Al/Ti = 26 and 60, the number average molecular weight (M_n) was found to be 227 000 and 330 400, respectively, and the weight average molecular weight (M_w) was found to be 1 260 600 and 1 516 400, respectively. The polymer produced with Al/Ti = 26 and 60 were found to have a polydispersity index of 5.6 and 4.6, respectively. These are within the expected range for supported catalysts. Scanning electron micrographs confirmed that the polymer particles had the same spherical morphology as the catalyst particles and one of the objectives of preparing the supported catalyst was realized.

The yields obtained in this work were found to be lower than those presented in the literature. The first explanation for this is the inadequate agitation of the growing polymer particles. The melting and agglomeration which resulted led to active site deactivation and therefore to the low yields observed. The second reason could be that the prepared catalyst had a much lower specific surface area than those used in the literature. This is possible even though much effort had been made in this work to increase the specific surface area of the catalyst, firstly by dealcoholation of the support and secondly by repeating the treatment of the catalyst with $TiCl_4$.

With the exception of the inadequate mixing, the rest of the reactor system was successfully used to carry out the necessary polymerization reactions. The temperature and pressure control systems worked accurately and the catalyst injection system made it possible to inject the catalyst without contamination. Also, although product yields were not optimised, the difficulties associated with synthesizing an air and moisture sensitive Ziegler-Natta catalyst have been overcome. The synthesized catalyst was capable of polymerizing ethylene and of replicating its morphology into the morphology of the polymer.

I, Omasha Naicker, declare that to the best of my knowledge, the work contained in this document is my own, unless stated to the contrary in the text. This thesis has not been submitted for degree purposes, in part or in whole, to any other university.

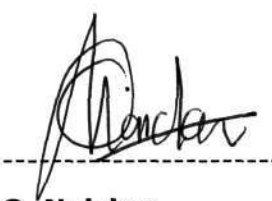

O. Naicker

As the candidate's supervisor, I, Prof. M. Starzak, have approved this thesis for submission.

Prof. M. Starzak

Acknowledgements

I wish to thank first of all my mum, Pat Naicker, my sister, Kashni Naicker, and my dad, Ronnie Naicker, for their love, support and guidance over the course of my studies. Without your strength and motivation the completion of this work would not have been possible.

I want to also thank my two supervisors Prof. M. Starzak and Dr. R. Rawatlal. To Dr. Rawatlal, thank you for allowing me the opportunity to undertake such a study. It was this opportunity that has allowed me to gain the knowledge and confidence that I now have. To Prof. Starzak, the immense time and effort that you have put into the final dissertation is greatly appreciated.

I wish to thank the staff of the mechanical workshop in Department of Chemical Engineering: Les, Ken, and Kelly, for using their experiences and talents to assist me in attaining my goals.

I want to thank Gregory Moodley from the Department of Chemistry. I truly appreciate the great interest that you have taken in my work and I hope to one day return the many favours.

Finally, I wish to thank the National Research Foundation (NRF) for their financial support.

Table of Contents

List of Figures

Chapter 1

Chapter 2

Chapter 3

Chapter 4

Chapter 5

List of Tables

Chapter 1

Chapter 2

Chapter 3

Chapter 4

Chapter 5

List of Abbreviations

Abbreviation	Description
ccp	cubic close packed
CSTR	continuous stirred tank reactor
DBP	dibutyl phthalate
DIBP	diisobutyl phthalate
DIOP	diisooctyl phthalate
EB	ethyl benzoate
ED	external electron donor
FBR	fluidized bed reactor
FTIR	Fourier transform infrared
GPC	gel permeation chromatography
hcp	hexagonal close packed
HDPE	high density polyethylene
ICP	inductively coupled plasma
ID	internal electron donor
IR	infrared
LDPE	low density polyethylene
LLDPE	linear low density polyethylene
MAO	methyl aluminoxane
MFI	melt flow index
M_n	number average molecular weight
M_w	weight average molecular weight
MWD	molecular weigh distribution
PDI	polydispersity index
PE	polyethylene
PP	polypropylene
PSD	particle size distribution
SEC	size exclusion chromatography
SEM	scanning electron microscopy
SSC	single-site catalysts
TEA	triethylaluminium
UHP	ultra high purity
XRD	X-ray diffraction

Chapter 1

Preliminaries

In this chapter a general introduction to the polymerization of ethylene with heterogeneous Ziegler-Natta catalysts is given. Since the discovery of these catalysts there have been significant improvements in the catalyst system and the historical development is briefly outlined here. An explanation of the mechanism of Ziegler-Natta catalysis and of the physical and mechanical properties of polyethylene, such as polymer density, chain length, and molecular weight, then follows. Polyethylene is produced commercially by a number of diverse processes but the gas phase process is of sole interest in this work and only the commercial gas phase processes are elaborated on. The advantages and disadvantages of these gas phase processes are also highlighted. An overview of a typical polymerization process then follows and the chapter is concluded by highlighting objectives of this study and by a brief overview of each of the chapters that follow.

1.1 Introduction

Although both the science and technology of polymers had advanced remarkably by the early 1950s formidable challenges remained to be surmounted. The abundant supply and low cost of hydrocarbons meant that hydrocarbon polymers represented a highly useful class of substances. Particularly attractive targets were polymers which could be made from the smallest and most abundant such hydrocarbons, ethylene and propylene, containing two and three carbon atoms respectively. The general ability of hydrocarbon molecules to join together to form long chains had long been recognized; however, in the case of ethylene and propylene this presented a significant challenge. The polymerization of ethylene had been accomplished but only at uneconomically high temperatures and pressures and yielding polymers whose properties left much to be desired. The polymerization of propylene remained to be achieved.

In 1953, while engaged in basic research on the reactions of compounds containing aluminium-carbon bonds German chemist Karl Ziegler, working at the Max Planck Institute for Coal Research in Mulheim, discovered that by adding salts of certain metals (e.g. Ti or Zr) these compounds resulted in highly active catalysts for the polymerization of ethylene under relatively mild conditions. Furthermore, the polymers formed in this way had chains that were longer and more linear, and these polymers therefore had superior properties such as strength, hardness and chemical inertness, making them useful in many applications.

Building on Ziegler's discovery, Italian chemist Giulio Natta, working at the Milan Polytechnic Institute, demonstrated that similar catalysts were effective for the polymerization of propylene. With such catalysts it became possible to achieve exquisite control of the chain length and structures of the resulting polypropylene polymers and therefore also of their properties. In 1963, the Nobel Prize in Chemistry was awarded to both Ziegler and Natta for their discoveries in the field of the Chemistry and Technology of Polymers.

Industrial applications of Ziegler-Natta catalysts were realized almost immediately and, with various subsequent refinements, continue to expand. The uses of polyethylene and polypropylene extend to virtually every facet of industry and daily life, including construction and building materials, containers, toys, sporting goods, electronic appliances, textiles, carpets and medical products. In many of these applications polymers replace other materials, such as glass and metals, but their distinctive properties have also given rise to entirely new applications. The billions of tons of polyolefins (essentially homopolymers and copolymers of ethylene and propylene) which are manufactured each year clearly indicate the commercial significance of Ziegler-Natta catalyzed polymerization processes. Also, the thousands of patents and articles describing numerous variations of the Ziegler-Natta catalyst system make polyolefin production technology a very active area of research.

1.2 Ziegler-Natta catalysts

A Ziegler-Natta catalyst is comprised of at least two parts: a transition metal component and a main group metal alkyl compound. The transition metal component is usually either titanium or vanadium and the metal alkyl compound is usually an aluminium alkyl. In common practice, the titanium component is called the "catalyst" and the aluminium alkyl is called the "co-catalyst" and it is the combination of the two that make up the active catalyst. The importance of these catalysts lies in their ability to produce stereoregular polymers from ethylene, and isotactic (methyl groups oriented uniformly) polymers from propylene. Improvements in the catalyst system since their discovery have been significant, and a brief summary of their evolution is outlined here.

1.2.1 The first generation - titanium trichloride catalysts

The first commercial catalysts resulted from the industrial extensions of Natta's work on the relationship between the crystal structure of titanium chlorides and the overall activity and selectivity of the catalysts. $TiCl_3$ was prepared from $TiCl_4$ by many different routes including reduction with hydrogen, irradiation and reduction with alkylaluminiums. Natta found that four structural modifications existed (named α, β, γ, and δ). The brown β-$TiCl_3$ had a chain like structure and had moderate activity and low stereoselectivity and was therefore not economically attractive. More stereospecific $TiCl_3$ (α, γ, δ) were formed upon thermal treatment of the β-phase and had a deep purple colour and a layer lattice structure. These catalysts, however, were economically infeasible and attempts were made to include a third component (electron donors such as triethylaluminium, TEA) to improve stereoselectivity. Another attempt to improve catalyst performance was ball-milling which resulted in an activity increase due to the reduction in size of the primary crystallites. The addition of a Lewis base to the catalyst was later attempted, essentially in order to improve the stereospecificity of the polymers, however, the higher stereospecificity did not correspond to an increase in activity.

1.2.2 The second generation – elimination of catalyst poisons

In the case of the second generation catalysts, it became apparent that the presence of co-precipitated $AlCl_3$ led to the formation of the catalyst poison $AlEtCl_2$, and that the large size of the catalyst ($TiCl_3$) crystallites resulted in a low proportion of active Ti sites. The removal of the co-precipitated $AlCl_3$, by washing with hydrocarbons at elevated temperatures, resulted in an approximate 30% increase in activity. It was also noted that by transforming the brown β-$TiCl_3$ into the stereoselective δ-$TiCl_3$ at low temperatures (<100 °C) in the presence of $TiCl_4$, which acted as a catalyst for the change of phase, resulted in smaller primary crystallites. The success of the second generation catalysts was due to the new morphology of the catalyst particles, which were highly porous active catalysts with high surface areas.

1.2.3 The third generation – supported catalysts

The prehistory of the third generation catalysts began in 1960, when Shell patented a catalyst for propylene polymerization that used $TiCl_4$ supported on $MgCl_2$. In 1968, Montecatini and Mitsui independently patented catalysts prepared from $TiCl_4$, $MgCl_2$ and an electron donor, and activated by a mixture of trialkylaluminium with another electron donor. These catalysts were formed by physically or chemically supporting catalyst molecules on the surface of a solid support. Since only the sites located at the surface of the support were available for polymerization, supports with high specific surface areas such as silica and magnesium dichloride ($MgCl_2$) were preferred. This generation of catalysts brought about a 50-fold increase in activity.

1.2.4 The fourth generation – homogenous catalysts

The fourth generation of catalysts, based on metallocene compounds, is now evolving towards industrial success. In 1986 Kaminsky and Sinn discovered that methyl aluminoxane (MAO)-activated homogeneous metallocene catalysts were capable of polymerizing propylene and higher olefins. Practical applications of metallocene catalysts require their pre-adsorption onto solid supports such as alumina or silica gels.

Although the metallocene-based single-site catalysts (SSC's) have recently been shown to have the ability to produce precisely tailored polymers, the high activity supported Ziegler-Natta catalysts are set to dominate polyolefin production for at least the next few decades.

1.3 Polymerization chemistry

Ethylene is the smallest α-olefin and because steric demand is minimal the aspect of stereoregularity does not play a role. Three types of polymerization mechanisms have been found to result in polymer:

- radical polymerization
- true anionic polymerization, and
- co-ordination polymerization

Ziegler-Natta type catalysts, such as the first generation $TiCl_3$ catalysts, supported catalysts such as the $MgCl_2$ supported catalysts and homogenous catalysts all polymerize by co-ordination polymerization. The repeating structural unit of polyethylene is demonstrated in Figure 1-1 and the resulting linear polymer is referred to as high-density polyethylene (HDPE).

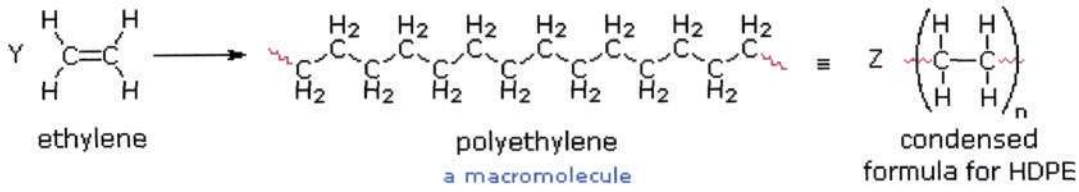

Figure 1-1 Polyethylene Polymerization

Ziegler-Natta catalysts are a combination of a transition metal catalyst like $TiCl_4$ and a co-catalyst which is usually based on group III metals like aluminium. Most often the catalyst/co-catalyst pair is $TiCl_4$ with Al $(C_2H_5)_3$. In the interior of a $TiCl_4$ crystal each titanium is surrounded by six chlorines, but on the surface a titanium atom is surrounded by only five chlorine atoms, making it reactive. The co-catalyst donates one of its ethyl groups to titanium, but removes one of the chlorines in the process. The Al remains co-ordinated to one of the carbon atoms of the ethyl group that it has just transferred to the titanium, and also to one of the adjacent chlorine atoms. *The now active titanium still has one empty orbital to be filled and this is where* polymerization occurs.

A polymer chain is initiated when a monomer molecule attacks an active titanium centre. There are two electrons in the π-system of a carbon-carbon double bond, and these electrons are used to fill the empty orbital of the titanium. The atoms then rearrange themselves to form a slightly different structure, once again leaving the titanium atom with one empty orbital (Figure 1-2). The polymer chain grows as monomer is inserted between the chain and the active site, thus increasing the chain length. The polymer bulk accumulated around the catalyst particle is an agglomeration of numerous polymer chains.

A chain will grow at a catalytic site until it reacts with a terminating agent which causes a scission from the site. When a polymer chain is terminated, it joins the bulk polymer material accumulated around the catalyst. This frees the catalytic site for chain initiation and subsequent propagation. The chief terminating agent is considered to be hydrogen and it is deliberately added to the reaction mixture for this purpose. However, chains may also be terminated by the co-catalyst and the monomer.

The reactions discussed above may be classified as series and parallel reactions. The growth of a polymer chain occurs sequentially; only one monomer unit can be inserted between the catalytic site and the polymer chain at a time. However, other reactions (catalytic site and chain termination reactions) can occur simultaneously.

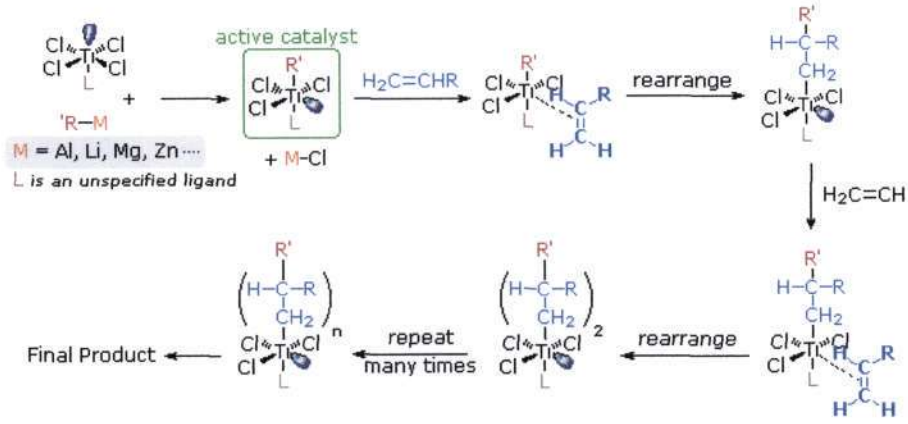

Figure 1-2 Mechanism of Ziegler-Natta Catalysis

1.4 Physical and mechanical properties of polyethylene

Although polyethylene (PE) is the simplest of the polyolefins it has been and remains to be the most extensively studied polymer. This is due to the fact that the term "polyethylene" can no longer be used to refer to a single polymer. Instead, it encompasses an array of ethylene-based materials that differ from each other in several respects, which include molecular weight and distribution, chain length and the presence/absence of branches.

Physical and mechanical properties of polyethylene depend on density, crystallinity, molecular weight and distribution, chemical composition, and other characteristics. These variables are controlled by polymerization conditions and are not mutually independent. The essential variable which affects all the physical properties is the chain microstructure of the polyethylene. Backbone linearity contributes to improve tensile strength and tear properties, while branching increases the toughness of the material. Commercial resins are mainly specified by density, molecular weight (melt index) and molecular weight distribution (melt flow ratio). The processing and end-use properties are mainly governed by these variables.

1.4.1 Polymer density

Polyethylene is normally classified as low density (LDPE) at 0.910-0.930 g/cm^3 and high density (HDPE) at 0.931-0.970 g/cm^3 (Figure 1-3). Low density polyethylene is further classified as low-density polyethylene (LDPE) and linear low density polyethylene (LLDPE) based on polymer chain microstructure and synthesis process. The density of polyethylene depends largely on the following factors: the number of branches, branch chain length, branch frequency distribution, chemical composition distribution and molecular weight and distribution. In general, the density of polyethylene decreases with an increase of branch numbers and the crystallinity of polyethylene decreases significantly with an increase in branch frequency and size. Therefore any physical properties related to crystallinity, such as stiffness and yield stress will be affected by branching. Also, density decreases with an increase in molecular weight, this is due to the inhibition of crystallization by longer molecular chains.

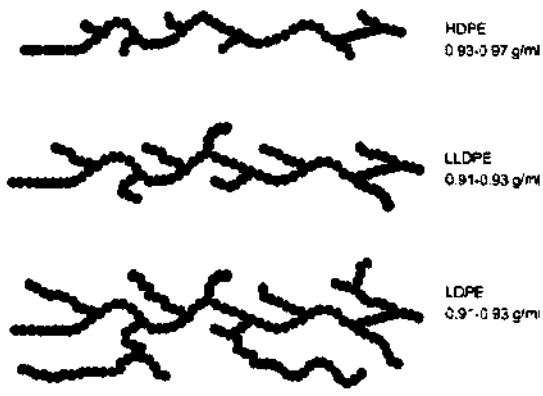

Figure 1-3 Schematic of Molecular Structures of Polyethylene

1.4.2 Chain length

Polymerization occurs by the sequential addition of monomer to the polymer chain. The termination reaction occurs in parallel, with hydrogen being the chief terminating agent. It is generally accepted (Long Chain Assumption) that the length of the polymer chain growing at a catalytic site does not affect the termination reaction, which proceeds at a rate determined solely by the temperature and the concentration of the terminating agent. Chains are continuously terminated and the probability of a chain growing to a certain length decreases with increasing chain length. Also, shorter chains have a smaller molecular weight and therefore constitute a smaller mass fraction than the longer chains. These factors together contribute to the overall shape of the chain length distribution, as is depicted in Figure 1-4. The chain length distribution is characterized by two measurable indices, known as the Melt Flow Index (MFI) and Polydispersity Index (PDI). These are related to the viscosity of the molten polymer and correspond to the average chain length and statistical spread respectively.

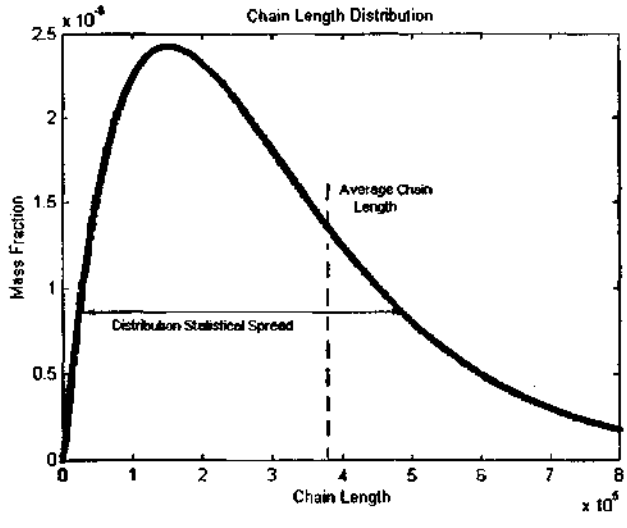

Figure 1-4 Typical Chain Length Distribution

1.4.3 Molecular weight and distribution

Unlike simple pure compounds, most polymers are not composed of identical molecules. The high density polyethylene (HDPE) molecules, for example, are all long carbon chains, but the lengths may vary by thousands of monomer units. Because of this, polymer molecular weights are usually given as averages. Two experimentally determined values are common: M_n ($M_n = \Sigma n_i M_i$), the number average molecular weight is calculated from the mole fraction distribution of different sized molecules in a sample, and M_w($M_w = \Sigma w_i M_i$), the weight average molecular weight is calculated from the weight fraction distribution of different sized molecules. Since larger molecules in a sample weigh more than smaller molecules, M_w is necessarily skewed to higher values, and is always greater than M_n.

1.4.4 Tacticity

Symmetrical monomers such as ethylene and tetrafluoroethylene can join together in only one way. Monosubstituted monomers, on the other hand, may join together in two organized ways, illustrated in Figure 1-5, or in a third random manner. Most monomers of this kind, including propylene, join in a head-to-tail fashion, with some randomness occurring from time to time.

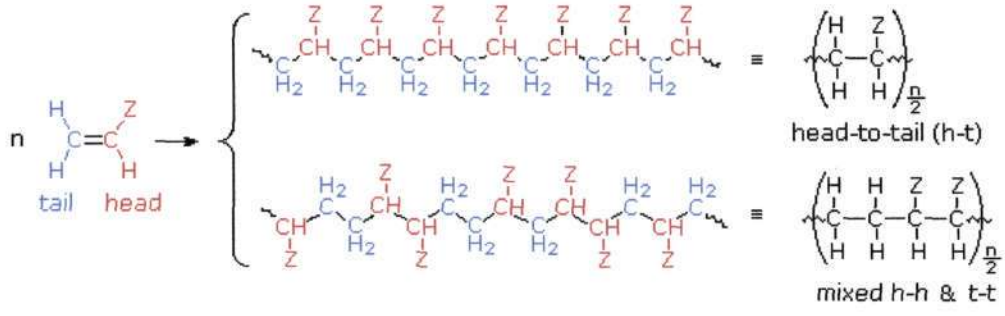

Figure 1-5 Regioisomeric Polymers from Substituted Monomers

If the polymer chain is drawn in a zig-zag fashion, as shown above, each of the substituent groups (Z) will necessarily be located above or below the plane defined by the carbon chain. Consequently three configurational isomers of such polymers can be identified. If all the substituents lie on one side of the chain the configuration is called isotactic. If the substituents alternate from one side to another in a regular manner the configuration is termed syndiotactic. Finally, a random arrangement of substituent groups is referred to as atactic. Examples of these configurations are shown in Figure 1-6.

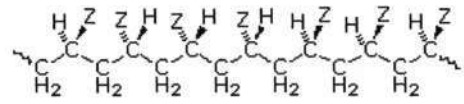

atactic

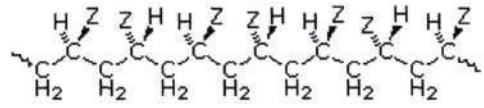

syndiotactic

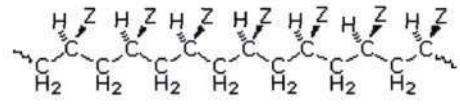

isotactic

Figure 1-6 Atactic, Syndiotactic and Isotactic Configurations

1.5 Polyethylene production processes

Commercial polyethylene production processes can be classified into the following five categories (Xie *et al.*, 1994):

Table 1-1 Polymerization Processes and Reactor Operating Conditions

	high press. process	**high press. bulk process**	**solution**	**slurry**	**gas phase**
reactor type	tubular or autoclave	autoclave	CSTR	loop or CSTR	fluidized or stirred bed
reactor press., atm	1200-3000	600-800	100	30-35	30-35
temp, °C	130-350	200-300	14-200	85-110	80-100
mechanism	free radical	coordination	coordination	coordination	coordination
polymerization location	monomer	monomer	solvent	solid	solid
density, g/cm^3	0.910-0.930	0.910-0.955	0.910-0.970	0.930-0.970	0.910-0.970
melt index, g/10min	0.10-100	0.80-100	0.50-105	<0.01-80	<0.01-200

Of the processes described in Table 1-1 the gas phase polymerization process is the most recently developed and the most versatile. Since its emergence the process has been challenging the other existing processes for market share, particularly, in the production of LLDPE, due to its economical and technological advantages. The distinguishing characteristic of gas phase polymerization is that the system does not involve any liquid in the polymerization zone.

The first commercial gas phase polymerization plant was constructed by Union Carbide in 1968, using a fluidized bed reactor. This process was developed initially for HDPE production but the success of the novel technology led to the extension of the process to LLDPE, which was produced initially on a commercial reactor in 1975. The process, commonly referred to as the UNIPOL process, has been licensed worldwide with more than 25 licenses and is operated in 14 countries. The production of LLDPE using gas phase processes is more difficult than the production of HDPE because the difference between the melting point and the polymerization temperature is much lower for LLDPE. The catalyst types and equipment design developed for HDPE cannot be used to produce LLDPE because of the potential for agglomeration of polymer particles (Xie *et al.*, 1994). Hence significant engineering and chemistry research had to have been carried out, to ensure the success of gas phase LLDPE production, by Union Carbide.

In about 1964 BASF developed a gas phase ethylene polymerization process using the Phillips catalyst and this resulted in the construction of a commercial gas phase HDPE plant in Germany in 1976. BASF uses a continuous stirred bed reactor for gas phase ethylene polymerization. The reactor is equipped with an anchor agitator and is operated at a higher pressure and temperature than those employed in the UNIPOL process. Magnesium-supported titanium halides, aluminium alkyl compounds and silica-supported modified chromium oxide catalysts are used for HDPE production.

The AMOCO (Standard Oil Company) gas phase polymerization process was developed in the mid-1970s. A compartmented horizontal stirred bed reactor is used with the reactor being divided into several stirred polymerization zones which are separated by weirs. The distinguishing feature of the AMOCO process, compared with the previous processes, is that it can be operated like a set of continuously stirred tank reactors (CSTRs) in series. Tracer studies on the commercial reactor show the RTD in the AMOCO process to be roughly equivalent to that of three to five well stirred tanks in series.

Soon after the Union Carbide process was introduced, Naphtachimie developed a gas phase polymerization reactor using a fluidized bed and a commercial scale plant was commissioned in 1975. The gas phase polymerization technology was later transferred to BP Chemicals. The BP chemicals gas phase process now has a capacity of 170 000 tons/year and can produce both LLDPE and HDPE. The major distinction of this process from the UNIPOL process is that pre-polymer particles rather than catalyst particles are fed into the fluidized bed reactor. Pre-polymerization has advantages in polymer particle size control and control of the catalyst activity in the fluidized bed. This process uses a combination of a stirred tank reactor and a fluidized bed reactor in series.

Typical reactor operating conditions and production capabilities of the gas phase processes discussed above are summarized in Table 1-2 (Xie *et al.*, 1994).

Table 1-2 Ethylene Gas Phase Polymerization Processes and Reactor Operating Conditions

	Union Carbide	BASF	AMOCO	BP Chemicals
reactor type	fluidized bed	stirred bed	horizontal stirred bed	stirred reactor and fluidized bed
catalyst	supported Ti, V and $CrCO_3$	supported CrCO3	supported Ti and $CrCO_3$	supported Ti and $CrCO_4$
catalyst size, μm	30-250			~50 for prepoly.
pressure, atm	20-30	~35	20-40	15-25
temperature, °C	75-110	100-110	70-110	70-115
co-monomer	1-butene or 1-hexene	1-butene	propylene or 1-butene	1-butene or 1-hexene
MW control	H_2	H_2	H_2 and temperature	H_2
density, g/cm³	0.91-0.97		0.95-0.98	0.91-0.96
polymer part. size, μm	500-1300			300-1200

1.6 The advantages/disadvantages of the gas phase process

Of the billions of tons of polyethylene produced each year, a large proportion is produced in gas-phase reactors using Ziegler-Natta catalysts. One benefit of gas phase polyethylene production is that there is no solvent present in the reactor system to be recovered and processed. Another advantage is that the gas-phase processes usually operate at more moderate temperatures and pressures than the high pressure or liquid phase polymerization systems.

When compared with the slurry and solution processes the gas phase processes have many distinct advantages. Slurry-based processes produce polyethylene covering a broad range of melt indexes; however the range of densities attainable is limited. As density decreases, resin solubility in the diluent increases and at a density of about 0.930g/cm³ sufficient dissolution occurs to foul the reactor. Slurry processes are therefore not suitable for LLDPE production. On the other hand, solution processes can produce polyethylene over a broad range of densities, but only a limited range of molecular weights can be attained. As molecular weight increases solution viscosity also increases and at some point the increased viscosity limits reactor operability and productivity. Thus solution processes are not suitable for producing high molecular weight polyethylene. Gas phase processes, which do not involve any liquid phase in the reaction zone, are constrained by neither solubility nor viscosity. The gas phase process can therefore be used to produce a complete range of polyethylene with densities of 0.91-0.97g/cm³ and melt indexes of <0.01g/10min up to 200g/10min. Furthermore, with gas phase processes construction costs are reduced by up to 30% and operating costs by up to 35% when compared to conventional liquid phase processes.

Compared with the slurry and solution processes the gas phase processes do however have disadvantages. The reactor operating temperature is limited to the resin softening point, and the productivity of the catalyst is therefore also limited. The poor heat transfer efficiency of the gas phase is also a disadvantage and additional inert heat transfer agents are therefore required to

maintain stable reactor operating conditions at high production rates. There is also a possibility of sintering and agglomeration of the polymer particles due to the formation of local hot spots when a high-activity catalyst is used. Another disadvantage is that as polymerization progresses, fine particles will deposit on heat transfer areas, compressor blades, and sloped walls of the reactor. Sensitivity to variation in operating conditions, such as flow rates of catalyst and monomer feed and polymer discharge is also a disadvantage. Also, the temperature in the reaction zone must be maintained above the dew point of the reactants to avoid condensation and below the melting point of the polymer to prevent particle melting and agglomeration.

1.7 An outline of a typical polymerization process

In a heterogeneous Ziegler-Natta polymerization reaction, the catalyst constitutes the solid phase and the continuous phase of the reactor contains monomer(s), either in the form of a gas or a liquid. In slurry reactors, the monomer(s) are either dissolved in an inert hydrocarbon diluent or, in the specific case of propylene, present as pure monomer. Gas phase reactors may contain up to 50% (v/v) nitrogen in addition to monomer(s). For all processes, hydrogen may be used as the chain terminating agent to control the average molecular weight. Regardless of the nature of the continuous phase, the monomer must diffuse through the boundary layer around the catalyst particle and through its pores to reach the active sites, where polymerization takes place. Depending on the catalyst type, the rate of polymerization might reach 10^4-10^5 insertions per second (McKenna and Soares, 2001). The fast-forming polymer will deposit on the catalyst surface and pores. Monomer must then adsorb and diffuse through this polymer layer to reach the active sites.

In many cases, pre-polymerization catalysts may be used. Pre-polymerization is a precisely controlled polymerization process under mild reaction conditions that precedes the polymerization process itself and in which the active sites will always be covered with a layer of polymer. This process is conducted in a separate reactor and is a useful technique to enhance catalyst stability as well as activity, and to eliminate the formation of hot spots in the catalyst particles.

As soon as the polymerization reaction begins the catalyst pores will be saturated with polymer. The desired effect for all catalysts used in industrial olefin processes at this stage is for the support to rupture into many fragments. The catalyst particle does not lose its overall integrity at this stage because the polymer already formed in the particle holds the individual fragments together. One of the main objectives of pre-polymerization is to ensure better control of this fragmentation step. Fragmentation is a desirable phenomenon since particle fragmentation produces porous polymer particles, thereby facilitating monomer access to the active sites.

Once the particle has fragmented, the volume of the polymer inside the particle continues to grow as monomer diffuses to the active sites (supposedly through increasingly thicker layers of polymer). One of the consequences is the well-known replication phenomenon: the shape of the particle size distribution curve of the polymer particles at the end of polymerization closely approximates the shape of the particle size distribution curve of the catalyst at the beginning of polymerization. Good replication is supposed to occur when there is an adequate balance between the mechanical strength of the catalyst particle and catalytic activity. This process of expansion continues until polymerization is terminated. The fraction of catalyst fragments in the final polymer particles is very small and does not need to be removed from the polymer product.

1.8 Overall objectives and motivation for the study

In the public literature on ethylene polymerization with $MgCl_2$-supported Ziegler-Natta catalysts there is a general lack of kinetic data that can be used for reactor design and control of polymer properties. This is in spite of intensive research efforts and the successful application of these catalyst systems in industry. The reason for this is that olefin polymerizations on a small scale are rather difficult to execute and the lack of fundamental kinetic models is therefore related to the difficulty in obtaining high-precision kinetic data. For kinetic studies, control of operating parameters such as temperature and pressure is highly important and high precision in the experiments demands close control of these parameters for the duration of the reaction. In addressing the issues mentioned above, the solution lies in firstly designing and constructing competent reactor systems.

The first and foremost goal of this study is to therefore design and construct a reactor system for the gas-phase polymerization of ethylene using a heterogeneous Ziegler-Natta catalyst. The system is to include high efficiency temperature and pressure control systems and the reactor is to be a spinning basket reactor. Basket reactors, like the Berty stationary catalyst basket reactor, are commercially available for laboratory investigations; however, information on their usefulness and limitations for gas phase olefin polymerization is limited in the literature. Although stirred bed reactors are easier to design and operate, polymer particle morphology is easily destroyed by the stirrer used for agitation. In this work the effectiveness of containing the catalyst and hence the growing polymer particles in a porous basket is investigated. The basket is intended to spin with the aim of minimizing temperature and concentration gradients in both the gas and solid phases.

In order to undertake quantitative investigations using the designed reactor system, a catalyst capable of polymerizing ethylene is required. The third generation Ziegler-Natta catalyst, which is formed by physically or chemically supporting catalyst molecules on the surface of a solid support, is reported to be more than 50 times more active than the previous generation catalysts and is the most widely used in industry. It was therefore decided to synthesize such a catalyst in this study. $MgCl_2$ must first be activated before it can be used as a catalyst support. The re-crystallization (precipitation) method for $MgCl_2$ activation is preferred to the ball milling

method since it can be used to produce support particles having a spherical morphology. From these support particles, catalyst particle shaving a similar morphology are produced. These are then used to produce spherical polymer particles. Polymer particle morphology is an important characteristic since it is a major factor in determining process viability. For the synthesis of the catalyst, a special experimental set-up consisting of Schlenk type glassware, vacuum and nitrogen lines and manifolds, mercury bubblers, a glove bag, double tipped needles, and gas-tight syringes, is necessary. This is because the support, the catalyst, and the chemicals used in their synthesis are extremely air and/or moisture sensitive and these will deactivate or explosively react if they come into contact with air or moisture.

Finally, gas phase ethylene polymerization experiments are to be carried out using both the synthesized catalyst and the constructed reactor system. A series of experiments to determine the effect of temperature, pressure and the Al/Ti molar ratio on the polymerization yield are to be carried out. These experiments are essentially aimed at investigating the effect of catalyst composition and process conditions on polymer properties and polymer yield. The experiments are also aimed at assessing the efficiency of the reactor system, with special interest in the temperature and pressure control systems and the spinning basket.

1.9 Dissertation outline

The outcomes of the goals mentioned above are presented and discussed in the chapters that follow. The organization of the chapters and their contents are summarized below.

Chapter 2 is a review of the fundamental aspects of Ziegler-Natta catalyzed polyolefin polymerization. An extensive survey of the literature relating to this study is presented there. Firstly, the preparation procedures used in the synthesis of Ziegler-Natta catalysts are investigated. Both the prevailing ball milling method and the more recently developed re-crystallization methods are looked at. This is followed by a comprehensive look at the design of gas phase polymerization reactor systems presented in the literature. Methods of reactor temperature control and catalyst injection are also focused on. The chapter is concluded by discussing the mechanisms and reactions proposed for Ziegler-Natta catalysts and the interaction of the catalyst with the co-catalyst.

In Chapter 3 a detailed description of the novel lab-scale reactor system that has been designed and constructed for investigating the kinetic behaviour of olefin polymerization reactions using a heterogeneous catalyst is given. The reactor design, the feed and exit gas systems, the catalyst injection system and the reactor temperature and pressure control systems are described in detail and elaborately illustrated.

In Chapter 4 an explanation of the experimental procedures and equipment used in the synthesis of the $MgCl_2$ support and the Ziegler-Natta catalyst is given. A spherical $MgCl_2$ support is synthesized and impregnated with $TiCl_4$ and an internal electron donor using special Schlenk

techniques for the manipulation of anhydrous and air sensitive chemicals. Both the support and the final catalyst are fully characterized by scanning electron microscopy (SEM), X-ray diffraction (XRD), inductively coupled plasma (ICP), and Infrared Spectroscopy (FTIR) analyses. The results of polymerization tests carried out to assess if the catalysts were capable of polymerizing ethylene are thereafter discussed.

In Chapter 5 the reactor pre-treatment and polymerization reaction experimental procedures are firstly described. The results of the gas phase ethylene polymerization experiments which were undertaken to investigate the effects of the Al/Ti molar ratio, temperature, and pressure on the polymerization yield and polymer properties are thereafter presented and discussed.

In Chapter 6 the conclusions of this work are highlighted and recommendations for future investigations are given.

Chapter 2

Literature Review

Research on Ziegler-Natta catalysts for α-olefin polymerization in the early 1960s led to the discovery of active $MgCl_2$ as the ideal support for $TiCl_4$. As a result, subsequent research predominantly focused on improving the performance of these catalysts. Researchers have extensively investigated the effects of different methods of activating $MgCl_2$ and the effects of several combinations of internal and external electron donors. In the first part of this review the catalyst, with particular regard to preparation methods and the role of individual components used in its synthesis are discussed. Both the prevailing ball-milling support preparation method and the more recently developed re-crystallization (precipitation) methods are looked at.

One of the most important features of ethylene polymerization involving heterogeneous Ziegler-Natta catalysts is the fact that these catalysts are uniquely capable of replicating their morphology into the morphology of the resulting polymer particles. Developments with respect to catalyst and polymer morphology are therefore also discussed.

The lack of fundamental kinetic models for ethylene polymerization is somewhat related to the difficulty in obtaining high-precision kinetic data. High precision in the experiments demand close control of operating parameters and the problem then lies in designing and constructing competent reactor systems. In the literature, various reactor systems are described and these systems are compared here. Both the advantages and disadvantages are addressed and the challenges faced in laboratory studies are outlined. The various methods used for reactor temperature control and for catalyst injection are also reviewed.

The chapter is concluded by discussing the mechanisms and reactions proposed for Ziegler-Natta catalysts and interaction of the catalyst with the co-catalyst.

2.1 $MgCl_2$-supported Ziegler-Natta catalysts: preparation methods

The discovery of active magnesium dichloride ($MgCl_2$) as the ideal support for the fixation of titanium tetrachloride ($TiCl_4$) and its derivatives has opened a new era in the field of Ziegler-Natta catalysis, both from an industrial and a scientific viewpoint. $MgCl_2$-supported Ziegler-Natta catalysts for the polymerization of olefins have had enormous commercial success in simplifying polymerization processes and improving polymer quality. At the same time, scientific research has tried to rationalize and understand the structure and the behaviour of the new catalytic systems. However, reaching an in-depth knowledge was not as rapid as the commercial development, and many concepts are still under discussion. Catalysis is therefore the most active area of research in ethylene polymerization with worldwide participation of both industrial and academic laboratories. The extent and variety of research work reflects not only the great interest and extensive commercial applications in this area but also the complexity of catalysts for ethylene polymerization.

The use of supports in heterogeneous catalysis was well understood by the 1950s and was highlighted by the discovery of highly active chromium trioxide catalysts supported on silica which could polymerize ethylene under mild conditions of temperature and pressure to produce predominantly linear, high density polyethylene (Hogan and Banks, 1958). At about the same time Natta and co-workers demonstrated that only a small percent of the titanium atoms (<1%) in first generation catalysts were active. It then became evident that higher catalytic activities were likely to be achieved through the use of transition metal compounds supported on appropriate matrices. It was ultimately the discoveries by Montecatini-Edison Co. and Mitsui Petrochemicals Ind. that catalysts prepared from $MgCl_2$, $TiCl_4$, and an electron donor, and activated by a mixture of trialkylaluminium and a second electron donor, could result in polypropylene with a high yield and good stereospecificity that have set the scene for much of the present explosion in catalyst development. Since then some of the most promising catalysts have resulted from the use of $MgCl_2$ as supports.

The fact that $MgCl_2$ seems almost uniquely suitable as a catalyst support has been widely attributed to the near isomorphism of $MgCl_2$ and $TiCl_3$ crystals. $MgCl_2$ exists in three distinct crystalline forms: the most common is the cubic close-packed (ccp) form, referred to as α-$MgCl_2$, a thermodynamically less stable hexagonal close-packed (hcp) form, referred to as β-$MgCl_2$ and a rotationally disordered version of the hcp crystal form, referred to as δ-$MgCl_2$. The cubic close-packed form is very similar in structure to γ-$TiCl_3$ while the hexagonal close-packed form is very similar in structure to α-$TiCl_3$. Crystals of both $TiCl_3$ and $MgCl_2$ are comprised of two planes of chlorine atoms sandwiching a plane of metal atoms.

The major findings of academic studies on $MgCl_2$-supported catalysts have been comprehensively reviewed and the main reasons that $MgCl_2$ is most widely used as a catalyst support can be summarized as follows (Chien *et al.*, 1987):

- $MgCl_2$ has crystalline forms similar to those of $TiCl_3$ (conventional Ziegler-Natta catalyst). This distinct feature suggests that $MgCl_2$ should have the ability to mimic the structure of active $TiCl_3$ and the ability to efficiently incorporate $TiCl_4$.
- $MgCl_2$ possesses desirable morphology as a support. Mercury porosimetry results showed that $MgCl_2$ is a highly porous polycrystalline material as a result of a large number of uniformly distributed micro-cracks (Chien *et al.*, 1983). The structure of $MgCl_2$ is sufficiently resistant to fracture by mechanical manipulation, but weak enough so that its internal structure can be broken down during polymerization. The porous morphology permits the diffusion of monomer into the interior of the catalyst particles and serves to determine the morphology of the polymer. This replication phenomenon, which has long been known for the $TiCl_3$ catalyst, has also been observed for the $MgCl_2$-supported catalyst.
- $MgCl_2$ has a lower electronegativity compared with those of other metal halides. Supports having electronegativities less than that of $TiCl_3$ are thought to promote the co-ordination of monomer molecule to Ti via π-back donation. This means that a metal halide with a lower electronegativity than $TiCl_3$ will increase productivity in ethylene polymerization. $MgCl_2$ also enhances chain-transfer reactions because the number average molecular weight (M_n) decreases with an increase in Mg/Ti ratio (Karol, 1984).
- Finally, $MgCl_2$ is inert to the chemicals used for polymerization and it can be left in the final product without a requirement for deashing.

In order to be successfully used as a catalyst support, $MgCl_2$ must first be converted to a form which can efficiently incorporate $TiCl_4$, a process referred to as activation. This can be done by various methods such as ball milling, vibratory milling, spray drying, precipitation of $MgCl_2$ from solution, and chemical conversion starting with Mg salts. The two most widely used methods are the ball milling and the precipitation methods. Ball milling with $MgCl_2$ can be carried out with $TiCl_4$ alone or with an electron donor (Lewis base), usually ethyl benzoate (EB). In the latter case, titanium incorporation takes place by refluxing with $TiCl_4$. These $MgCl_2$/EB/$TiCl_4$ catalyst systems may be activated with trialkylaluminium compounds and used for the polymerization of ethylene. However, for propylene polymerization the addition of an electron donor (external donor) to the trialkylaluminium solution is necessary in order to achieve high stereospecificity. The ball milling support preparation method is discussed in section 2.1.1. The active $MgCl_2$ support can also be prepared by the re-crystallization (precipitation) method. This method has the advantage of producing polymer of favourable morphology for industrial use and has, as a result, been widely used in commercial production. The re-crystallization method, which is the method used for the preparation of the support in this work, is discussed in section 2.1.2.

2.1.1 Catalyst preparation by ball milling

Highly active $MgCl_2$-supported catalysts can be obtained by the mechanical treatment of mixtures of $MgCl_2$ and $TiCl_4$. The ball-milling of $MgCl_2$ produces a disordered crystal structure. A reduction in the crystallite size also occurs during milling but reaches a rather large limiting size. As the crystallite size decreases, its surface energy increases to cause re-crystallization. Therefore, at a certain point the $MgCl_2$ crystallites are subject to re-agglomeration and no further size reduction or deformation is possible.

During ball milling the $MgCl_2$ structure undergoes substantial variations which considerably affect the catalyst performance. Giannini (1981) has reported that during ball milling the X-ray reflection at d = 2.5 Å gradually disappeared and was replaced by a broad halo at d = 2.65 Å, a position intermediate between reflections for cubic and hexagonal structures. This behaviour was attributed as arising from stacking faults induced by the rotation of Cl-Mg-Cl layers. Modelling studies carried out by Galli *et al.* (1984) demonstrated that the changes which occurred in the crystal structure corresponded to a destruction of α-$MgCl_2$ and creation of rotational disorder, i.e. δ-$MgCl_2$. This change was correlated to an increase in activity. From radial atomic distribution analysis undertaken by Zakharov *et al.* (1986) it was suggested that the presence of crystal distortions seemed to be preferential sites for $TiCl_4$ binding. Barbe *et al.* (1987) suggested that these sites may be on the edges of the crystallites and that they were created by breakage across stacking layers and were coordinatively unsaturated with two vacancies where $TiCl_4$ can bind. Vermel *et al.* (1980) found that $TiCl_4$ entered the $MgCl_2$ defects and brought about some ordering while Zakharov *et al.* (1986) suggested that the titanium entered the subsurface of the $MgCl_2$ and was consequently inaccessible to the monomer.

In addition to crystallite transformation, a size reduction also occurs during ball milling. Kashiwa (1980) stated that when $TiCl_4$ is co-milled with $MgCl_2$, $TiCl_4$ acts like a wedge, breaking up the $MgCl_2$ crystals. He identified three stages of titanium fixation, with the polymerization activity increasing up to the last stage. Initially, $TiCl_4$ was fixed onto the $MgCl_2$ surface with subsequent wedging (i.e. after 10 hours of milling). The second stage consisted of freshly fixed titanium participating in re-aggregation of particles (10-50 hours). Finally, no new titanium was fixed and only re-aggregation occurred (>50 hours). After a long enough milling time (~60-70 hours) no further improvement in crystallite size reduction and activity were noticed. This was attributed to the re-aggregation of the catalyst particles. Kashiwa also found that co-milling $TiCl_4$ with $MgCl_2$ typically resulted in an average titanium content of around 4 wt%.

Keszler *et al.* (1980) discovered that the crystallite size was reduced dramatically for up to 60 hours of milling, and decreased slowly thereafter. Chien *et al.* (1983) reported that the ultimate crystal size was produced after 30-60 hours of milling. Typical crystallite sizes reported are 50 Å and 70 Å. Chien also reported that 20 Å diameter $MgCl_2$ particles were agglomerated into 4000 Å particles when ethyl benzoate was used. This could be broken up by subsequent treatment and milling times of 120 hours were typically used to achieve limiting size reduction. Mercury

porosity work carried out by Chien on the catalyst at this stage of milling showed that it was nonporous and as a result the active centres were said to be on the surface.

Data on the performance of catalysts prepared by co-milling $MgCl_2$ and $TiCl_4$ have been widely reported. Gerbasi *et al.* (1984) found that the activity for ethylene polymerization clearly depended on the length of the mechanical treatment, i.e. it increased with milling time reaching a maximum and it thereafter decreased. The initial increase of activity was found to be linked to the disorder produced by gradually ball milling and consequently to the increasing number of sites available for active Ti fixation. Kashiwa *et al.* (1984) attributed the subsequent activity decrease to a decrease in surface area caused by the agglomeration of small particles.

The re-crystallization observed when co-milling $MgCl_2$ and $TiCl_4$ can be inhibited by an additive which complexes with the substrate to reduce its surface energy. This is one of the functions of the Lewis base, most commonly ethyl benzoate. The structural changes observed in the support when co-milling with ethyl benzoate are similar to those observed when co-milling with $TiCl_4$, namely a reduction in crystallite size and introduction of crystal distortions. Chien *et al.* (1983) have investigated the effects of ball milling $MgCl_2$ with ethyl benzoate by means of BET, mercury porosity, and X-ray techniques, and have concluded that the milled material (60 hours) has a higher surface area, smaller pore radii, higher pore surface area and smaller crystallite dimensions than that of un-milled material. They suggested that size reduction is possible since ethyl benzoate is able to stabilize the $MgCl_2$ crystallites by coordination, through its carbonyl function, to newly expose faces created by the milling action.

Calorimetric data presented by Keszler *et al.* (1981) suggested the presence of two ethyl benzoate adsorption processes. One was thought to be simple surface adsorption and the second was the result of an endothermic $MgCl_2$ crystal lattice destruction, followed by the exothermic formation of a $MgCl_2$/ethyl benzoate complex. According to Keszler ethyl benzoate did not penetrate the $MgCl_2$ crystal matrix but was limited to surface reactions. Chien *et al.* (1982) however believed that ethyl benzoate must penetrate the crystal lattice without rupturing it since the amount incorporated was three to four times that required to form a monolayer. Keszler *et al.* (1980) found that an ethyl benzoate/$MgCl_2$ molar ratio of 0.17 resulted in the smallest crystal size reduction. Sergeev *et al.* (1983), on the other hand, observed no minimum. They rather observed that the crystal size decreased monotonically with the ethyl benzoate/$MgCl_2$ ratio.

Once the support is prepared, the active titanium is incorporated onto the support surface by refluxing the $MgCl_2$/ethyl benzoate co-ground mixture with $TiCl_4$, typically at 80°C for 2 hours. According to Zakharov *et al.* (1986), $TiCl_4$ displaces ethyl benzoate from unsaturated portions of the $MgCl_2$ crystallite and binds there during this process. They also found that the crystallite size was increased by the treatment. Sergeev *et al.* (1983) suggested growth in only the (110) direction. This means that $TiCl_4$ attaches to the unsaturated portion of only one face, implying that ethyl benzoate may block $TiCl_4$ fixation on certain parts of the $MgCl_2$ crystallite. Work

carried out by Busico *et al.* (1985) indicates that the (100) and (110) faces have different Lewis acidities (the latter being more acidic). This has an effect on the ease of removal of the Lewis base from the different $MgCl_2$ faces. Ethyl benzoate is more easily removed from the (100) face and $TiCl_4$ therefore binds there more easily, but it is inhibited somewhat from fixing to the (110) face. According to Busico this potential site blocking mechanism can be an explanation for the improved stereospecificity of $MgCl_2$/ethyl benzoate-supported catalysts.

According to Kashiwa (1980), ethyl benzoate is removed from the $MgCl_2$ surface as a complex with $TiCl_4$. It is believed that this yellow complex is inactive for polymerization and remains unfixed. The weight percent of Ti incorporated into the catalyst typically ranged from ~0.75 to 8. Keii *et al.* (1982) found that a titanium weight percent greater than 2 provided no additional activity and was probably in the form of an inactive $TiCl_4$/ethyl benzoate complex. The active titanium was thought to be fixed as a monolayer. Estimation of the concentration of active centres by site poisoning with CO was carried out by Doi *et al.* (1982) and it was found that only 1 to 10% of the available titanium appeared to form active centres. Also, not all the ethyl benzoate is removed by $TiCl_4$ treatment and Kashiwa (1980) proposed that some formed an integral part of the active site.

Table 2-1 Approximate Dimensions of $MgCl_2$-Supported Catalysts (Chien, 1987)

composition	diameter Å	pore volume cm^3/g	surface area m^2/g
$MgCl_2$ (HCl treated)	~4000	0.41	
$MgCl_2$/EB	700-1500	0.41	2.0-7.0
$MgCl_2$/EB/PC/$AlEt_3$	300-500	1.2	50-70
$MgCl_2$/EB/PC/$AlEt_3$/$TiCl_4$	25-170	1.3	100-150

Table 2-1 shows approximate dimensions of $MgCl_2$ supported catalysts obtained by ball milling, where PC refers to *p*-cresol and $AlEt_3$ to triethylaluminium. From the table it can be seen that $MgCl_2$-supported catalysts have large surface areas and internal pore volumes and that both the surface area and the pore volume change with modifier composition. Incorporation of $TiCl_4$ with such a support results in dispersion or isolation of the titanium centres so that the population of active centres which are accessible for polymerization increases dramatically compared with that of unsupported conventional Ti catalysts. This is the main reason why supported Ti catalysts have productivities that are much higher that those of conventional catalysts. In addition, magnesium ions can stabilize active titanium ions from deactivation, enhance chain transfer processes (average M_n of PE decreases when Mg/Ti ratio increases), and lead to narrow molecular weight distribution (MWD) for polyethylene production (Karol, 1984). According to Chien (1987), both internal Lewis base (ethyl benzoate) and internal alcohol (*p*-cresol) increase the surface area and pore volume but do not compete for the same surface sites of the $MgCl_2$ crystal. This was concluded since they found the content of ethyl benzoate on the support to be the same after the addition of internal alcohol and concluded that the Lewis base and internal alcohol must therefore adsorb on different planes of the $MgCl_2$ crystal.

2.1.2 Catalyst preparation by the re-crystallization method

In recent years much attention has been given to the re-crystallization (precipitation) method for $MgCl_2$ support preparation. The method involves dissolving $MgCl_2$ in an alcohol followed by the re-crystallization of the $MgCl_2$ from solution by various techniques. The spherical, porous, re-crystallized $MgCl_2$ has a crystal structure that is much more suitable for supporting $TiCl_4$.

Ferraris *et al.* (United States Patent, 1981) were among the first to invent high activity and high stereospecific catalysts that allowed for the formation of olefin polymers having controlled morphology. The method proposed essentially consisted of forming an emulsion of an adduct of $MgCl_2$ and ethanol with a liquid that is immiscible with and does not react with the adduct. The emulsion was then made to pass through a pipe under turbulent conditions and was quenched at the outlet of the pipe causing an immediate solidification of the adduct. The resulting $MgCl_2$ support was in the form of spherical particles having an average diameter between 1 and 100 μm, a surface area higher than 500 m^2/g and porosity higher than 0.5 cm^3/g. They found that the reaction product of the Ti compound and support maintained the morphology of the support while the surface area and porosity decreased. The polymer particles that resulted from the use of these catalysts were also found to be spherical.

Prior to the above mentioned invention, catalysts with high activity and stereospecificity were known but they did not allow one to obtain polymers with controlled morphology, high flowability, and a narrow particle size distribution. Galli *et al.* (United States Patent, 1976), on the other hand, described a polymerization catalyst that resulted in olefin polymers in the form of spherical particles having a controlled particle size distribution but the activity and stereospecificity were inadequate for practical use.

Hu and Chien (1988) also prepared highly disordered $MgCl_2$ by a re-crystallization method. The basis of the catalyst preparation was to precipitate $MgCl_2$ from its emulsion with the alcohol and dispersant by the addition of $TiCl_4$ in the presence of an ester. Two series of catalysts were made, both consisted of $MgCl_2$ solutions in 2-ethylhexanol with the first containing ethyl benzoate and the second containing phthalic anhydride. Reactions of these solutions with $TiCl_4$ with or without another ester produced the final series of catalysts. The two esters used during the titanium treatment were ethyl benzoate (monoester) and diisobutyl phthalate (diester). It was found that the monoester modified catalysts differed from the diester modified catalysts in every respect. By comparison the diester modified catalyst contained half as much Ti per Mg, had more than 10 times the pore volume, more than 100-fold the surface area, about 50% higher productivity, and greatly increased stereospecificity.

Internal Lewis bases such as ethyl benzoate are used as anti-agglomeration agents in support preparation by ball milling and it has been found that the ultimate crystallite sizes are attained in their presence. Another major purpose of ethyl benzoate is to coordinate the acidic sites and thus inhibit their non-specific polymerization of monomer, and to increase the number of stereospecific sites. Hu and Chien (1988) used this rationale when preparing their catalysts.

They claimed that it was important that the re-crystallization of $MgCl_2$ occurred slowly so that a large number of very small crystallites were formed but not in the thermodynamically stable cubic close packed (ccp) structure. They therefore introduced an ester to the solution of $MgCl_2$ in ethanol prior to precipitation with $TiCl_4$ claiming that due to the known effects of ethyl benzoate in ball-milling it was likely that its addition would prevent the $MgCl_2$ from growing too rapidly and will also prevent crystallites from growing without much disorder. Kothandaraman and Devi (1994), Chung *et al.* (1995) and Choi *et al.* (1996) also added the electron donor to the $MgCl_2$-alcohol solution prior to precipitation.

Catalysts prepared by the precipitation of the $MgCl_2$-ester-alcohol solution with $TiCl_4$, with no further ester addition, showed the highest Ti contents but it was found that 30% of the Ti belonged to Cl_3TiOR. That is, the Ti found bonded to the $MgCl_2$ support was in the form of both $TiCl_4$ and Cl_3TiOR, of which the Ti in Cl_3TiOR was inactive for polymerization. These catalysts had the lowest BET surface area and pore volumes and also had the lowest productivity and stereospecificity. When these catalysts were further treated with $TiCl_4$, the surface area and pore volumes increased significantly, while only a small increase in the productivity was noticed. According to Hu and Chien (1988), this implied that surface area and porosity could not simply be correlated with catalytic activity.

When the support was treated with an ester modifier during the first $TiCl_4$ treatment the amount of alcohol in the catalyst was reduced by 80%. This was attributed to the exchange and replacement of Cl_3TiOR by the modifier in the $MgCl_2$ complexes and resulted in a two-fold increase in activity. The amount of Ti was, as a result, found to be lower if an ester was added during precipitation with $TiCl_4$. With a second $TiCl_4$ treatment they found that there was a further decrease in the Ti content, implying that the Ti formed complexes with the ester which adsorbed on the surface and which could be extracted with $TiCl_4$.

Kothandaraman and Devi (1994) used a silicon halide, $SiCl_4$, to precipitate the $MgCl_2$-alcohol complex out of solution and, as with Hu and Chien (1988), an ester was added prior to precipitation. The purpose of the silicon halide was to react with the alcohol and to at least partially remove it from the precipitated support. They found that at least 50% of the alcohol was removed with this method, resulting in an increase in the specific surface area of the support. When these supports were treated with $TiCl_4$ the remaining alcohol was completely removed and the surface area and porosity were further increased.

When investigating the effect of different alcohols on the surface area of the supported catalysts, Kothandaraman and Devi found that it increased in the following order (depending on the alcohol and the electron donor used):

1. *p*-cresol < *n*-butanol < *n*-pentanol < *n*-hexanol < *n*-octanol
2. *n*-butanol < *t*-butanol
3. *n*-hexanol < 2-ethyl-1-hexanol
4. no electron donor < ethyl benzoate < dibutyl phthalate

From these results they concluded that alcohols with higher carbon numbers and branching were more efficient in increasing the surface area of the catalysts. The presence of the electron donors also facilitated in increasing the surface area and among the esters the diester (dibutyl phthalate) was found to be more efficient than the monoester (ethyl benzoate). They also found that a higher surface area directly resulted in a higher productivity. Among the various alcohols and esters tested for the chemical activation of the support, 2-ethyl-1-hexanol and dibutyl phthalate resulted in the highest surface area and highest productivity.

Kothandaraman and Devi (1991) also studied the difference in X-ray diffraction patterns of both hand-ground anhydrous $MgCl_2$ and of $MgCl_2$-supported catalysts. They found that X-ray diffraction pattern of the hand-ground $MgCl_2$ showed reflections corresponding to a more thermodynamically stable cubic close packed arrangement while the patterns of the supported titanium catalysts showed a highly disordered structure of $MgCl_2$, mostly with a hexagonal close packed arrangement.

Chung *et al.* (1995) investigated the effect of ethanol in the preparation of the $MgCl_2$-support. The method of re-crystallization by solvent evaporation was used. Dibutyl phthalate was added prior to re-crystallization and the support was treated with triethylaluminium (TEA) prior to being treated with $TiCl_4$. In order to investigate the effects of ethanol they prepared two different catalyst supports, one with 30 mL of ethanol and the other with 100 mL, both with the same mass of $MgCl_2$ (0.05 mol). They found that the supports changed into an amorphous state after they were treated with TEA due to the removal of the ethanol in the form of aluminium ethoxide which was formed by the reaction of TEA with the ethanol in $MgCl_2.n$EtOH. The surface area of the support was found to drastically increase and the ethanol content decrease after the treatment with TEA. The ethanol content was found to further decrease after the $TiCl_4$ addition, implying that the ethanol was also removed in the form of titanium ethoxide by the reaction of $TiCl_4$ with the ethanol in $MgCl_2.n$EtOH. A further increase in the surface area was noticed after the $TiCl_4$ addition. It was found that although the treatment with TEA and $TiCl_4$ did not remove all of the organic compounds in the support, the surface heterogeneity of both the supports and the catalyst were found to increase when ethanol was removed in the form of aluminium ethoxide and titanium ethoxide.

When the effects of the different amounts of ethanol on the characteristics of the supports and catalysts were compared it was found that the support prepared with 100 mL of ethanol had a larger surface area and smaller average particle size than that prepared with 30 mL of ethanol. This meant that the support with the smaller particle size was formed during re-crystallization when it was treated with very large amounts of ethanol due to the decreased $MgCl_2$ concentration in the ethanol droplets in the inert dispersant. Chung *et al.* (1995) proposed that is was likely that the ethanol in the support prepared with 100 mL and with the smaller average particle size had a higher probability of reacting with the TEA. This meant that the support prepared with 100 mL of ethanol underwent an enhanced ethanol removal upon treatment with TEA. On the other hand, the ethanol in the support prepared with 30 mL had a much higher

probability of reacting with $TiCl_4$. This was concluded because the Ti content in the support prepared with 100 mL of ethanol was lower and from this it was further concluded that the large amounts of aluminium ethoxide in the support prepared with 100 mL ethanol retarded the Ti impregnation.

The catalyst prepared with 100 mL of ethanol showed a higher activity and isotactic index than the catalyst prepared with 30 mL of ethanol. This effect was noticed both in the presence and absence of the external electron donor, ethyl benzoate. The enhanced isotactic index was found to be mainly due to very large amounts of aluminium ethoxide acting as an electron donor. The enhanced activity was found to be a result of two factors: 1) the large amounts of aluminium ethoxide in the catalyst prepared with 100 mL of ethanol retarded Ti impregnation, and 2) the small amounts of ethanol forming small amounts of inactive titanium ethoxide upon titanium impregnation.

Forte and Coutinho (1996) also reported on the preparation of $MgCl_2$/internal donor/$TiCl_4$ catalysts with controlled morphology. Diisooctyl phthalate (DIOP) or diisobutyl phthalate (DIBP) were used as internal electron donors (ID) and unlike the research work discussed above, the internal donors were added during support titanation. The supports were precipitated by quenching the liquid adducts in isoparaffin at -20°C. For catalysts prepared with DIBP no particle breaking was observed during the support titanation or during polymerization. The contrary was observed for catalysts prepared with DIOP. The method used for precipitation involved transferring the reaction mixture through a 3 mm tube and quenching it at the outlet. It was found that that the rate of transference, which was controlled by the reactor pressure, affected the average diameter of the supports. The largest average diameter of 112 μm was obtained for a reactor pressure of 1.5 atm while an average diameter of 58 μm was obtained for a reactor pressure of 5 atm.

For the preparation of the support, the ethanol/$MgCl_2$ molar ratio was varied in the range 1-10, and the best results in terms of particle size and morphology were obtained between 2.5 and 4. Forte and Coutinho found that for ratios lower than 2.5 it was not possible to obtain the adducts in a totally melted form and for ratios higher than 4 it was not possible to gain good control of the support morphology. The support did not precipitate for higher ratios investigated. It was also found that the Ti incorporated into the catalyst was dependent on both the internal donor used and on the initial amount of alcohol incorporated into the support. The Ti content was found to be the same if the support was dealcoholated by heating before titanation. However, when the support was dealcoholated with TEA the Ti content was found to be higher. The degree of dealcoholation was found to have a strong influence on the porosity and surface area of the supports and catalysts. The catalysts prepared without an internal electron donor were found to have poorer morphologies and lower activities than those prepared with an internal donor.

A comparison of the effects of ethanol and propanol on the morphology of both the support and catalyst has also been made (Choi *et al.*, 1996). Supports were prepared by the re-crystallization method involving solvent evaporation and dibutyl phthalate, the internal donor, was introduced to the $MgCl_2$-ethanol solution prior to support precipitation. It was found that the average size of the support prepared with propanol was larger than that prepared with ethanol. It was also found that the size of the catalyst particles were much smaller than that of the support, regardless of the alcohol used, implying that the support was changed into smaller particles upon Ti impregnation. The propanol treated catalyst, however, underwent a more severe particle size decrease than the ethanol treated catalyst. The surface area of the catalyst treated with propanol was found to be larger than that of the ethanol treated catalyst and the propanol treated catalyst showed a lower alcohol content and higher dibutyl phthalate (internal electron donor) and Ti contents than the ethanol treated catalyst.

Smaller amounts of alcohol remained in the propanol-treated catalyst after treatment with $TiCl_4$, i.e. when both types of catalysts were treated with $TiCl_4$ propanol was more readily removed than ethanol. From this it was concluded that since $MgCl_2$ forms a $MgCl_2$-alcohol complex by activation with alcohols it is likely that ethanol, a stronger Lewis base than propanol, interacts more strongly with $MgCl_2$ than propanol does. Also, the $MgCl_2$-ethanol complex formed may retard the Ti impregnation on the support and this was the reason proposed for the higher Ti content in the catalyst prepared with propanol than in the catalyst prepared with ethanol.

The propanol-treated catalysts also showed a better performance than the ethanol-treated catalysts. It was also found that when the catalyst prepared with ethanol was reacted with triethylaluminium (TEA), the isotactic index (I.I.) was enhanced. The enhanced I.I. was attributed to the formation of aluminium ethoxide (formed by the reaction of TEA with ethanol), which acted as an electron donor. The catalyst prepared with propanol also showed a high I.I. and this was due to the isospecific active function of propanol, which forms aluminium propanoxide. In addition to this, the catalyst prepared with ethanol showed a lower catalytic activity and it has been suggested that the large amounts of aluminium ethoxide formed blocked the TEA from approaching and activating the active sites of the catalyst.

Fregonese *et al.* (1999) investigated the effect of $ZnCl_2$ as a doping salt in $MgCl_2$ supports. $ZnCl_2$ was found to be an ideal doping agent as its X-ray diffraction pattern closely resembles that of $MgCl_2$ and these salts result in reasonably homogeneous mixtures on a molecular level. It was found that the catalyst activity increased for both ethylene and propylene polymerization on increasing the content on Zn in the catalyst up to 0.73 wt%. For a higher Zn content, the activity was found to decrease. The higher activity of the doped catalysts was attributed to a higher structural disorder which made the catalytic sites kinetically more active. Polydispersity was not affected by the $ZnCl_2$ contents investigated and it was concluded from this that the doped and undoped catalysts contained active sites which were basically the same.

In investigating the kinetics of ethylene polymerization with morphology-controlled $MgCl_2$-supported $TiCl_4$ catalysts Wu *et al.* (1999) used pre-polymerized catalysts. The pre-polymerized catalyst was obtained by ethylene pre-polymerization at mild conditions in heptane using a catalyst in which $TiCl_4$ was supported on spherical $MgCl_2$ support prepared by melt quenching (quick cooling) of a $MgCl_2$-ethanol complex. In order to achieve proper performances of catalysts in terms of morphology and activity, this small amount of polymerization was carried out in a reactor operated in slurry mode under mild conditions of low temperature (30°C) and low monomer pressure (62 kPa). The majority of the polymerization was subsequently carried out in a gas-phase reactor.

Parada *et al.* (2002) undertook a comparative study to investigate the performance of $TiCl_4$ catalysts supported on $MgCl_2$ re-crystallized through different techniques. $MgCl_2$ was dissolved in 1-hexanol and re-crystallized through solvent evaporation under vacuum, quick cooling to -5°C and precipitation with $SiCl_4$ solution in hexane. A catalyst was also prepared by directly precipitating the liquid adduct with $TiCl_4$. The variations of the dealcoholation levels due to the different re-crystallization techniques were found to highly influence the catalytic activity. The catalysts synthesized with the supports that were re-crystallized by $SiCl_4$ addition were found to be the most active.

The preparation of active $MgCl_2$-support by quick cooling or by solvent evaporation of $MgCl_2.n$ROH liquid adducts has been often reported on in the literature. According to Parada *et al.* (2002) the alcohol elimination is not complete through these techniques and the presence of alcohol in the support is undesirable as it reacts with $TiCl_4$ during impregnation producing titanium alkoxides which are inactive for polymerization. They therefore investigated the effect of a precipitating agent, $SiCl_4$, in the re-crystallization of $MgCl_2$ and found that it was effective in eliminating alcohol from $MgCl_2.n$ROH adducts and directly generated alkoxysilanes which acted as electron donors.

From the investigations carried out by Parada *et al.* (2002) it was found that the amount of supported titanium depended greatly on the preparation method used. The catalyst obtained from the re-crystallization of $MgCl_2$ by precipitation with $TiCl_4$ and by quick cooling showed the lowest values. The support re-crystallized by solvent evaporation had an intermediate value while that re-crystallized by precipitation with $SiCl_4$ was found to have the highest content. This behaviour was related to the degree of dealcoholation of the adducts by the various methods. There were no traces of ethanol in the support prepared by $SiCl_4$ precipitation while ethanol still remained in those prepared by the other methods. The re-crystallization techniques significantly influenced the activity of the catalysts and that re-crystallized by $SiCl_4$ precipitation was found to have the highest activity followed by that prepared by cooling, solvent evaporation, and finally by $TiCl_4$ precipitation-impregnation. It was suggested that the formation of inert complexes such as titanium alkoxides, which do not participate in the formation of active sites, were decisive in the catalytic performance. The reaction rate curve for the $SiCl_4$ precipitated catalyst had a maximum activity more that 2.5 times that of those prepared by the other methods. This

behaviour was attributed to two things. Firstly it was attributed to a better distribution of active sites. This was as a result of a higher interaction of $TiCl_4$ with $MgCl_2$ during impregnation. Secondly, alkoxysilanes rather than titanium alkoxides were formed and these acted as an internal Lewis base. The alcohol that remained on the catalysts prepared by solvent evaporation and quick cooling was found to react with the catalyst activator (triethylaluminium) to form aluminium alkoxides which acted as electron donors and were found to enhance the isotactic index.

Some of the most important preparation conditions affecting the performance and morphology of $MgCl_2$-supports for Ziegler-Natta catalysts are shown in Table 2-2.

Table 2-2 Important Conditions for Supported Catalyst Preparation (Ye *et al.*, 2002)

Factor	Affected Aspect
Reagent purity	Catalyst performance
Agitation speed	Particle size and particle size distribution
Time-temperature profile	Performance and composition
Reagent ratios	Particle shape and stereospecificity
Order of reagent addition	Morphology and performance

Ye *et al.* (2002) found that poor purity of the reagents led to poor morphologies. When $MgCl_2$ had absorbed some humidity, the surfaces of the spherical support particles were irregularly spiny. This was due to the complexes between H_2O and $MgCl_2$ which had a negative effect on the $MgCl_2$ dissolving in the ethanol and dramatically influenced the crystallizing process by affecting the velocity of crystallization in certain directions and therefore resulting in the formation of irregular, non-spherical particles.

They further confirmed that the amount of ethanol added during support preparation strongly affected the re-crystallization process of the $MgCl_2$. When excessive amounts of ethanol were used it was impossible for the $MgCl_2$ to re-crystallize completely within a commercially profitable time. Also, excessive ethanol resulted in the adducts being too fragile due to the greater number of defects created by the ethanol absorbing on (100) and (110) faces of the $MgCl_2$ crystal structure.

Spherical $MgCl_2$ supports prepared by the re-crystallization method have also recently been extended to being used as supports for metallocene catalysts. In order to use metallocene catalysts in the existing slurry or gas phase processes, a procedure of impregnation of the catalyst on a support is necessary. According to Cho and Lee (2003), since all commercial polymerization processes use heterogeneous systems, the preparation of heterogeneous metallocene catalysts is a prerequisite for the existing processes.

2.2 Catalyst and polymer morphology developments

One of the most important features of ethylene polymerization involving heterogeneous Ziegler-Natta catalysts is the fact that these catalysts are uniquely capable of replicating their morphology into the morphology of the resulting polymer particle. There are distinct commercial advantages, particularly for gas phase polymerization, in using spherical catalyst particles of narrow particles size distribution, and as a result there has been considerable effort in recent years to prepare catalysts in this form.

All the Ziegler-Natta catalysts used commercially, i.e. both $TiCl_3$ and $MgCl_2$-supported catalysts, consist of primary crystallites, the average size of which varies from about 5 nm to 20 nm depending on the catalyst type, which are agglomerated into larger particles, typically 1-50 μm (van der Ven, 1990). The primary crystallites are held together in a mesh network leaving voids which form the internal pore structure of the catalyst particle. This pore network is essential for high catalyst efficiency since it is through these pores that monomer and co-catalyst can reach the innermost crystallites. It is on the surface of these crystallites that polymerization occurs.

There are a number of reasons why polymer morphology is a major factor in determining process viability. Fine particles pack poorly, limiting reactor capacity and retaining substantial amounts of polymerization solvent on centrifuging the final slurry. Catalyst powders with a diameter less than 100 μm neither flow well nor pack closely. On the other hand, much coarser particles are difficult to keep in suspension. The shape of the polymer particles is also of primary importance, with spherical particles being preferred on account of their high packing efficiency. Particle porosity must also be optimized since a certain degree of porosity is necessary in order to allow the monomer to reach the innermost crystallites (active centres), while a very high porosity results in low density polymer particles which limit reactor capacity and hence process economics.

The phenomenon of replication is usually observed such that the polymer particles formed are essentially enlarged replicas of the catalyst particles used. The only exceptions occur when polymer agglomeration or break-down occur as a result of wrongly selected process conditions. Poor agitation can lead to agglomeration while the exposure of the catalyst to uncontrolled or abnormally high initial polymerization rates can result in fragmentation (catalyst explosion).

The ultimate objectives when preparing supported catalysts is that they are spherical and have a high bulk density. Galli (1982) listed the five primary properties that a catalyst must possess if the polymer granule produced is to be a faithful replica of the catalyst particle: (1) High surface area of the catalyst particle, (2) High porosity of the catalyst particle, with a correspondingly high number of cracks even in the innermost zones, (3) Free access of monomer throughout the catalyst particle, including the innermost regions, (4) Homogenous distribution of the active centers throughout the catalyst particle, and (5) Mechanical strength high enough to withstand manipulations without fragmentation. The first four properties ensure that the whole catalyst particle takes part in the polymerization process while the last aspect refers to eliminating, or at

least minimizing, the risk of catalyst explosion and hence loss of morphological control in the initial stages of the reaction. In such cases where catalysts may fail to withstand the initial forces exerted on it during polymerization, a certain degree of polymerization, referred to as pre-polymerization, can be carried out. Pre-polymerization is carried out under mild reaction conditions and enough polymer is synthesized to hold the catalyst together when it is subjected to the main reactor conditions.

The phenomenon of replication can best be understood by considering how the polymer particles grow during the polymerization process. Active centers are located on the edges of the primary crystallites, which comprise the catalyst particle, thus polymer is formed throughout the catalyst particle on each of the numerous crystallites. As polymerization proceeds, the catalyst particle is split up into progressively smaller units which become uniformly distributed throughout the growing polymer particle. The catalyst particle is split up by the growing mass and once a sufficient polymer yield has been achieved the catalyst will be homogenously dispersed throughout the polymer particle in the form of primary crystallites.

Boor (1979) reviewed various proposals that explained exactly how a polymer chain might grow and crystallize about the catalytic centers. As far as replication is concerned the relevant issue is that the polymer acts as "cement" holding together the millions of primary crystallites within the expanding matrix of the polymer particle. For supported catalysts, the primary particle is the support material, i.e. $MgCl_2$ or silica. Both Barbe *et al.* (1983) and Galli *et al.* (1984) have observed that polymer grows on the edges of $MgCl_2$ crystals treated with $TiCl_4$ and activated with TEA. Since polymer size and shape have been found to replicate the catalyst size and shape, it has been suggested that $MgCl_2$ or silica particles favour the most isotropic distribution of $TiCl_3$ active centres. Figure 2-11 shows the replication relationship between a silica supported catalyst and the resulting polymer particles (Xie *et al.*, 1994).

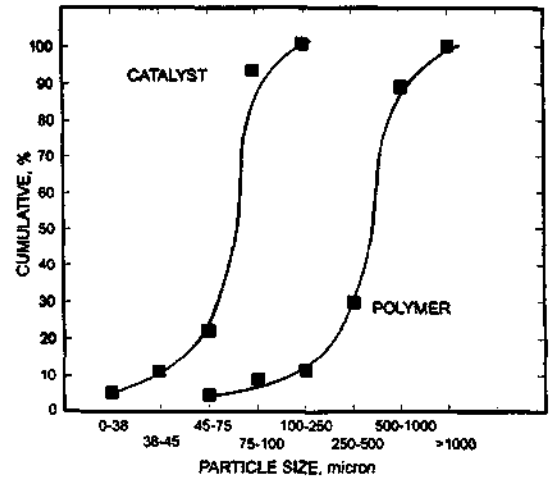

Figure 2-1 Particle Size Replication for Ethylene Polymerization with Silica-supported Ziegler-Natta Catalysts (Xie *et al.*, 1994)

2.3 Laboratory gas-phase polymerization reactor systems

The commercial production of linear low and high density polyethylene is carried out using both slurry- and gas-phase processes. However, following the development of the UNIPOL process by Union Carbide, the majority of new polyethylene production facilities have utilized gas phase processes in which polymer particles are grown in a stirred or fluidized bed reactor.

Despite the rapid commercial acceptance of the gas-phase process, most laboratory evaluations of new catalysts are still carried out in the slurry phase using reactors in which the catalyst particles are suspended in a hydrocarbon solvent (Lynch and Wanke, 1991). This is not only due to the relatively easy construction and operation (typically at a total pressure near atmospheric) of slurry phase reactors, but also due to the excellent heat transfer characteristics of these reactors.

Reaction kinetics and polymer properties resulting from slurry operation are however not directly transferable to gas phase operation. Although in many cases the kinetics are quite similar, there is also some evidence that certain aspects of polymerization kinetics of the gas phase process differ from that of the liquid slurry process (Choi and Ray, 1985). Keii (1972) has shown that ethylene polymerization rates for gas-phase operation are an order of magnitude lower than those observed when the catalyst is suspended in a toluene slurry. It has also been shown by Choi and Ray (1985) that for propylene polymerization the overall activation energy for gas-phase operation is significantly less than that observed for polymerization carried out in a liquid slurry. These observations show that for the investigation of gas phase kinetic behaviour, it is best that experiments be performed in a gas-phase reactor.

2.3.1 Gas phase polymerization reactors

In this section the reactor systems for gas phase polymerization presented in the literature are discussed. Also, since good mixing of the polymer particles and the surrounding gas is essential for reaction heat removal and to prevent thermal runaway in the particles, some attention is focused on the methods of agitation.

Doi *et al.* (1982) undertook gas phase polymerization experiments at constant pressure in a 600 cm^3 glass reactor equipped with a Teflon stirrer and three side arms. The glass reactor does however impose pressure limitations and reactions were only carried out at atmospheric pressure.

Choi *et al.* (1985) carried out gas phase propylene polymerization experiments in a 1 L autoclave stirred bed reactor equipped with a specially designed U-shaped stirrer for the uniform mixing of solids. The laboratory reactor was cable of operating at temperatures and pressures used commercially. The reactor system is shown in Figure 2-2.

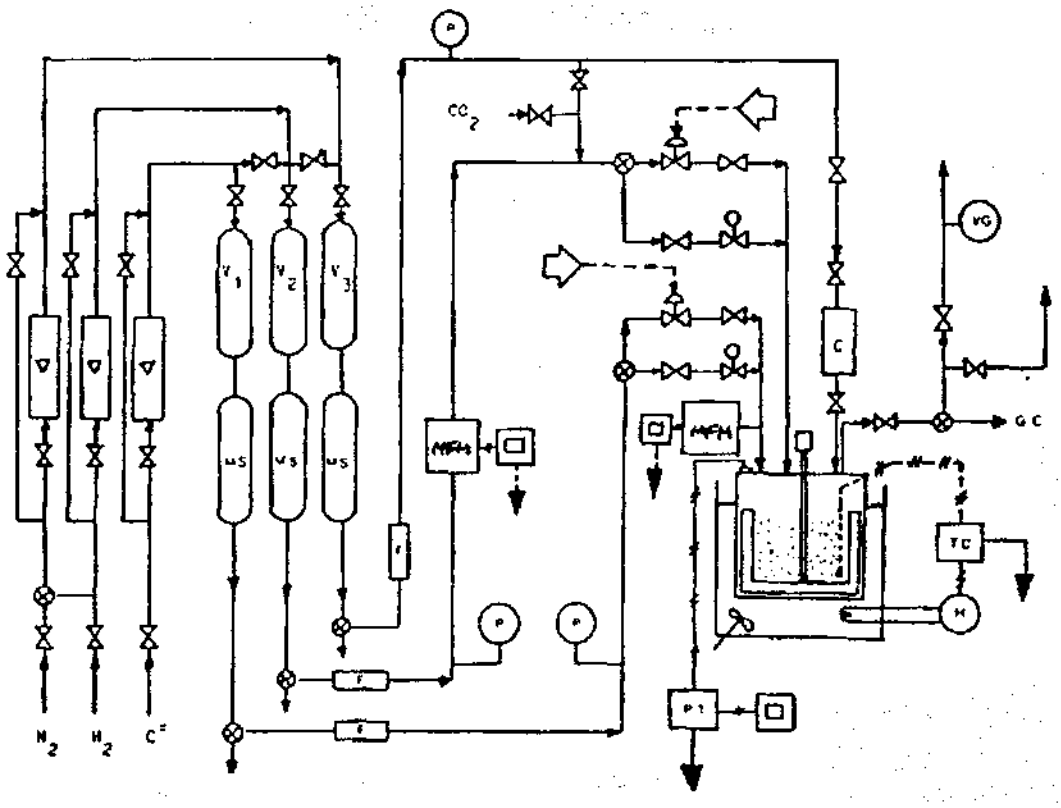

Figure 2-2 Gas Phase Stirred Bed Reactor for Propylene Polymerization Designed by Choi *et al.* (1985) (C = catalyst injection bomb; F = inline filter; H = heater; MFM = mass flow meter; MS = molecular sieves; V1, V2, V3 = oxygen scavenging columns; VG = vacuum gauge; TC = temperature controller; PT = pressure transducer)

Spitz *et al.* (1988) also designed a gas phase reactor system capable of commercial operating conditions for ethylene polymerization experimentation. The reactor had a volume of 675 cm^3 and was constructed from stainless steel. To avoid the problem of grinding by the stirrer, the unusual approach of having the entire reactor oscillate vertically (6cm stroke, 7Hz) was employed. Not much detail was given regarding the effectiveness of this method of stirring which is important given the tendency of growing polymer particles to agglomerate.

Weist *et al.* (1989) used a 20 mm diameter fluidized bed reactor to study polymer morphology developments at the initial stages of polymerization. The reactor performance was however not described.

In 1991, Lynch and Wanke designed a well instrumented semi-batch reactor for studying the gas-phase polymerization of ethylene using heterogeneous Ziegler-Natta type catalysts. The reactor could be operated over the entire range of temperatures and pressures used in the commercial production of linear low and high density polyethylene. The reactor vessel was cylindrical in shape and was constructed from 316 stainless steel with a wall thickness of 1.3 cm, an inside diameter of 11.4 cm and a depth of 10.2 cm. The internal volume was approximately 1 L. Stirring of the reactor contents was achieved by using an Autoclave Engineers Ltd. Model

1.5-1-5K Magnedrive stirrer driven by a variable speed DC motor. Variable angle paddle-type stirring vanes were attached to the stirrer shaft. The optimal locations of the stirring vanes were determined by using a reactor bottom section constructed from Lexan with dimensions and thermocouple positions identical to the steel bottom. The state of mixing with various amounts of polyethylene resin in the Lexan vessel was examined and the final locations of the stirrer vanes thus determined. In order to promote mixing the vanes at the bottom were angled upwards and the vanes at the top were angled downwards. A schematic of the reactor system is shown in Figure 2-3.

To improve reactor mixing and heat transfer, Dusseault (1991) designed an 800 cm^3 horizontal cylindrical stirred reactor with both internal cooling coil and external cooling/heating jacket. The agitator was designed in such a way that the entire polymer bed could be turned over.

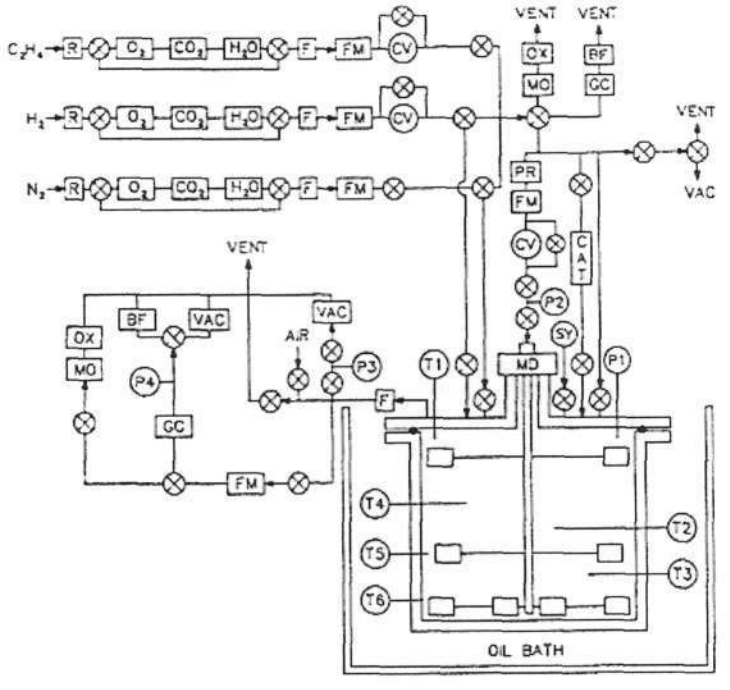

Figure 2-3 Schematic of the Gas Phase Ethylene Polymerization Reactor System Design by Lynch and Wanke (1991) (BF = bubble flow meter; CAT = injection port for solid catalyst; CV = control valve for flow controller; F = filter; FM = flow transducer; GC = gas chromatograph; MD = magnetically coupled stirrer; MO = moisture analyzer; $O_2/CO_2/H_2O$ = gas purifiers; OIL BATH = constant temperature oil bath; OX = oxygen analyzer; P1-4 = pressure gauges; PR = pressure regulator; R = gas cylinder regulator; T1-6 = thermocouples; SY = syringe injection port for liquid co-catalyst VAC = vacuum pump)

Han-Adebekun *et al.* (1997a, b, c), for their gas phase polymerization kinetic investigation, used a 1 L stainless steel stirred bed reactor which was manufactured by Parr Instrument Co. (Figure 2-4). The reactor system was originally designed by Choi and Ray (1985) as a vertical reactor for propylene polymerization studies using unsupported catalysts. Thereafter the reactor was modified by Chen for ethylene/propylene copolymerization studies with feedback control of

temperature, pressure, and composition using online gas chromatography (GC). Chen found that horizontal operation provided better particle agitation and improved reactor heat transfer. The reactor was then further modified to incorporate a liquid feeding system, rapid response monomer composition control using on-line Fourier transform infrared spectrometry (FTIR), and hydrogen partial pressure control using on-line thermal conductivity. This final system, operated in a horizontal position with a U-shape stirrer, was that used by Han-Adebekun and co-workers in their investigations.

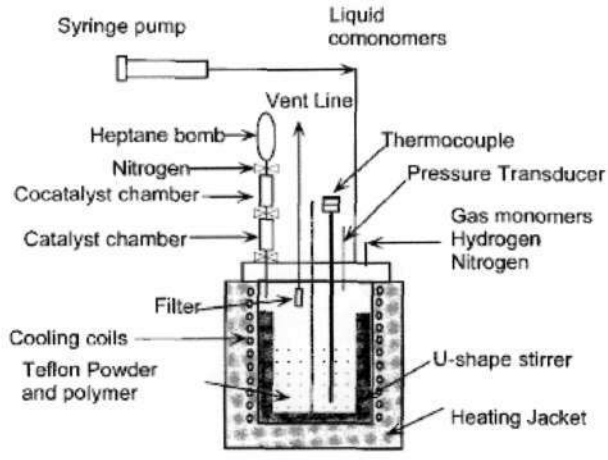

Figure 2-4 The Stirred Bed Reactor used by Han-Adebekun *et al.* (1997, a, b, c)

In investigating gas phase ethylene polymerization kinetics, Kissin *et al.* (1999) carried out experiments in a 500 cm^3 stainless steel reactor equipped with a manometer, a magnetic drive stirrer (anchor stirrer), and an external heating jacket.

Samson *et al.* (1999) used a jacketed, 1 L glass reactor (Buchi) for reaction pressures of up to 12 bar. The glass reactor enabled the operator to visually observe the mixing rate. The agitator consisted of two stirrers mounted on the same shaft (Figure 2-6). The upper stirrer consisted of four vertical blades. To prevent powder from sticking to the walls and to improve heat transfer to the reactor jacket, two blades have a clearance of 1 mm from the reactor wall, while the other two blades are placed closer to the stirrer shaft to provide mixing in the centre. To further improve mixing, the horizontal bars supporting the blades are shaped like propellers. The lower stirrer is a propeller that has been mounted to stir up the powder from the bottom end of the stirrer shaft, 1 mm above the reactor bottom. The agitator used was heavy and was rotated 1 mm from the glass wall with rotation speeds up to 1500 rpm and as a result an additional bearing had to be constructed to balance the stirrer and to prevent it from touching the reactor wall.

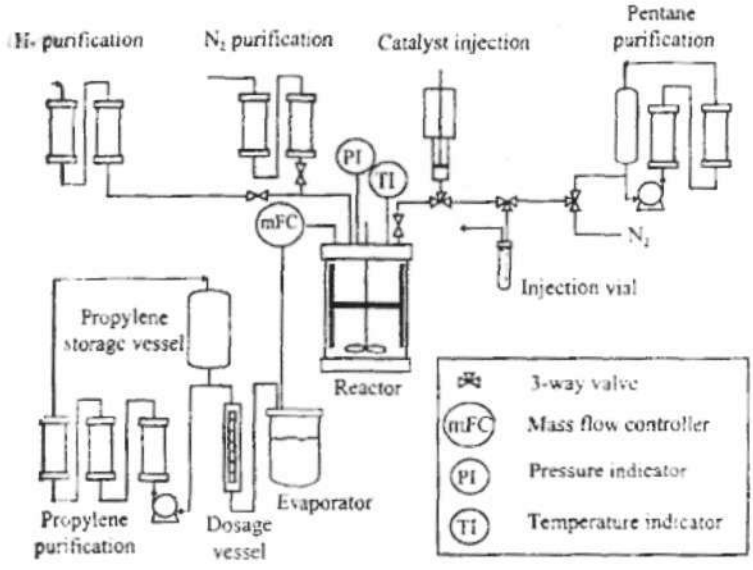

Figure 2-5 Experimental Setup for Gas-Phase Polymerizations designed by Samson *et al.* (1999)

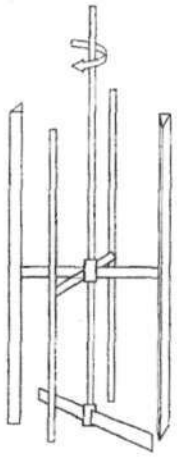

Figure 2-6 Agitator used in the Experimental Setup shown in Figure 2-5

Mannan *et al.* (2004) made improvements to the reactor constructed by Lynch and Wanke (1991) as they felt that it was inadequate in controlling the reaction temperature when high activity catalysts were used. A 2 L vessel, constructed from 316 stainless steel, was attached to a flange that contained all the ports for feeding reactants, catalysts and co-catalysts into the reactor. A magnetically driven stirrer (Autoclave Engineers Magnedrives) was used for stirring of the reactor contents. They tested various types of stirrers by replacing the stainless steel reactor with a Plexiglass replica to visually observe the degree of solids agitation obtained with the various stirrers and at different stirrer speeds. The optimal stirrer configuration consisted of a pitched anchor-type stirrer attached to the bottom of the stirrer shaft and two variable-angle paddle-type stirring vanes attached towards the top of the stirrer shaft (Figure 2-9). They achieved good mixing of the solids with this configuration even for stirring speeds above 300 rpm. The reactor system can be seen in Figure 2-7 and Figure 2-8.

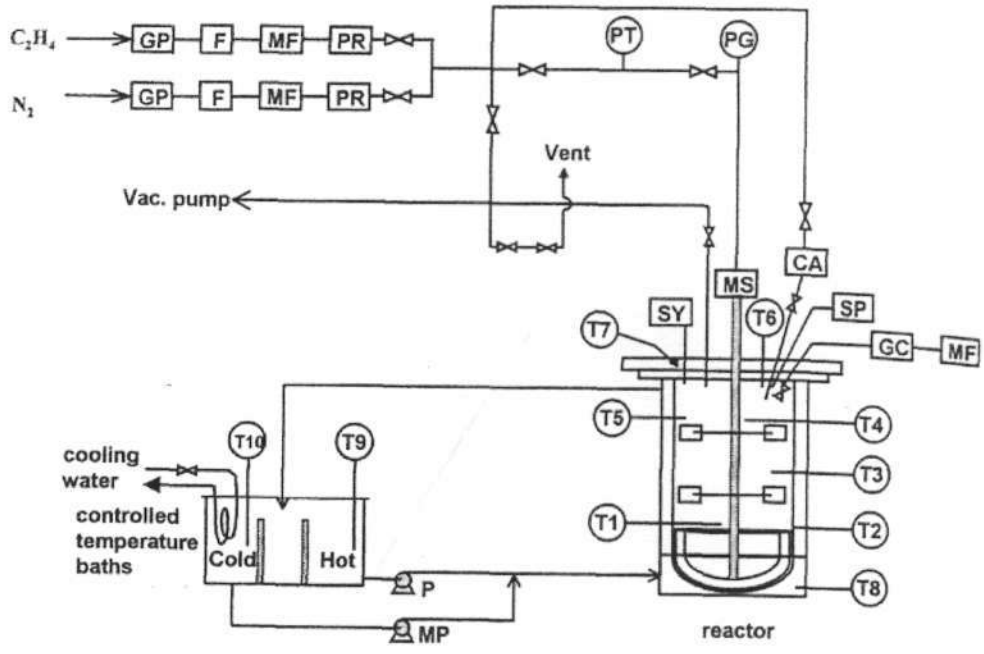

Figure 2-7 Schematic of the Reactor System Designed by Mannan *et al.* (2004) (CA = catalyst injector; GC = gas chromatograph; GP = gas purifiers; F = 7μm filter; MF = mass flow meter; MP = metering pump; MS = MagneDrive stirrer; P = centrifugal pump; PG = pressure gauge; PR = pressure regulator; PT = pressure transducer; SP = syringe pump; SY = syringe injection port; T_i = thermocouples)

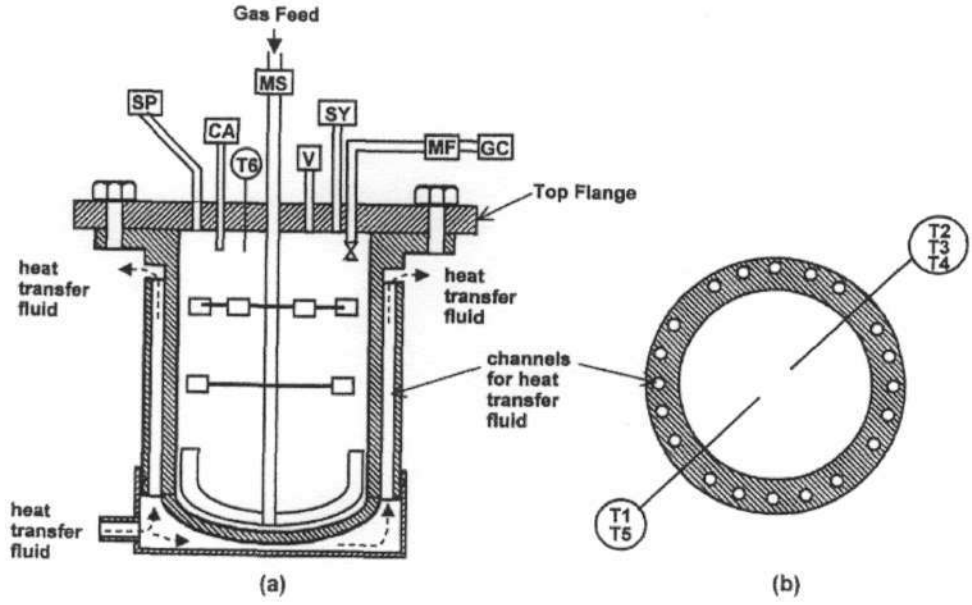

Figure 2-8 Reactor Design: (a) Vertical Cross Section of Reactor; (b) Horizontal Cross-Section of Reactor (Mannan *et al.*, 2004)

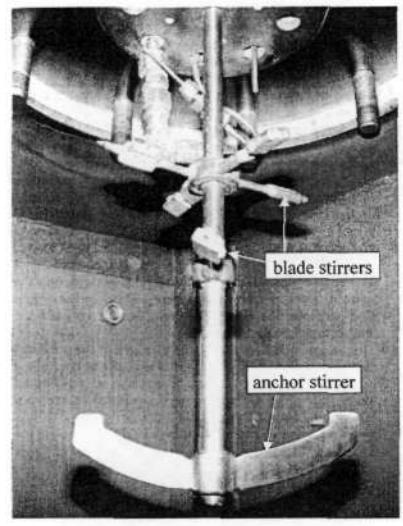

Figure 2-9 Photograph Showing the Pitched Anchor Stirrer, the Blade Stirrers and the Bottom of the Reactor Flange of the Reactor Designed by Mannan *et al.* (2004)

2.3.2 Reactor temperature control

The successful operation of a polymerization reactor depends on careful control of the reaction temperature. The reaction temperature is dependent on the rate of polymerization and if the rate is too large the reaction temperature increases uncontrollably (thermal runaway) until catalyst deactivation occurs when melting polymer encapsulates the catalyst particles (Lynch and Wanke, 1991).

For temperature control Lynch and Wanke (1991) immersed their 1 L reactor into a 26 L bath filled with low viscosity white mineral oil. The temperature of the oil was maintained to within ±0.1°C of the set-point by a Lauda Model MS constant temperature immersion circulator, which, when used in combination with a cooling coil, enabled the bath to be operated between 5 to 120°C. The temperature bath was raised to 3 cm above the top surface of the reactor during operation. The temperature in the reactor was monitored by means of six sheathed, Type J thermocouples situated at various radial and axial locations, shown in Figure 2-3.

According to Xie *et al.* (1994), the reactor temperature control systems shown in Figure 2-10 and designed by Choi *et al.* (1985), Lynch and Wanke (1991) and Dusseault (1991) provide satisfactory temperature control only within a very restricted operating temperature range. With highly active catalysts the initial polymerization rate is very high, making the initial heat difficult to remove with an oil or water bath cooling system. According to Xie, in order to carry out gas phase ethylene polymerization under commercial operating conditions, the reactor must be able to provide fast heat removal to avoid hot spots in the reactor and should be able to provide adequate mixing to disperse the small amounts of catalyst powder.

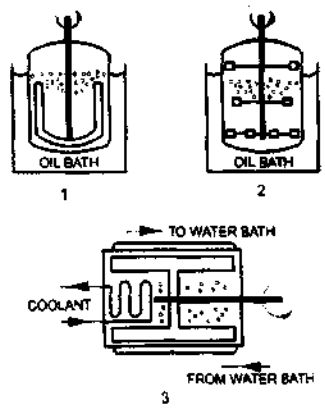

Figure 2-10 Laboratory Reactor Temperature Control (1) Choi *et al.* (1985); (2) Lynch *et al.* (1991); (3) Dusseault (1991), (Xie *et al.*, 1994)

Han Adebekun *et al.* (1997, a, b, c) maintained reactor temperature control by using a combination of heating and cooling; an electrical heating jacket was used to provide a constant heating source while cooling was achieved by both ambient air and external cooling water which was pumped from an isothermal bath through copper coils soldered to the outside of the reactor (Figure 2-11). The reactor temperature was maintained by a balance between the voltage supply to the heating jacket and the temperature set-point for the water bath. They managed to maintain the reaction temperature to within ±0.5°C of the 50°C set point for most of the duration of the reaction. Slightly larger oscillations however existed for the first 30 minutes, during the initial stages of the reaction, where deviations from the set point exceeded 2°C.

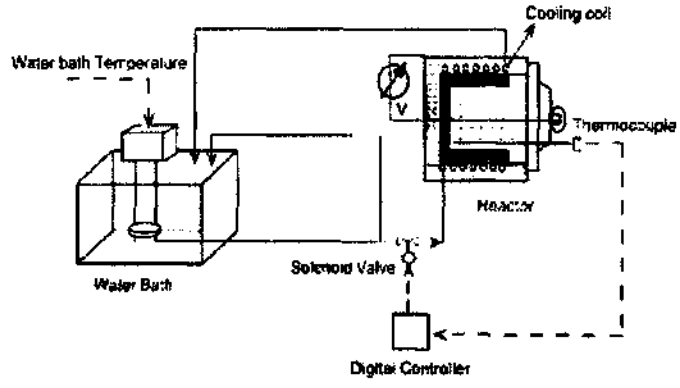

Figure 2-11 The Temperature Control System Used by Han-Adebekun *et al.* (1997)

The temperature control system designed by Samson *et al.* (1998), and used for both their gas and liquid phase experiments, enabled them to maintain temperature control with a maximum overshoot of 0.5 to 1°C in the first few minutes of the reaction. Thereafter the reaction temperature was maintained constant to within 0.1°C. The control system comprised separate control circuits for the reactor cover plate and the reactor jacket. The temperature of the cover plate was always set to a few degrees above the reaction temperature. The control circuit for the reactor jacket comprised cold and hot water streams, a pipe that injected cold water directly

into the inlet pipe of the reactor jacket, and a Eurotherm 900 EPC proportional-integral-derivative (PID) control unit. The separate hot and cold streams were used to heat the reactor in a few minutes from pre-polymerization conditions to higher reaction temperatures.

In more recent work by Lynch, Wanke and co-workers, (Mannan *et al.*, 2004), they described the reactor temperature control system previously designed by them (Lynch and Wanke, 1991) as being inadequate for controlling the gas phase temperature when highly active catalysts were used. They consequently constructed a new reactor system with improved temperature control. For heat transfer to and from the reactor, 20 cylindrical channels, 6.35 mm (1/4 inch) in diameter and 181 mm long, were drilled into the wall of the reactor; the spacing of the channels is shown in Figure 2-8(b). Temperatures at various locations in the reactor were measured by 8 thermocouples (3 mm stainless steel sheathed Type J thermocouples); the locations of these thermocouples are shown in Figure 2-7. Electrical heaters (Omega cartridge heaters; 6.35 mm in diameter and 89 mm long) were imbedded in the top flange and a digital temperature controller was used to control the temperature of the flange at the desired set-point.

The temperature of the reactor was controlled by the flow of silicon oil (Dow Corning 200 Fluid, 50 centistokes) through the channels in the reactor wall. The temperature of the oil entering the channels in the reactor was controlled by mixing hot and cold silicon oil prior to the entry of the oil to the bottom of the reactor. The flow rate of the hot oil was constant at about 4 L/min. The flow rate of the cold oil was varied by the variable speed metering pump (Micropump Inc. Series 2200 magnetic drive gear pump, Model GD-M35 PVSE close-coupled to 0.5 hp, DC TEFC motor with a 4-20 mA remote signal-speed control). The speed of the metering pump was controlled by the PID controller where the output from thermocouple 1 was the input to the PID controller. The flow rate varied from 0, for the runs without PID temperature control, to as high as 8 L/min. The ability to make rapid controlled changes of the heat transfer fluid flowing through the channels in the reactor walls was necessary to control rapid changes in gas-phase temperatures inside the reactor. According to Mannan *et al.* (2004) the response to gas-phase temperature changes is slow for reactors immersed in circulating liquid baths such as that used by Lynch and Wanke (1991). They also claim that the temperature control system designed by them should have a more rapid response to internal temperature changes than that used by Han-Adebekun *et al.* (1997a, b, c) which consisted of cooling coils soldered to the external surface of the reactor.

2.3.3 Catalyst injection methods for gas phase polymerization

Due to the extreme sensitivity of Ziegler-Natta catalysts to air and moisture in the atmosphere, special methods have had to be devised for their introduction into the reactor. Also, due to the high reactivity of the catalysts, only a small amount (usually in the order of milligrams) is required for laboratory scale polymerization experiments using 0.5-1.0 L reactors (Xie *et al.*, 1994). Inert particles are therefore usually added into the reactor to assist with the initial dispersion and mixing of the catalyst.

For good dispersion of the small quantities of catalyst in the reactor Doi *et al.* (1982) used approximately 4 cm^3 of glass beads (0.5 cm diameter). Keii (1972) and Dusseault (1991) also used glass beads. Spitz *et al.* (1988) used salt (KCl) or polyethylene powder to assist with dispersion. Choi *et al.* (1985) introduced a small volume of ~1 mm glass beads to the reactor prior to the injection of the catalyst mixture. Lynch and Wanke (1991) used 450 µm of Teflon powder. Kissin *et al.* (1999) used large diameter HDPE particulate resin (25 g) as seedbed material. The resin was pre-treated in three steps: (1) heating at 95°C in a nitrogen flow for 60 minutes, (2) vacuuming at 30-40°C for 60 minutes, and (3) pressurizing the reactor with ethylene and treatment with 1.5-3.0 mmol $AlEt^3$.

In reactions conducted by Han-Adebekun *et al.* (1997, a, b, c) approximately 160 g of Teflon resin (Grade 9B, E.I. Du Pont, average particle diameter = 650 µm) was used as seed bed material. The amount of bed material was selected to insure that good heat conduction through the reactor wall was obtained as well as to guarantee that the dense phase temperature could be measured with a thermocouple.

Samson *et al.* (1999) claimed that without a support bed the injected catalyst easily sticks to reactor walls resulting in bad reproducibility and low activity. They therefore used a certain amount of inert particles to prevent catalyst particles from sticking to each other and to the walls of the reactor. They tested polypropylene powder as support bed material but found that the yields obtained were too low. They concluded that this was probably due to the impurities in the porous polypropylene particles of the support bed which were too many and too difficult to scavenge in the cleaning procedure. They found that a further problem was the separation of the polypropylene support bed and the polymer produced. A support bed of dried NaCl crystals was therefore used. The crystals were non porous and were easily dried in a vacuum oven at temperatures above 100°C. At the end of the reaction the polymer product produced was separated from the support bed by simply washing with water.

Xie *et al.* (1994) claimed that glass beads may grind the catalyst during the initial stage of polymerization and that because salt is sensitive to moisture, elaborate drying procedures are required. They also claimed that although polyethylene powder is effective for initial mixing, it is not good for polymer property analysis because newly produced polymer can not be separated from the initial polymer powder. They do however state that polyethylene powder may be useful for polymerization rate measurements where separation from the seedbed is not required.

Besides the various types of support beds used there are also variations in the methods of catalyst injection into the reactor. Doi *et al.* (1982) introduced the catalyst (0.1-0.5 g) and 1.0 cm^3 of $Al(C_2H_5)_3$ in a heptane slurry into their reactor. The solution was mixed for 1 minute at the polymerization temperature under a nitrogen atmosphere and then the catalyst mixture was dried under vacuum for 4 minutes to remove heptane.

For propylene polymerization, Choi *et al.* (1985) also injected the catalyst ($TiCl_3$.1/3.$AlCl_3$ and DEAC) as a mixture in a small amount of n-heptane. The reactor was thereafter evacuated for approximately 1 hour before the monomer feed was started. The same system was later used by Yoon and Ray (1987) in their investigations of propylene polymerization kinetics. They described the catalyst injection system to consist of two bombs in series (Figure 2-2). The first contained a pre-weighed quantity of catalyst and co-catalyst while the second contained 10 mL of purified heptane to wash the residual catalyst contained in the first bomb into the reactor. Complete removal of heptane from the reactor was achieved by evacuating the reactor at reaction temperature for 15 minutes.

According to Lynch and Wanke (1991), the catalyst injection method employed by Choi *et al.* (1985) has two potential problems. Firstly, pre-mixing the catalyst and co-catalyst prior to injection into the reactor could result in catalyst deactivation due to over-reduction of the catalyst, particularly for co-catalysts such as TEA. Secondly, pre-mixing of the catalyst and co-catalyst in n-heptane requires the subsequent evacuation of the reactor to remove the n-heptane to prevent the possibility of a small slurry mixture in the reactor. This evacuation removes some of the co-catalyst and it is therefore not possible to accurately determine the ratio of the co-catalyst to catalyst (Al/Ti molar ratio) under reaction conditions.

The catalyst injection system devised by Lynch and Wanke (1991) for their kinetic investigations of gas phase polymerisation using Ziegler-Natta catalysts can be seen in Figure 2-3, labelled CAT. The catalyst holder was constructed from a stainless steel quick connect (Swagelok QF series) with plug valves (Nupro SS-4P4T) attached on either end. The quick connect and the plug valves have essentially no internal constrictions permitting a free flow of sample through the holder. Catalyst samples (typically 0.05 to 0.3 g ± 0.0001 g) were placed in to the male half of the quick-connect with approximately 0.1 g of Teflon powder (450 μm particle size) placed on either side of the catalyst sample. When the female half of the quick connect was attached with the plug valves closed, the sample holder (which was filled in a glove box) could be removed from the glove box and connected to the top flange of the reactor without contaminating the catalyst. The liquid co-catalyst used was diethylaluminium chloride (DEAC) and was injected into the reactor vessel through a septum port connected to the top flange of the reactor (SY in Figure 2-3). Catalyst introduction into the reactor was achieved by having a nitrogen or hydrogen pressure on the upstream side of the catalyst holder which was higher than the pressure in the reactor. The catalyst sample was pushed into the reactor by quickly opening and closing the valves on either side of the holder.

The catalyst injection system used by Han-Adebekun *et al.* (1997, a, b, c) can be seen in Figure 2-4. The system is designed to allow for the control of the pre-contact between the catalyst and the co-catalyst for the Ziegler-Natta catalyst. The three-chamber design makes it possible to control both the ageing time as well as the co-catalyst to catalyst ratio. The diluent (heptane or hexane) wash is required in order to further rinse out any possible catalyst residue.

Samson *et al.* (1998, 1999) used the same method of catalyst injection for both their gas and liquid phase experiments. The injection system, which safeguards inert conditions during catalyst injection into the reactor, is shown in Figure 2-12. The catalyst components were prepared and weighted in a 20 mL vial in an inert atmosphere. The vial was then sealed with a rubber septum and connected to the reactor by two sharpened capillaries which were continuously flushed with nitrogen to avoid contamination. The three way valve above the vial was then opened to add a few millilitres of pentane through one of the capillaries to the vial. Thereafter the catalyst was suspended in the pentane and the content was sucked into the injector by the continuous shaking action of the vial. The contents were then injected into the reactor. The injection procedure was repeated several times with fresh pentane to flush the vial and lines to the reactor to avoid catalyst losses.

According to Samson *et al.*, this injection method is effective for high activity catalysts because suspension of the catalyst in an inert hydrocarbon enhances de-agglomeration, minimizes the effective size of the catalyst particles, and helps to avoid the thermal runaway of particles. One drawback, however, is the introduction of liquid. Although the amount of liquid introduced into the reactor is relatively small (10 to 15 mL), it has to be removed so that the reactor can contain only pure gas phase monomer around the particles. If the liquid is left in the reactor, the result is a concentrated slurry reaction rather than a gas phase reaction, at least in the first stage of the reaction. Further on in the reaction, the liquid may become completely absorbed in the formed polymer, but even then it will influence the concentration of the polymer. It is therefore essential that the liquid be removed from the reactor. Samson *et al.* have used relatively volatile pentane and removed it by evaporation through repeated pressurization and venting with the monomer. Depending on the reactor temperature, two to five cycles of pressurization to 10 bars and subsequent venting to atmospheric pressure proved to be more than sufficient to evaporate all the liquid from the reactor. Evaporation could be completed in 5 minutes, as each of the pressurizing and venting cycles took about a minute. They assumed the losses of co-catalyst (TEA) and electron donor by entrainment with the evaporating liquid to be negligible due to the boiling points of those components being above 200°C.

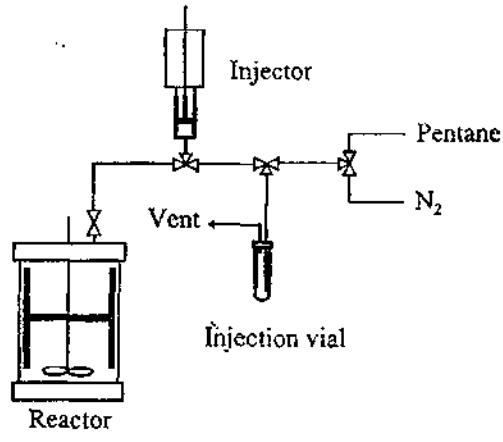

Figure 2-12 Catalyst Injection System Designed by Samson *et al.* (1999)

2.4 Ziegler-Natta polymerization

2.4.1 Mechanisms and reactions for Ziegler-Natta polymerization

The chemical reactions for ethylene polymerization can be envisioned as occurring at the interface between the solid catalyst and the polymer matrix, where the active centres are located. From gas-state monomer to solid-state polymer, ethylene experiences a dramatic physiochemical transition within a very short time. Although extensive research efforts have been focused on Ziegler-Natta catalyst systems since their discovery in the early 1950s, no definitive, unequivocal chemical reaction mechanisms have been developed to fully describe the kinetic behaviour of ethylene homo/co-polymerization. Nevertheless, the key elementary reactions have been established, which include formation of active centres, insertion of monomer into the growing polymer chains, chain transfer reactions, and catalyst deactivation. Most of the proposed mechanisms are based on information about polymerization rate, molecular weight and its distribution, polymer chain microstructure, and active centre concentrations.

Among the proposed polymerization mechanisms, the one proposed by Cossee (1964) seems to be the best representation of what is happening at the active centre (Figure 2-13). The titanium atom is in an octahedral coordination environment with one site vacant and an adjacent coordination site bonded to an alkyl group (polymer chain). For supported catalysts this structure is created when bound $TiCl_4$ reacts with aluminium alkyls (TEA).

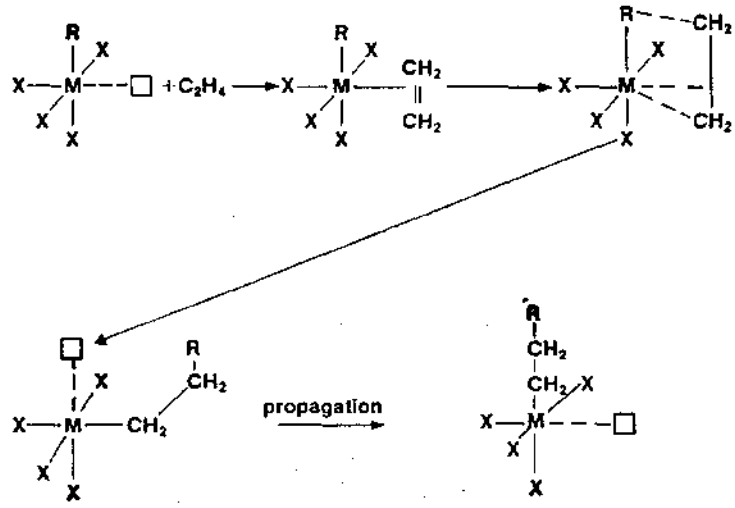

Figure 2-13 Cossee Mechanism (Cossee, 1964)

The two-step mechanism for propagation involves π-coordination of an incoming monomer by the titanium atom at its vacant coordination site, followed by insertion, via a four-centre transition state, into the titanium-alkyl (polymer) bond. It should be noted that for stereospecific polymerization, the growing polymer chain must migrate back to its original

position after each insertion in order to maintain sterically identical propagation steps. The weakness of this mechanism is that the active Ti^{3+} has only one outer shell available for the formation of π back-bonding, which is a requirement for metal-olefin π-bond formation (Cossee, 1964). However, Burfied (1984) has documented analogous examples of metal-olefin π-bond formation which supports the existence of such a species.

Ystenses (1991) examined the Cossee mechanism and proposed the so-called "triggering" mechanism to account for weaknesses such as the required polymer–Ti bond migration step (to maintain stereoregularity) and strained coordination geometry (due to the presence of the vacant coordination site). He hypothesized that insertion of π-coordinated monomer is initiated by incoming monomer. The active site is coordinatively saturated, i.e., the vacancy of the Cossee mechanism is always occupied by monomer (or Lewis base). Monomer is unable to insert without the aid of a second (incoming) monomer. In other words, monomer is an integral part of the active site as it is required for active site formation.

Which part of the two-step mechanism is the slowest has been widely discussed. Cossee (1964) and Pino and Mulhaupt (1985) suggested that monomer insertion is rate controlling because of a greater activation energy. The suggestion was supported by Keii *et al.* (1982) based on their analysis of the structure of the transition state. According to Dusseault and Hsu (1993), the experimental data (a linear relationship between activity and [M]) presented by Keii suggest olefin coordination as rate determining. Monomer insertion as the rate controlling step predicts a lowering of reaction order with respect to concentration of monomer, while π-coordination control would have strictly first-order kinetics. Dusseault and Hsu suggest that the contradiction in the data presented by Keii might have been due to too narrow a range of concentrations tested.

Support for π-complex formation as rate determining comes from Zakharov *et al.* (1976) and is based on kinetic data and quantum mechanical calculations. A review of experimental data by Kissin (1985) led him to conclude that coordination is rate controlling and that only at low temperatures does insertion become rate determining. This was confirmed by Burfield (1984). However, at higher temperatures Burfield was noncommittal, stating that both steps may take on a role in determining the overall rate.

By 1978, the inhibition of polymerization by and dependence of polymer properties on a co-catalyst and hydrogen for the Ziegler-Natta catalyst were known, and attempts at developing reaction schemes that defined the elementary reactions had already been made (Natta, 1959). Bohm (1978a) attempted to revise these early reaction schemes for the third generation supported catalysts by assuming that polymerization was preceded by the formation of a complex between the catalyst and co-catalyst. With Cossee's mechanism in mind, Bohm (1978a) proposed perhaps the most comprehensive elementary reactions involved in the ethylene polymerization process (Figure 2-14).

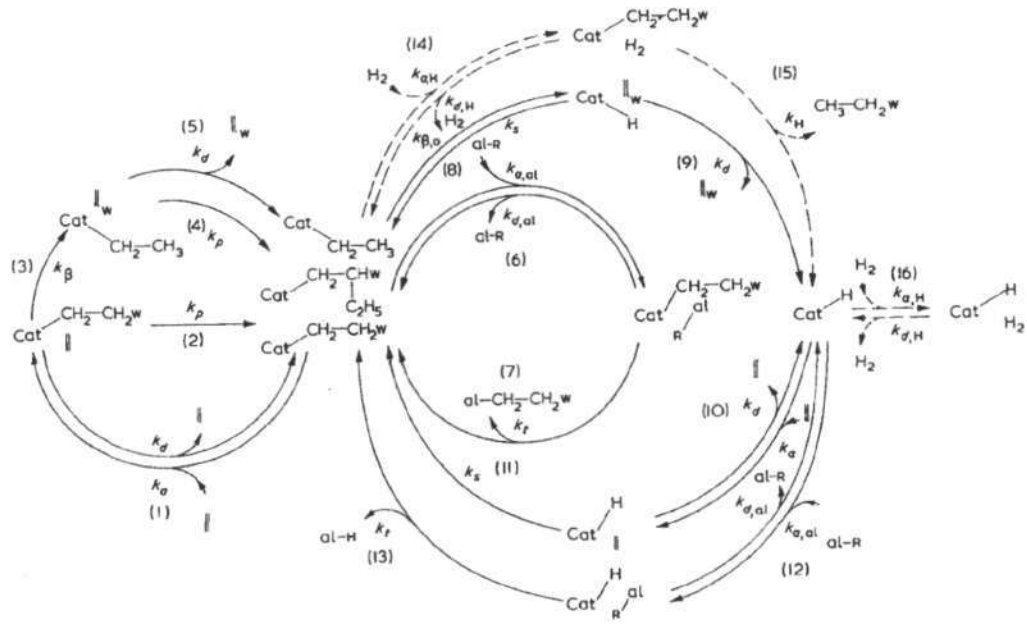

Figure 2-14 Reaction Scheme of a Ziegler-Natta Polymerization Process (Cat, catalytic active centre; || ethylene molecule; w, polymer chain; $||^{w}$, polymer chain with a vinyl group. al. 1/3 Al; R, alkyl group (for example C_2H_5); H, H_2, hydrogen atom or hydrogen molecule)

Since the commercial production of LLDPE and HDPE consists of a copolymerization process, copolymerization mechanisms are required to understand kinetic behaviour and polymer properties. Bohm's reaction model has therefore been modified and extended to ethylene copolymerization processes in recent modelling studies (Villermaux *et al.*, 1989; de Carvalho *et al.*, 1990; McAuley *et al.*, 1990; Lorenzini *et al.*, 1991; Hutchinson *et al.*, 1992). Furthermore, to illustrate multimodal distribution of polymer chain composition and broad molecular weight distribution, the multiple active centre concept has been adopted in recent modelling studies (Rawatlal, 2004). A comprehensive chemical reaction mechanism should therefore not only include reactions proposed by Bohm (1978) but also reactions involving multi-components at different active centres.

Whether each type of active centre has the same or different reaction mechanisms is still uncertain (multiple centre formation itself has not been proven fundamentally). If one assumes that all the active centres perform the same reaction mechanisms, but with different reaction rates for each elementary reaction, then elementary reactions which are commonly adopted in modelling studies can be summarized as in Table 2-3 (Xie *et al.*, 1994), where C_p is the catalyst potential active centre; P^*_0 is the active centre without polymer chain; $P^*_{m,n,i}$ is the active centre with *m* units of monomer 1 and *n* units of monomer 2, with the third subscript *i* denoting the chain terminal monomer type bonded to the active centre; $q'_{m,n}$ is a dead polymer chain with a terminal double bond; and $q_{m,n}$ is a dead polymer chain without a terminal double bond. For simplification of notation, no subscript is shown corresponding to the type of active centre. The reactions shown in Table 2-3 should be considered to occur at each type of active centre and are summarized based on Ti-based catalysts.

Table 2-3 Summary of Elementary Reactions for Ethylene and α-Olefin Copolymerization (Xie *et al.*, 2004)

Reaction	Rate Constant	Description
Activation		
$C_p \rightarrow P^*_0$	K_{as}	spontaneous activation
$C_p + [A] \rightarrow P^*_0$	K_{aA}	activation by aluminium alkyl (A)
$C_p + [E] \rightarrow P^*_0$	K_{aE}	activation by electron donor (E)
$C_p + [H_2] \rightarrow P^*_0$	K_{aH}	activation by hydrogen (H_2)
$C_p + [M_1] \rightarrow P^*_0 + [M_1]$	K_{aM1}	activation by monomer 1 (M_1)
$C_p + [M_2] \rightarrow P^*_0 + [M_2]$	K_{aM2}	activation by monomer 2 (M_2)
Initiation		
$P^*_0 + [M_1] \rightarrow P^*_{1,0,1}$	K_{i1}	initiation of M_1 by normal active centre
$P^*_0 + [M_2] \rightarrow P^*_{1,0,2}$	K_{i2}	initiation of M_2 by normal active centre
$P^*_{H,0} + [M_1] \rightarrow P^*_{1,0,1}$	K_{iH1}	initiation of M_1 by active centre with H
$P^*_{H,0} + [M_2] \rightarrow P^*_{1,0,2}$	K_{iH2}	initiation of M_2 by active centre with H
$P^*_{A,0} + [M_1] \rightarrow P^*_{1,0,1}$	K_{iA1}	initiation of M_1 by active centre with A
$P^*_{A,0} + [M_2] \rightarrow P^*_{1,0,2}$	K_{iA2}	initiation of M_2 by active centre with A
$P^*_{E,0} + [M_1] \rightarrow P^*_{1,0,1}$	K_{iE1}	initiation of M_1 by active centre with E
$P^*_{E,0} + [M_2] \rightarrow P^*_{1,0,2}$	K_{iE2}	initiation of M_2 by active centre with E
Propagation		
$P^*_{m,n,1} + [M_1] \rightarrow P^*_{m+1,n+1}$	K_{p11}	propagation of chain type 1 with M_1
$P^*_{m,n,1} + [M_2] \rightarrow P^*_{m,n+1,2}$	K_{p12}	propagation of chain type 1 with M_2
$P^*_{m,n,2} + [M_1] \rightarrow P^*_{m+1,n,2}$	K_{p21}	propagation of chain type 2 with M_1
$P^*_{m,n,2} + [M_2] \rightarrow P^*_{m,n+1,2}$	K_{p22}	propagation of chain type 2 with M_2
Chain transfer		
$P^*_{m,n,i} \rightarrow P^*_0 + q'_{m,n}$	K_{fspi}	spontaneous chain transfer or β-elimination
$P^*_{m,n,i} + [H_2] \rightarrow P^*_{H,0} + q'_{m,n}$	K_{fHi}	chain transfer to hydrogen (H_2)
$P^*_{m,n,i} + [A] \rightarrow P^*_{A,0} + q'_{m,n}$	K_{fAi}	chain transfer to aluminium alkyl (A)
$P^*_{m,n,i} + [E] \rightarrow P^*_{E,0} + q'_{m,n}$	K_{fEi}	chain transfer to electron donor (E)
$P^*_{m,n,i} + [M_1] \rightarrow P^*_{1,0,1} + q'_{m,n}$	K_{fM1i}	chain transfer to M_1
$P^*_{m,n,i} + [M_2] \rightarrow P^*_{1,0,2} + q'_{m,n}$	K_{fM2i}	chain transfer to M_2
Deactivation		
$P^*_{m,n,i} \rightarrow C_d + q_{m,n}$	K_{dspi}	spontaneous deactivation
$P^*_{m,n,i} + [Z] \rightarrow C_d + q_{m,n}$	K_{dZi}	deactivation by impurities or poison (Z)
$P^*_{m,n,i} + [A] \rightarrow C_d + q_{m,n}$	K_{dAi}	deactivation by aluminium alkyl (A)
$P^*_{m,n,i} + [E] \rightarrow C_d + q_{m,n}$	K_{dEi}	deactivation by electron donor (E)
$P^*_{m,n,i} + [H_2] \rightarrow C_d + q_{m,n}$	K_{dHi}	deactivation by hydrogen (H_2)
$P^*_{m,n,i} + [M_j] \rightarrow C_d + q_{m,n}$	K_{dMij}	deactivation by monomers
Other reactions		
$P^*_{1,0,1} + q'_{r,s} \rightarrow P^*_{r+1,s,1}$	K^*_{p1}	formation of short chain branches
$P^*_{1,0,2} + q'_{r,s} \rightarrow P^*_{r,s+1,2}$	K^*_{p2}	formation of short chain branches
$P^*_{m,n,1} + q'_{r,s} \rightarrow P^*_{m+r,n+s,1}$	K^*_{p1}	formation of long-chain branches (rare)
$P^*_{m,n,2} + q'_{r,s} \rightarrow P^*_{m+r,n+s,2}$	K^*_{p2}	formation of long-chain branches (rare)

Hutchinson *et al.* (1992) considered transformation reactions, which are assumed to form different active centres. If an active centre formed by transformation in independent of the

original polymer chain, then the effect of a transformation reaction is on the initiation reactions which have been shown in Table 2-3. If an active centre formed by transformation depends on the original polymer chain produced by this centre, then the formation of each active centre must be treated individually. The detailed mechanisms of transformation reactions have however not been given by Hutchinson. Formation of short-chain branches was proposed by Bohm (1978). It was assumed that a polymer chain with a terminal double bond will participate in propagation at an active centre with one monomer unit. Formation of long-chain branching is unlikely for Ziegler-Natta polymerization systems.

2.4.2 Catalyst and co-catalyst interaction

In order for the $MgCl_2$-supported catalyst to be active for polymerization, it has to be contacted with a trialkylaluminium such as triethylaluminium (TEA) or triisobutylaluminium (TIBA). TEA is most commonly used. It is well known that in conventional catalyst systems a chemical interaction between the catalyst and the metal-alkyl takes place which essentially leads to a variation of the transition metal oxidation state. This is likewise true with the $MgCl_2$ catalysts; however, in this case there are many possible reactions, given the greater complexity of the system. The activating action of the aluminium alkyl is twofold. First, it reduces Ti^{4+} to Ti^{3+} and secondly it alkylates the Ti^{3+}. The process is shown in Figure 2-15. The reverse activation mechanism (i.e. alkylation followed by reduction) has been suggested by Nirisen *et al.* (1986). Differentiating between the two is difficult; however most researchers prefer reduction followed by alkylation.

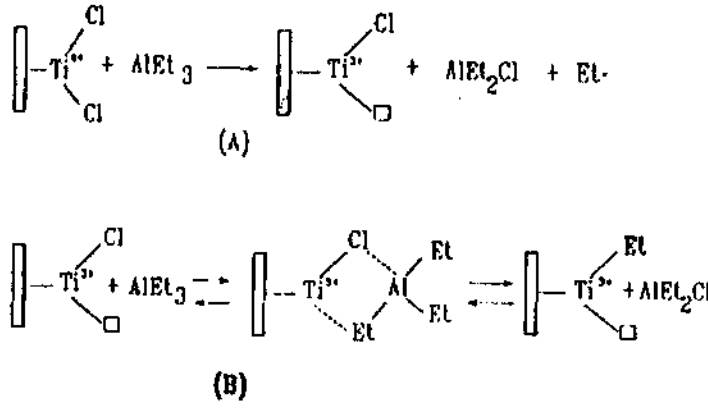

Figure 2-15 Activation Process: (A) Reduction of $TiCl_4$ as proposed by Kashiwa and Yoshitake (1984), and (B) Alkylation Reaction proposed by Chien *et al.* (1985)

Typically the alkyl aluminium is used in excess of a stoichiometric ratio with respect to the molar concentration of active titanium centres. Uses of excess TEA had led to the suggestion that, in addition to the activation processes, aluminium alkyl acts as a scavenger of impurities or forms a complex with monomer required for polymerization.

In the case of supported catalysts, Baulin *et al.* (1980) observed that, when using $AlEt_3$ under conditions similar to that of the polymerization (T = 70°C, Al/Ti = 150–200), more that 90% of the Ti^{4+} was reduced (85% Ti^{3+} and 15% to Ti^{2+}). He was, however, not able to find any quantitative correlation between the degree of Ti reduction and catalytic activity, even though the latter is clearly decreased by pre-contact between catalyst and aluminium alkyl.

An even stronger reduction (80% Ti^{2+} and 20% Ti^{3+}) has been reported by Kashiwa and Yoshitake (1984) for a $TiCl_4$/EB/$MgCl_2$ catalyst after a two-hour reaction with $AlEt_3$ (Al/Ti = 50) at 60°C. They observed that the catalyst obtained was only slightly active for the polymerization of ethylene and completely inactive for propylene polymerization. They concluded that a direct relationship existed between activity and the Ti oxidation state.

With a similar catalyst, but containing the Ti in different oxidation states from the beginning (45% Ti^{4+}, 42% Ti^{3+} and 12% Ti^{2+}), Chien and Wu (1982) observed that after treatment with a 3:1 TEA and MPT (methyl-para-toluate) mixture for 10 minutes at 50°C and Al/Ti = 20, approximately 90% of the initial Ti^{4+} had been reduced to Ti^{3+} (85%) and Ti^{2+} (15%). Similar values have also been reported by Zakharov *et al.* (1984) for $TiCl_4$/$MgCl_2$ catalysts treated with TEA at T≤ 20°C and Al/Ti ≤ 20.

Fregonese *et al.* (2001) found that Ti^{4+} fixed on a $MgCl_2$ support undergoes extensive reduction, even to Ti^{2+} when the catalyst is activated in a large excess of co-catalyst or by increasing the activation temperature (Table 2-4).

Table 2-4 Activation Temperature Effect on both Oxidation State Distribution and Activity (Fregonese *et al.*, 2001)

T (°C)	Ti (IV)%	Ti(III)%	Ti(II)%	Activity (kg PE/gTi h)
20	60	13	27	29
40	**36**	32	**32**	**n.d.**
55	**18**	44	**38**	**n.d.**
70	**10**	34	**56**	34

Polymerization conditions: Al/Ti = 50; P = 2 atm; aging time = 2 hours

Although referred to different catalysts and reaction conditions, these results clearly show that, under polymerization conditions, a considerable reduction of the oxidation state of Ti, even to Ti^{2+} under the most severe conditions, must be taken into account.

Bohm (1978b) monitored the monomer consumption rate for suspension polymerization of ethylene and estimated instantaneous rates of polymerization, reporting that the catalyst activity depended on the co-catalyst/catalyst ratio. He attributed the high activity of the catalyst to a large number of active sites, which he found to be an order of magnitude greater

than previous generations of catalysts. He concluded that the polymerization rate was not hindered by pore diffusion or extra-particle mass transfer resistance.

Soga *et al.* (1981) investigated ethylene/propylene co-polymerization in the presence and absence of TEA. They found that the polymer product characteristics changed considerably depending on whether TEA was used. In addition, it was observed that polypropylene incorporation decreased with increasing TEA whilst ethylene incorporation slightly increased. Since TEA promotes reduction of the titanium sites to the lower oxidation states, these observations supported their earlier conclusions (Soga *et al.*, 1980) that propylene polymerizes on Ti^{3+} whereas ethylene polymerizes on both Ti^{3+} and Ti^{2+}. In a later study by Soga *et al.* (1982), additional olefins (1-hexene, 1,3-butadiene) were considered, and a correlation between catalyst activity and titanium oxidation state was established. It was found that Ti^{3+} was active for all α-olefins whereas Ti^{2+} was active only for ethylene. No reason for the exceptional behaviour of ethylene was proposed.

Keii *et al.* (1982) studied the effect of TEA on catalyst behaviour for slurry polymerization of propylene and concluded that Langmuir-Hinshelwood kinetics governed catalyst behaviour. They used a CO inhibition technique to estimate the number of active centres. The method involved exposure to a solution containing CO, which tended to suppress certain oxidation states of titanium. An important conclusion was that there appeared to be two kinds of sites, one that promoted isotactic growth and another that encourage atactic growth. They further reported that the activity decay was observed to be second order, and understood this to be a result of reduction by TEA.

In the early 1980s, there were two theories for the observed catalyst activity decay. The first postulated that deactivation was a result of the oxidation state change mentioned above. The second hypothesis was that due to the continuous accumulation of polymer around the catalytically active metal sites, monomer mass transfer resistance increased, resulting in the observed decay. *Doi et al.* (1982) applied the CO inhibition technique in kinetic studies conducted in gas phase polymerization and reported that, for gas phase polymerization of propylene, activity increased rapidly followed by slow deactivation. They postulated that the polymerization rate depended on the titanium content as well as the catalyst surface area. The deactivation rate was found to be second order with respect to monomer concentration which they accounted for as being the reduction of titanium from the 3+ to the 2+ oxidation state, rather than polymer growth inhibition or monomer mass transfer limitations. They also report that the propagation rate constant was an order of magnitude greater than that for the previous generation catalyst.

Choi and Ray (1985) also considered gas phase propylene polymerization and investigated the effect of monomer and hydrogen concentrations, polymerization temperature and catalyst formulation. They concluded that at high temperatures, when polymer growth rates are higher, mass transfer limitations could play a role in catalyst productivity but chemical deactivation was

responsible for the activity decay. They found that first-order activity decay fitted their data adequately.

For propylene polymerization the Al/Ti ratio has a significant effect on the stereospecificity. Keii *et al.* (1984) found that at low ratios, highly isotactic polypropylene is formed, while at higher ratios there is a decrease in isotacticity. It is believed that stereospecific sites are activated first by TEA and as the aluminium concentration increases, atactic sites are formed. The creation of more active-centres by larger amounts of TEA is supported by Kashiwa and Yoshitake (1984) for non-stereospecific centres.

Kashiwa *et al.* (1986) believed that at high TEA concentrations, isotactic centres producing low molecular weight polymer were formed, while at low TEA concentrations, high molecular weight centres were formed. They suggested that the latter active centres may have a higher valence state than the former, although increased transfer reactions at high TEA concentrations are also a significant factor for molecular weight decrease.

Chien *et al.* (1989) determined the oxidation state composition (2+, 3+, 4+) of a catalyst and found that reduction of titanium by TEA is affected by the crystallographic support structure, which itself affects the stereospecificity of the catalyst sites. These researches also supported the kinetic rather than the mass-transfer limitation theory of catalyst decay. They showed that the CO inhibition technique has some serious limitations, and can significantly over-estimate the propagation rate constant.

Chien and Nozaki (1991) published evidence supporting the claim that the oxidation state determined catalyst activity. They observed that the presence of hydrogen correlated with a decrease in the 2+ oxidation state of titanium and the emergence of the 3+ state. They postulated a dissociative adsorption of hydrogen on a pair of adjacent Ti^{2+} ions as the mechanism for this reaction.

The molecular weight distribution typically broadens with an increasing Al/Ti molar ratio. However, at high Al/Ti ratios, chain transfer with the aluminium alkyl can counteract this. In particular, for polypropylene, increased Al/Ti broadens the isotactic fraction and leaves the atactic fraction unaffected. This was supported by the findings by Kashiwa *et al.* (1986) that the overall molecular weight distribution (MWD) is shifted downward, as well as broadened, as the TEA concentration increases. Keii *et al.* (1986) found that the number average molecular weight ($\overline{M_n}$) decreased rapidly with TEA concentration until it levelled off, with polydispersity also levelling off after an initial increase. The atactic polymers were affected more than the isotactic products.

The co-polymerization of ethylene and 1-hexene with a Ti based catalyst has been studied by Kissin (1995). He showed that as the polymer yield increased quickly with time, the hexene content in the polymer deceased, indicating that the active sites which readily incorporate 1-

hexene deactivate more quickly. Resolution of the GPC (gel permeation chromatography) curves into Flory components allowed the determination of the number of types of active sites. Five different sites were required to account for the entire GPC curve. The first active site had a high activity, hydrogen response (M_w = 9000) and 1-hexene incorporation (~25% mol) but a fast decay. These features gradually decreased for the other active sites, ending with the fifth one having poor activity and 1-hexene uptake (<0.3%mol), producing high molecular M_w (~320 000) and long lifetime. Kissin relates this different kinetic behaviour to different oxidation states (Ti^{3+} versus Ti^{2+}) as well as different ligands and location of active centres (crystal faces versus edges).

Han-Adebekun *et al.* (1997), in their studies of gas-phase polymerization with on-line gas-phase composition control were able to monitor the polymerization rate profile for variations in concentration of hydrogen, TEA, and monomer. An interesting observation was the emergence of a second peak in the ethylene polymerization rate profile, which had not been reported on previously. They explained the observation in terms of oxidation state variation of the titanium centres. Wu et *al.* (1999) also observed the second peak reported by Han-Adebekun *et al.* and conclude that two sites exhibiting different polymerization rates were responsible.

As is discussed above, a proposed reason for the deactivation of propylene catalysts is the over-reduction of the Ti centres to Ti^{2+}, because Ti^{2+} is considered to be able to polymerize ethylene but not propylene or higher α-olefins. However, Albizzati *et al.* (1997) dispute this mechanism. They prepared a Ti^{2+} compound which is active on its own and once supported on $MgCl_2$ gives reasonable yield in polypropylene polymerization (although lower than a standard $MgCl_2/TiCl_4$ catalyst). They concluded that catalyst deactivation during the polymerization cannot be attributed solely to over-reduction, but other mechanisms must also exist.

Hydrogen (used as a chain transfer agent for M_w control) usually deactivates or does not affect ethylene polymerization, but activates propylene polymerization. Formation of 'sleeping sites' is proposed to account for this effect. ^{13}C NMR studies by Kojoh *et al.* (1995) suggest that the propagation after 2-1 insertion of propylene is very slow, leading to a 'sleeping' site, which can be reactivated by H_2 chain transfer. Rishina *et al.* (1996) showed that $AlEt_3H$, acting as both a strong activator and chain termination agent, can partially reactivate sleeping sites.

The injection of co-monomer during ethylene and propylene polymerization also gives some interesting results, as was demonstrated by Wester *et al.* (1997). The two main effects observed, just after the injection of the co-monomer, are a rapid rate reduction followed by a slow but persistent rate increase. Different co-monomers have different effects on the polymerization rate, for example, 1-hexene induces a permanent increase in ethylene polymerization, whereas it has no effect on propylene polymerization. *Trans* and *cis* isomers of 2-butene have a similar minor effect in ethylene polymerization, whereas the *cis* 2-butene gives a significant reduction in propylene polymerization and the *trans* isomer has no effect. Steric

considerations are clearly important in rationalizing these effects, though relative mass transport of monomers and catalyst fragmentation arguments has been made.

Kissin *et al.* (1999) undertook an investigation of the kinetics of ethylene homo-polymerization reactions and ethylene/1-hexene co-polymerization reactions using a supported Ziegler-Natta catalyst. The kinetic data was analyzed using the concept of multicentre catalysis with different centres that respond differently to changes in reaction parameters. The catalyst contained five types of active centres that differed in the molecular weights of material they produced and in their co-polymerization ability. In ethylene homo-polymerization reactions, each active centre had a high reaction order with respect to ethylene concentration, close to the second order. In ethylene/α-olefin co-polymerization reactions, the centres that have poor co-polymerization ability retain this high reaction order, whereas the centres that have good co-polymerization ability change the reaction order to the first order. Hydrogen was found to depress activity of each type of centre in the homo-polymerization reactions in a reversible manner; however, the centres that co-polymerize ethylene and α-olefins well were not depressed if an α-olefin was present in the reaction medium. To explain the kinetic features, Kissin *et al.* proposed a new reaction scheme based on the hypothesis of low reactivity of the Ti-C_2H_5 bond in active centres.

Chapter 3

Gas Phase Laboratory Polymerization Reactor System

In this chapter the design of the novel lab-scale reactor system that has been constructed for investigating the kinetic behaviour of olefin polymerization reactions using a heterogeneous catalyst is described. More specifically, the gas phase semi-batch reactor system is to be used for ethylene homo-polymerization reactions using the supported Ziegler-Natta catalyst whose synthesis will be described in Chapter 4. The 0.7 L stainless steel reactor has been constructed in the mechanical workshop at the Department of Chemical Engineering, Howard College and is equipped with both temperature and pressure control systems. A specially designed catalyst injection system is used for the introduction of the solid catalyst and the liquid co-catalyst, both of which are air and moisture sensitive, into the catalyst basket. Feed gas dehydration and purification columns are employed for the removal of moisture and other impurities from the feed gases. These have been included since the presence of even minute quantities of moisture in the feed gases would deactivate active sites on the catalyst surface and using gases containing such impurities would gradually diminish catalytic activity and introduce an uncontrolled factor influencing the measured experimental yields. The reactor is also fitted with a spinning basket into which the catalyst is injected. The catalyst is contained in this basket for the duration of the reaction and the polymerization reaction takes place there. The spinning basket serves a dual purpose in that it is also used for agitation. In the sections that follow the reactor design, the feed and exit gas systems, the gas purification system, the catalyst injection system, and the temperature and pressure control systems are fully described and illustrated.

3.1 Introduction

The commercial production of polyethylene by catalytic gas-phase processes has grown significantly since the introduction of the Unipol process by Union Carbide in the 1970s. Since then there has been a definite shift in industry from slurry- and liquid- to gas-phase polymerization of olefins where polymer particles are grown in a stirred or fluidized bed. Today, gas-phase polymerization may even be the most important olefin polymerization process due to its relative simplicity and flexibility. In the gas phase process there is no solvent present in the reactor system to recover. Also, the gas phase process is usually operated at more moderate temperatures and pressures than the high-pressure or liquid-phase polymerization processes. In addition, the process offers a wide range of products, including low molecular-weight polymers. The gas phase process does however have a limitation in that the temperature in the reaction zone must be maintained above the dew point of the reactants to avoid condensation and below the melting point of the polymer to prevent particle melting and agglomeration.

Despite the rapid commercial acceptance of the gas-phase process, most laboratory investigations are still carried out in slurry phase reactors due to their simpler construction and relative ease of operation. Excellent heat transfer is obtained because of the liquid phase surrounding the catalyst-polymer particles and the good mixing/suspension of the particles in the hydrocarbon liquid medium. Reaction kinetics and polymer properties resulting from slurry operation are however not directly transferable to gas phase operation. Although in many cases the kinetics are quite similar, there is also some evidence that certain aspects of polymerization kinetics of the gas phase process differ from that of the liquid slurry process (Choi and Ray, 1985). Keii (1972) has shown that ethylene polymerization rates for gas-phase operation are an order of magnitude lower than those observed when the catalyst is suspended in a toluene slurry. It has also been shown by Choi and Ray (1985) that for propylene polymerization the overall activation energy for gas-phase operation is significantly less than that observed for polymerization carried out in a liquid slurry. These observations show that for the investigation of gas phase kinetic behaviour, experiments should be performed in a gas-phase reactor.

In the public literature on olefin polymerizations with highly active Ziegler-Natta catalysts there is a lack of kinetic data that can be used for reactor design and control of polymer properties. This is in spite of intensive research efforts and the successful application of these catalyst systems in industry. The reason for this is that olefin polymerizations on a small scale are rather difficult to execute (Samson *et al.*, 1999). According to Han-Adebekun *et al.* (1996) the lack of fundamental kinetic models is related to the difficulty in obtaining high-precision kinetic data. A complete kinetic study requires extensive experiments due to the vast number of combinations of important operating parameters (temperature, pressure, and hydrogen and monomer concentration) which influence these reactions. High precision in the experiments demand close control of these parameters for the duration of the reaction and the problem then lies in designing and constructing competent reactor systems.

There are basically two types of gas phase olefin polymerization reactors used industrially and in the laboratory, the fluidized bed reactor (FBR, used in the Unipol process and licensed by Union Carbide) and the continuous stirred bed reactor (CSBR, used and licensed by BASF and BP Amoco). However, many reactors containing catalyst baskets are also commercially available for catalysis research. Of these the Berty stationary catalyst basket reactor, where gas is circulated past a stationary fine wire mesh catalyst basket is the most widely used recycling gas phase catalytic research tool. The Carberry and the Mahoney-Robinson spinning catalyst basket reactors and the Mahoney-Robinson stationary catalyst basket reactors are also widely used for heterogeneous catalysis studies. According to Weekman (1974), who undertook a comparative study of a number of laboratory reactors and their limitations, the sampling and analysis of the product composition of these catalyst basket reactors present no problems since the catalyst is contained and no separation is required prior to analysis. Also, with enough mixing energy the system can be sufficiently mixed and isothermal. A further advantage is that the residence time of the solids is accurately known and with good mixing the gas residence times can also be measured quite accurately. The one disadvantage put forward by Weekman was the complexity of the design over that of the stirred bed reactor due to the requirements of containing the catalyst. Spinning basket reactors for olefin polymerization reactions have however not been reported on extensively in the literature.

3.2 Reactor design

In this section the reactor design, the catalyst basket, and the method of agitation employed are fully discussed. The 0.7 L capacity reactor is fully constructed from Type 316 Stainless Steel (T316SS) and so are all the process lines, valves and fittings. Although many metals are available for reactor construction T316SS has been chosen as it is the recommended material for use with most organic systems and it has been used previously (Choi *et al.*, 1985 and Han-Adebekun *et al.*, 1997a, b, c) for similar work. Furthermore, T316SS can be used with most commercial gases at temperatures and pressures within the required experimental range.

Although glass pressure vessels are commercially available for bench scale experimental investigations, they do pose several potential safety hazards at elevated temperatures and pressures. Should the vessel shatter during operation both flying glass and the release of hot flammable gases are foreseeable safety hazards. Issues such as geometry and annealing further complicate glass vessel design and provisions for dealing with differential thermal expansion, adequate thickness, and inspection and testing were also carefully considered. Therefore, although glass vessels do provide the opportunity for watching a polymerization reaction progress, a stainless steel vessel was preferred.

3.2.1 The reactor cylinder

According to Townsend *et al.* (2000), the larger the reactor being used for reaction kinetic investigations becomes, the less accurate is the kinetic data obtained. In smaller reactors both

composition and temperature gradients tend to be minimized. The fact that smaller reactors are more efficient for kinetic investigations is evident in that Choi *et al.* (1985), Han-Adebekun *et al.* (1997a, b, c), and Samson *et al.* (1999), have all made use of a 1 L reactor for their work. The reactor designed for this work has a capacity of 0.7 L. The reactor cylinder dimensions are shown in Table 3-1.

Table 3-1 Reactor Cylinder Dimensions

Material of construction	T316SS
Outside diameter (mm)	90
Wall thickness (mm)	3
Inside height (mm)	110
Capacity (L)	0.7

In Figure 3-1 the catalyst basket can be seen screwed into its holder and the four baffles positioned around the basket are meant to assist with mixing. The reactor cylinder is completely removable so that the basket and its contents can also be removed. The six holes drilled into the flange of the cylinder are to accommodate the cap bolts used to attach the reactor cylinder to the reactor head.

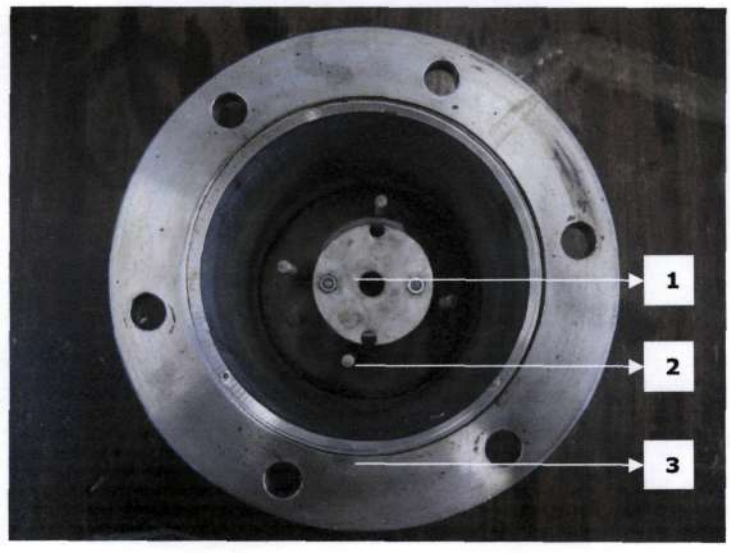

Figure 3-1 Stainless Steel Reactor Cylinder with the Catalyst Basket (1), Baffles (2), and Flange (3) to which Reactor Head is attached

A Tealon™ TF1590 (restructured PTFE) gasket is used between the flanges of the reactor head and cylinder to prevent gas leaks. The flat gasket is 3 mm thick and is kept firmly in place by the cap bolts that are used to secure the flange of the reactor head to the flange of the cylinder. The gasket material is able to withstand temperatures of up to 260 °C and pressures of up to 83 bar and is suitable for use in both chemical processing and hydrocarbon plants. Flat gaskets require an initial loading pressure in order to develop and maintain a tight seal and this is

achieved by tightening the cap screws in place. PTFE is slightly "plastic" and will flow under pressure, producing a seal that improves with each use as the gasket is forced into the flanges on the head and cylinder. It is also a very forgiving seal and does not require the special care needed to achieve a uniform loading which is essential when working with metal or other non-plastic gasket materials. An equally important advantage of the PTFE gasket is that it has essentially universal chemical resistance.

3.2.2 The reactor head

All ports for gas entry and exit, cooling water entry and exit, the PT-100 temperature sensor, and the catalyst and co-catalyst injection line are fitted onto the head of the reactor (Figure 3-2) and unlike the reactor cylinder which is removable the position of the reactor head is fixed and, as a result, all attachments to the reactor head also remain permanently in place. The sealed reactor is opened by simply removing the six cap screws holding the head and cylinder together and then lowering the cylinder away from the head, leaving all attachments undisturbed. The feed gases exit the gas inlet line below the basket so as to allow for the gases to rise up, be circulated by the spinning basket, and leave through a gas exit line attached to the head of the reactor. The gas inlet and exit lines share the same attachment on the reactor head with the inlet line being a ⅛" tube connected inside the ¼" exit line via a Tee connection, this can be more clearly seen in Figure 3-3. When the reactor is sealed, the PT-100 temperature sensor and the gas inlet line fit in the annular space between the outside of the catalyst basket and the inside of the cooling coils while the catalyst injection line extends into the basket through the hole on the top cover of the basket.

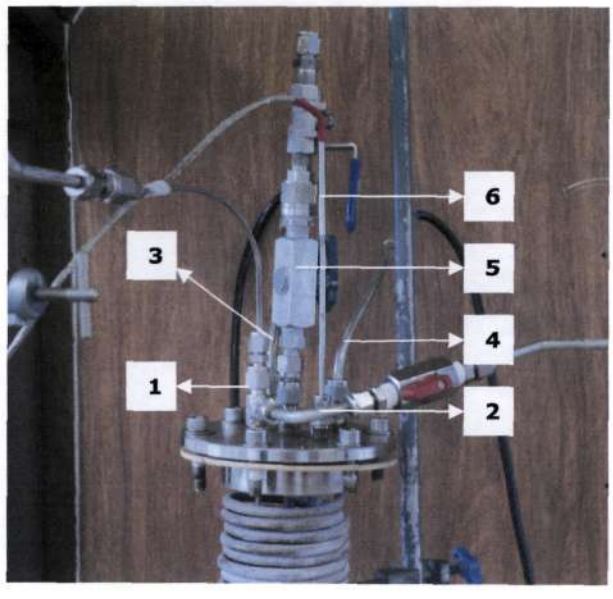

Figure 3-2 Reactor Head with Ports for Gas Entry (1) and Exit (2), Cooling Water Entry (3) and Exit (4), the Catalyst and Co-Catalyst Injection Line (5), and the PT-100 Temperature Sensor (6)

The Tealon gasket used between the flanges of the reactor head and cylinder and the cap screws used to seal the reactor can be seen in Figure 3-3.

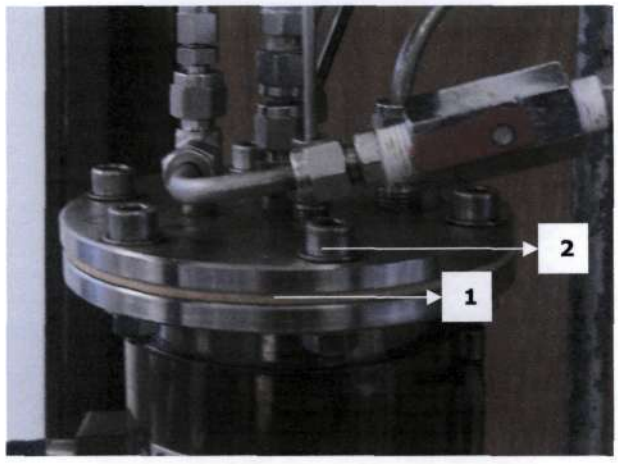

Figure 3-3 Reactor with Gasket (1) Between the Head and Cylinder and Sealed with Six Cap Screws (2)

3.2.3 The spinning catalyst basket

The solid catalyst and the liquid co-catalyst are both injected into the catalyst basket (Figure 3-4) and it is in this basket that the polymerization reaction occurs. The stainless steel basket is rigid, has a solid bottom, and is lined with mesh also made from stainless steel but with a pore size of 20 microns. The spinning basket has been included to hold the supported catalyst while not destroying the catalyst and the reaction product as would be the case if an impeller was used for agitation purposes. The dimensions of the catalyst basket are given in Table 3-2.

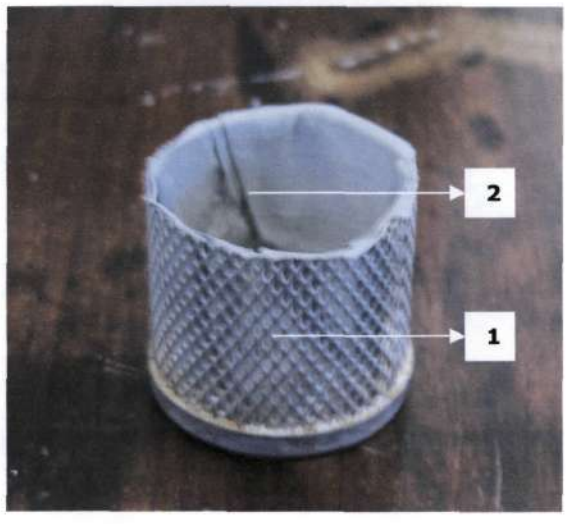

Figure 3-4 Catalyst Basket (1) Lined with Stainless Steel Mesh (2) with a Pore Size of 20µm

The 20 micron mesh is used because it has a pore size smaller than the smallest expected catalyst particle size while still allowing for inflow of the gaseous reactants. The top cover of the

basket is solid stainless steel and has a hole drilled into the centre to allow for the catalyst injection line to fit through when the reactor is sealed. The basket screws into a holder fitted in the reactor cylinder and can be completely removed from the reactor cylinder to remove reaction products and to replace the mesh after each reaction.

Table 3-2 Catalyst Basket Dimensions

Material of construction	T316SS
Basket Diameter (mm)	35
Basket height (mm)	30
Mesh pore size (μm)	20
Basket Capacity (cubic cm)	29

The holder to which the catalyst basket is screwed is designed to spin when the magnets attached to the motor positioned below the reactor cylinder spin (Figure 3-5). The speed at which the basket spins is dependant on the voltage applied to the motor. The spinning basket also serves as an impeller for stirring the reactants and the four fixed vertical baffles around the basket ensure good circulation over the surface of the contained catalyst. Good mixing of the surrounding gas is essential for reaction heat removal, to promote heat transfer, and to prevent thermal runaway in the particles, which would result in low yields and poor polymer quality. This method of agitation avoids gas leakage problems since there are no rotating seals involved in the agitation system. The motor therefore efficiently spins the basket while providing a gas-tight system.

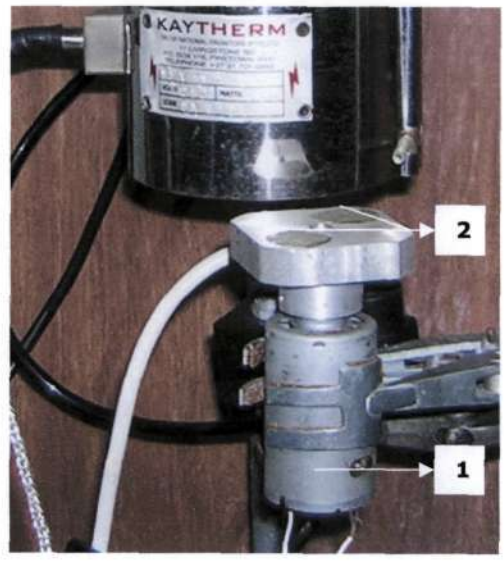

Figure 3-5 Variable Speed Motor (1) with Fitting Containing Two 2 Magnets (2)

The fully assembled reactor can be seen in Figure 3-6.

Figure 3-6 Fully Assembled Reactor

3.3 Reactor feed and exit gas systems

3.3.1 The feed gas system

The reactor feed system essentially consists of three gas streams, nitrogen (Afrox, UHP, 99.999%), hydrogen (Afrox, UHP, 99.999%), and ethylene (Afrox, 99.90%), each of which are individually dehydrated and purified prior to being introduced into the reactor. The reason for dehydrating and purifying the feed gas streams is that Ziegler-Natta catalysts are easily poisoned by both oxygen and moisture. The titanium component of the catalyst will hydrolyze on contact with moisture and release hydrogen chloride. The co-catalyst, triethylaluminium, is also extremely sensitive with aluminium alkyls being pyrophoric, i.e. they ignite spontaneously on contact with air, and with metal alkyls being explosively reactive on contact with water. A clean gas stream is therefore necessary to prevent deactivation of the catalyst and co-catalyst and to guarantee the quality of the analysis and the reliability of the results.

Each gas cylinder is connected to a molecular sieve column specifically designed to individually dehydrate and purify the respective gases which pass through them (Figure 3-9). When a gas cylinder is being replaced, the valve before the molecular sieve column is used to isolate the column from the atmosphere and prior to allowing the gas from the new cylinder to pass through the column the regulator and the tubing connecting the cylinder to the molecular sieve column is purged of air through the purge valve. This is aimed at prolonging the life of the molecular sieves and thereby postponing their regeneration. A schematic of the nitrogen gas inlet line leading up to the gas manifold is shown in Figure 3-7. The gas inlet lines for ethylene and hydrogen are the same as the nitrogen line with the only variation being that the content of the gas purification columns are different and that for the ethylene gas line, a pressure control valve is positioned between the purification column and the manifold. The flow control valve is

used to maintain the reactor pressure at the desired set-point by controlling the flow of ethylene into the reactor.

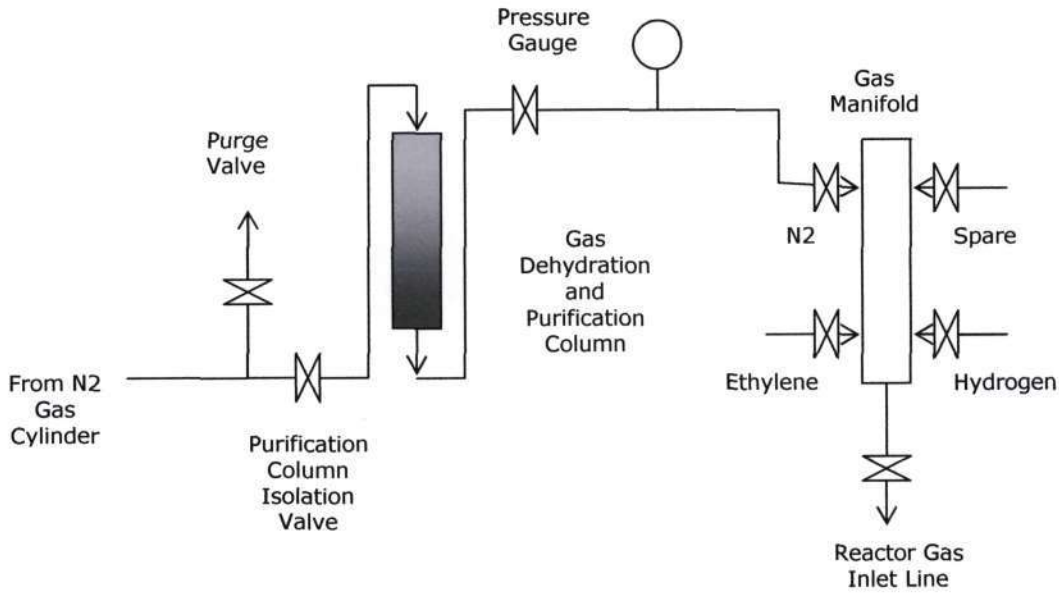

Figure 3-7 Schematic of the Nitrogen Gas Inlet Line

The gas manifold (Figure 3-8) has ports for the introduction of nitrogen, ethylene, and hydrogen gases and has two spare ports for additional gas feeds. The manifold allows for the simultaneous introduction of more than one gas and also allows for the gases to be mixed before entering the reactor through the gas inlet line. Since the feed gases are to be introduced into a vessel under pressure, the supply pressure must be greater than the pressure in the vessel to prevent reverse flow into the supply system. Safety prevention in the case of reverse flow is attained by the installation of a ¼" stainless steel inline Hoke safety check valve on the reactor gas inlet line, after the manifold. This valve will snap shut if the supply pressure is too low or if the pressure in the vessel should rise above the supply pressure. Check valves were also used on each gas inlet line, before the manifold, to prevent reverse flow of one gas into the inlet line of another.

Figure 3-8 Gas Manifold Showing Three Gas Inlet Ports and One Gas Outlet Port

3.3.2 Feed gas dehydration and purification

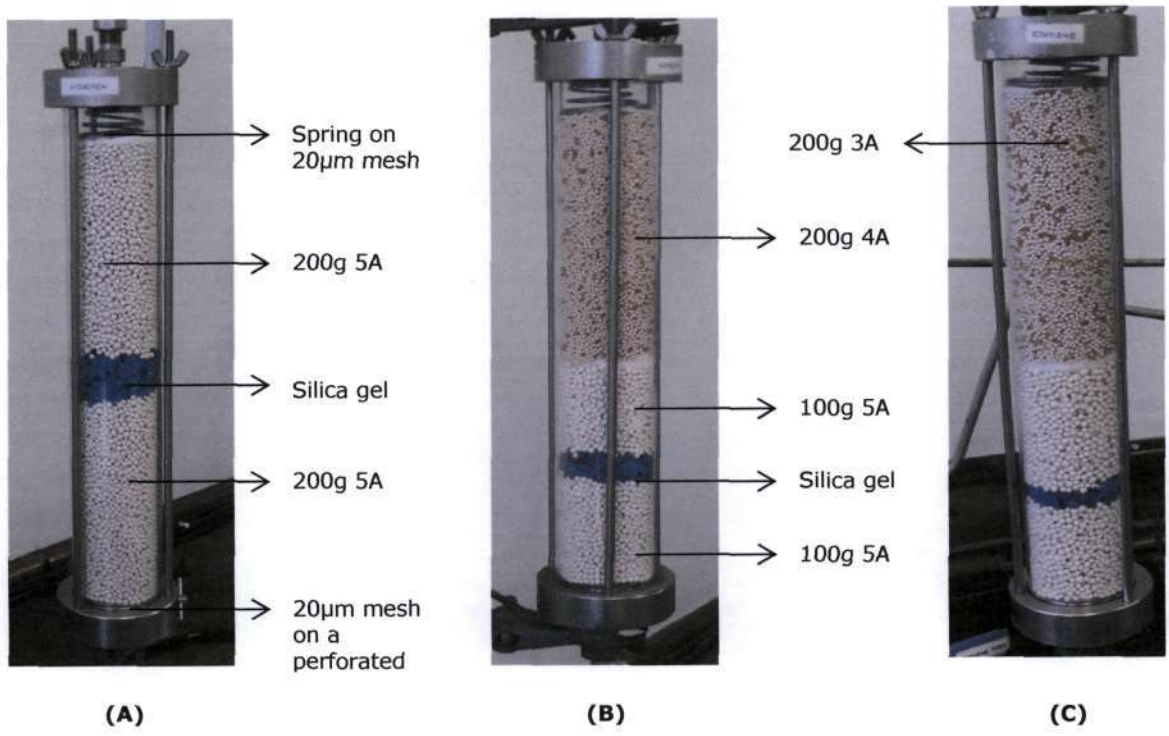

Figure 3-9 Gas Purification Columns for Hydrogen (A), Nitrogen (B) and Ethylene (C)

There are essentially three primary methods of removing water vapour from a gas stream. The first method is low temperature condensation, the second is compression of the gas so that the partial pressure of the water increases and condensation results and the third is the use of solid adsorbants. The gas dehydration and purification scheme employed in this work is based on the third method and involves passing the feed gases through fixed beds of molecular sieve adsorbants (Figure 3-9). The adsorption process makes use of the characteristics of porous solids endowed with large surface areas in order to selectively separate low concentrations of gas impurities from the gas streams. Molecular sieve adsorbants have an advantage over silica gel and activated carbon in that they are not only capable of removing water vapour from the gas streams but also selectively adsorb other contaminants.

The purification columns are positioned in a vertical position to prevent gas channeling and H_2O, CO and CO_2 (the oxygen containing compounds) are removed by passing the feed gases through the columns at ambient temperature. The columns (H=300mm, D=50mm) are constructed from polycarbonate, a transparent plastic through which the degree of saturation can be observed. 20 μm stainless mesh filters are placed on either end of the columns. At the bottom end of the column the mesh sits on a rigid perforated screen and at the top of the column it is placed on the molecular sieve particles which are firmly compressed by a spring. Molecular sieves 3A, 4A and 5A were used in the purification columns and were all purchased from Aldrich. Sieves 3A and 4A are self indicating, implying that they will change colour when saturated and because the 5A sieves are not a layer of blue silica gel was used between the particles to

indicate saturation by turning pink. When saturated, the molecular sieves and the silica gel can simply be regenerated by heating in an oven until they return to their original colour. The shut off valves on either side of the columns are used for isolating the columns from the atmosphere after they have been filled with regenerated particles in the glove bag and prior to them being re-installed.

The drying of high pressure gases through adsorption represents a purely physical process in the course of which water vapour (adsorbate) is bound to the drying medium (adsorbant) through binding forces of molecular adhesion. When a gas containing water is passed through a bed of freshly regenerated adsorbant, the water is adsorbed first near the inlet portion of the bed, and the dehydrated gas passes through the rest of the bed with only a small amount of additional drying taking place. As the adsorbant near the inlet becomes saturated with water at the condition of the feed gas, the zone of rapid water adsorption moves inward and ultimately passes through the entire bed. When this "adsorptive wave" reaches the outlet end, the water content of the product gas is observed to rise rapidly, signifying the "break-through point" for the particular operating conditions.

As with other mass transfer operations, the rate of transfer of water vapour from the gaseous phase is a function of the gas flow rate, the size and shape of the desiccant particles, and the properties of the gaseous and adsorbate phases. If the mass transfer coefficient is very high, the adsorptive zone will be quite abrupt; i.e. complete dehydration will be obtained until the break point is reached and at this time the water content in the product gas will rise very rapidly. If the mass transfer coefficient is quite low, or the bed is shallow, some water vapour may pass through with the gas from the start, and the water content of the exit gas will increase slowly as the entire bed becomes saturated. Most commercial installations fall between the two extremes in that there is first a period of maximum dehydration, then after a definite break point, the water content of the product gas is observed to rise at a moderate rate.

For a given total gas flow and desiccant bed volume, a deep bed is more effective than a shallow bed, in that it permits the desiccant to attain a higher average loading than a shallow bed and provides a higher degree of dehydration of the gas. These advantages are gained, however, at the expense of pressure drop since the deep bed must be operated at a higher gas velocity (Kohl, 1979). If a fixed bed is used for adsorption, it is possible to obtain a nearly adsorbate free gas effluent until the adsorbant in the bed approaches saturation. When the mass transfer zone, the zone where adsorption takes place, reaches the end of the bed breakthrough occurs and the concentration of the adsorbate in the effluent is the same as that in the feed. If it is required that the outlet concentration of the adsorbate should always be less than 5% of the concentration in the feed for example, the adsorbent needs to be regenerated long before the mass transfer zone reaches the end of the bed. The columns shown in Figure 3-9 are therefore self-indicating to indicate the degree of saturation and consequently indicate when regeneration is necessary.

The weaker physical or van der Waals forces are responsible for most adsorption phenomena and this explains why in general, compounds which have low vapour pressures are adsorbed in greater quantity than relatively non-condensable gases. Molecular sieves have the property of relatively high adsorption capacity at low concentrations of the material being adsorbed and have an unusually high affinity for unsaturated and polar-type compounds (Kohl, 1979). Molecular sieves also have very unusual properties with regard to both dehydration and the selective adsorption of other compounds. They are crystalline synthetic zeolites, whose crystal lattice contains numerous cavities connected with one another by pores having exactly defined diameters (3A, 4A, 5A, and 10A according to type of molecular sieve). If the water to be found in the pores and cavities is removed by heating, extremely active adsorbents are obtained which are eminently suited to drying gases. Experience has shown that the drying of gases with the aid of molecular sieves is more complete than with the customary drying agents. In contrast to adsorption by means of active charcoal grades, a selective separation of gases may take place when molecular sieves are used, since all molecules whose critical diameter is less than the pore diameter of the molecular sieve concerned are selectively adsorbed out of the mixture. In this way components can be removed from the gas mixtures almost quantitatively, even if only traces thereof are present. Due to their higher polarity, water, carbon dioxide and hydrogen sulfide are preferentially bound.

Molecular sieves permit separations to be carried out which are based on the following various effects:

Molecular sizes: Since the cavities in which the adsorption takes place are only accessible via the exactly dimensioned pores, only those molecules whose critical molecular diameter is smaller than the pore diameter (sieve effect) can be adsorbed. By critical molecular diameter is understood the geometrical dimensions of the molecules, which may be calculated using van der Waal's radii of the atoms which in principle is equal to the diameter of the circle circumscribing the molecule. In the case of elongated molecules, this circle describes the plane perpendicular to the axis of the molecule, and is thus the same size for all n-paraffins. The critical molecular diameters of some common molecules are presented in Table 3-3.

Table 3-3 Table of Critical Molecular Diameters of Some Common Molecules

H_2	2.4A	N_2	3A	HC≡CH	2.4A
CO_2	2.8A	CO	3.2A	$H_2C{=}CH_2$	4.25A
O_2	2.8A	NH_3	3.8A	$H_3C\text{-}CH_3$	4.44A
H_2O	2.6A	Cl_2	8.2A	n-paraffins	4.89A

Polarity: Polar molecules are more strongly adsorbed, with molecules of comparable critical diameter being adsorbed strictly in ascending order of polarity. Molecules already adsorbed are therefore displaced by those with a higher polarity.

Bond character: Unsaturated compounds are bound in preference to saturated compounds.

Molecular Weight: Within a homologous series, compounds having a higher molecular weight are somewhat preferentially adsorbed.

Some of the advantages of drying gases with molecular sieves are that in relation to other adsorbents the drying is more complete with dew points of -75 °C being obtained without difficulty. Even at extremely low partial pressures the drying effect is usually high. Also, the simultaneous removal of water and interfering gases from gas mixtures, even at elevated temperatures, is possible. They have an unusually long life, i.e. molecular sieves may be regenerated several hundred times without impairing their effectiveness. Another advantage is the drying of gas mixtures without the danger of chemical changes resulting from the action of the drying agent.

For drying using molecular sieve 3A, the pore diameter is such that both carbon dioxide and water can penetrate the pores. Water, with a heat of adsorption of 34 kcal/mol, is considerably more strongly held than carbon dioxide, with a heat of adsorption of 12, 2 kcal/mol. Therefore, since the heat of adsorption is more important for the drying effect than the pore diameter, the carbon dioxide is expelled from the pores. Carter and Husain (1974) studied this phenomenon for the adsorption of water vapour and carbon dioxide on 4A type synthetic zeolite. With equal partial pressures of water and CO_2 in the inert gas, they found that the water displaced the CO_2 adsorbed by the solid.

Triebe *et al.* (1995) studied the potential of molecular sieves 4A and 5A for the separations of CO_2, CO and NO from N_2. By calculating the separation factors (ratios of Henry's Law constants) for NO, CO and CO_2 from N_2 on the molecular sieves they were able to determine the best sieve for the removal of the contaminants from N_2. They found that CO is strongly adsorbed in both 4A and 5A zeolites, more so in the 5A, which they attribute to the presence of stronger adsorption sites (bivalent Ca^{++} cations as opposed to Na^{+} cations) available to interact with the strong CO dipole. It is therefore highly possible that the CO and CO_2 will be removed from the nitrogen stream using the 5A molecular sieves after the water has been removed by the 4A molecular sieves.

Triebe *et al.* (1996) investigated the adsorption of methane, ethane and ethylene on molecular sieves 4A and 5A, with specific interest being in the separation of ethylene from methane. It was found that both the 4A and 5A molecular sieves adsorb the ethylene from a stream of ethylene, ethane and methane gas. The zeolites were also found to have a greater affinity for light gas impurities such as CO_2 than for methane. From this it was concluded that the methane and ethane can not be removed from the ethylene feed gas stream and only H_2O, CO_2 and CO can be removed. The H_2O is firstly removed by passing the gas through the 3A molecular sieves and the CO_2 and CO are thereafter removed by the 5A molecular sieves.

Yang *et al.* (1995) investigated the separation of H_2/CO_2 and H_2/CO systems with zeolite 5A. Hydrogen gas is adsorbed less strongly by molecular sieves than almost any other species and the removal of CO_2 and CO from the hydrogen stream with the molecular sieves is therefore highly possible. This was confirmed by the experimental work carried out by Yang which showed a very high selectivity for CO_2 and CO over H_2 with the 5A molecular sieve. The 5A

molecular sieves were therefore used in the hydrogen purification columns to remove both water vapour and the CO_2 and CO contaminants.

3.3.3 The exit gas system

A schematic of the reactor gas exit line is shown in Figure 3-10. A stainless steel Hoke adjustable relief valve is used as a safety measure to relieve excess reactor pressure in the event of failure of the pressure control system. The relief valve is therefore a means of protecting the vessel in case of accidental overpressure. The purge valve on the reactor exit gas line is used to release gas from the reactor at the completion of a run. The vacuum pump is connected to the vacuum line and is used together with the nitrogen gas inlet line to attain an inert atmosphere in the reactor prior to catalyst injection.

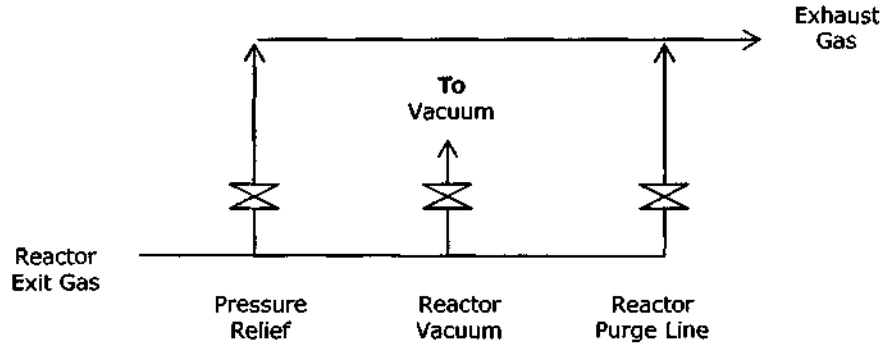

Figure 3-10 Schematic of the Reactor Gas Exit Line

3.4 Catalyst injection system

Due to the extreme sensitivity of the solid catalyst and liquid co-catalyst to the atmosphere, special methods had to be devised for their introduction into the reactor. The catalyst injection system designed safeguards inert conditions during injection and makes possible catalyst and co-catalyst pre-contact prior to injection.

The catalyst holder used for transferring the catalyst and co-catalyst from the glove bag to the reactor is constructed from a stainless steel full flow quick-connect (Swagelok QF series) with a stainless steel plug valve (Nupro SS-4P4T) attached downstream and a ball valve attached upstream (Figure 3-11). The quick-connect and the plug valve have essentially no internal constrictions thereby permitting free flow of sample through the holder. The filling of the catalyst holder with the catalyst and co-catalyst is to be done in the glove bag under an inert nitrogen atmosphere. With the plug valve closed, the solid catalyst and liquid co-catalyst (TEA, 1M solution in heptane from Aldrich) are inserted into the body of the quick-connect (Figure 3-12). The volume of TEA required is accurately measured with a Hamilton gas-tight syringe. When the stem of the quick connect is attached and the ball valve closed, the catalyst holder

can be removed from the glove bag and connected to the top flange of the reactor without contaminating the catalyst.

The catalyst holder forms part of the catalyst injection line. The rest of the injection line consists of a ¼" stainless steel tube fixed to the reactor head and which extends into the catalyst basket. When the catalyst holder is connected to the tube, the catalyst sample can simply be injected into the basket by opening the plug valve. Once the catalyst and co-catalyst are injected, 10 mL of hexane is injected into the septum port situated upstream of the ball valve in order to further rinse out any possible residues of the co-catalyst and catalyst on the walls of the injection line. The gas-tight syringe used for hexane injection is filled in the glove bag under a nitrogen atmosphere.

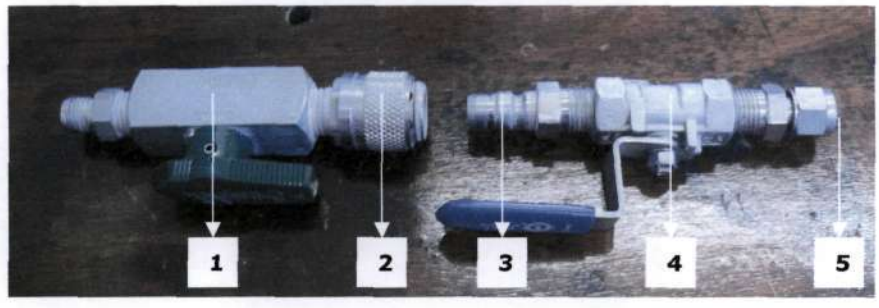

Figure 3-11 Body of Catalyst Holder (2) Attached to Plug Valve (1), Stem of Catalyst Holder (3) Attached to Ball Valve (4) and Septum (5) for Heptane Injection

Figure 3-12 Top View of the Body of the Injection Line

3.5 Reactor temperature control system

Ethylene polymerization reactions are known to be highly exothermic, with heat removal duties of 922 Kcal/Kg being reported (Ray *et al.*, 2000), and if the polymerization rate is too great the reaction temperature increases uncontrollably (thermal runaway) until catalyst deactivation occurs when melting polymer encapsulates the catalyst particles (Lynch and Wanke, 1991). Efficient heat removal from the reacting powder bed is extremely important in order to avoid problems such as particle melting and sintering, reactor fouling, and changes in polymer

properties. Also, good gas phase temperature control is required to obtain reliable activity profiles. Experimental results in the literature illustrate that activity profiles are a strong function of the gas-phase temperature and proper temperature control is therefore essential for the investigation of activation-deactivation behaviour of polymerization catalysts.

It has been shown that gas-phase polyolefin reactors are open-loop unstable and easily show excursions to high temperature steady states, which lead to polymer melting (Choi and Ray, 1988, McAuley *et al.*, 1995, Gorbach *et al.*, 2000), it has however also been shown that the unstable reactor can be stabilized through PID feedback control of the reactor temperature. In the literature, oil or water bath cooling systems are often reported on (Choi *et al.*, 1985, Lynch and Wanke, 1991) but these are highly inefficient. According to Mannan *et al.* (2004), the response to gas-phase temperature changes is slow for reactors immersed in circulating liquid baths. These reactor temperature control systems are therefore not adequate for a broad range of reactor operating conditions.

For this work, a combination of an electric band heater and stainless steel cooling coils are used in order to reach and maintain a steady state reaction temperature. An 800 W electrical band heater, custom made by Gilectric, is fitted onto the outside of the reactor cylinder to provide a constant heating source. The band heater, which is removable, is sized to the cylinder dimensions and can be seen alone in Figure 3-13 and fitted around the reactor cylinder in Figure 3-6. ¼ inch diameter stainless steel cooling coils are wound in a spiral configuration around the inside diameter of the reactor cylinder. The spiral cooling coil configuration consists of multiple loops and maximizes the available cooling area. Water is used as the cooling fluid inside the coils. When the reactor is sealed these coils fit in the annular space between the baffles surrounding the catalyst basket and the reactor cylinder wall. The cooling coils are shown in Figure 3-15. Both the cooling water inlet and exit lines enter and leave the reactor through fittings attached to the head of the reactor (Figure 3-14). The solenoid valve is installed on the cold water line with a flow connection to the cooling coil and an electrical connection to the digital controller. It is used to control the cooling water flow rate through the coils and an ON/OFF control approach is used where the valve is operated as either fully opened or fully closed.

The reaction temperature set-point is set on a digital controller while the instantaneous reaction temperature is measured with a PT-100 Class A temperature sensor. The sensor is encased in a metal sheath which protects it from physical damage and extends into the reactor on the same radius as the baffles surrounding the catalyst basket. A TTM-004 Toho digital temperature controller is used and has two separate PID control loops; one for heating and a second one for cooling. The first loop controls the voltage supplied to the band heater while the second loop, with its own self-tuning parameters, is used to activate a solenoid valve to control the flow of coolant through the installed cooling coil. A switch-over control approach is used and the temperature within the vessel is continuously displayed on the digital controller. The reactor temperature was however not continuously logged.

The reactor temperature is essentially maintained by a balance between the voltage supply to the heating jacket and flow of cooling water through the coils. A schematic of the control system is shown in Figure 3-16. The energy balance however also depends on the polymerization rate and the temperature difference between the reactor temperature and the ambient temperature. The system has been shown to be highly effective in controlling the exothermic polymerization reactions and it is possible to maintain the reaction temperature to within ±0.5 °C of the set point for the duration of the reaction. Slightly larger oscillations however existed for the first few minutes during the initial stage of the reaction.

Figure 3-13 Band Heater which Fits Around the Reactor Cylinder

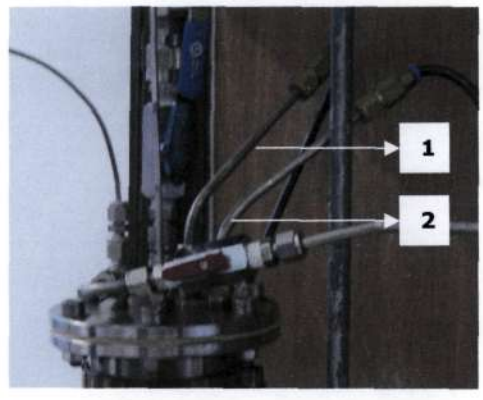

Figure 3-14 Cooling Water Inlet Line (1) and Cooling Water Outlet Line (2)

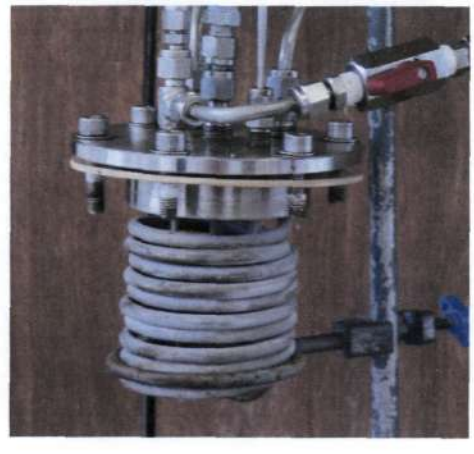

Figure 3-15 Reactor Cylinder with Spiral Cooling Coils

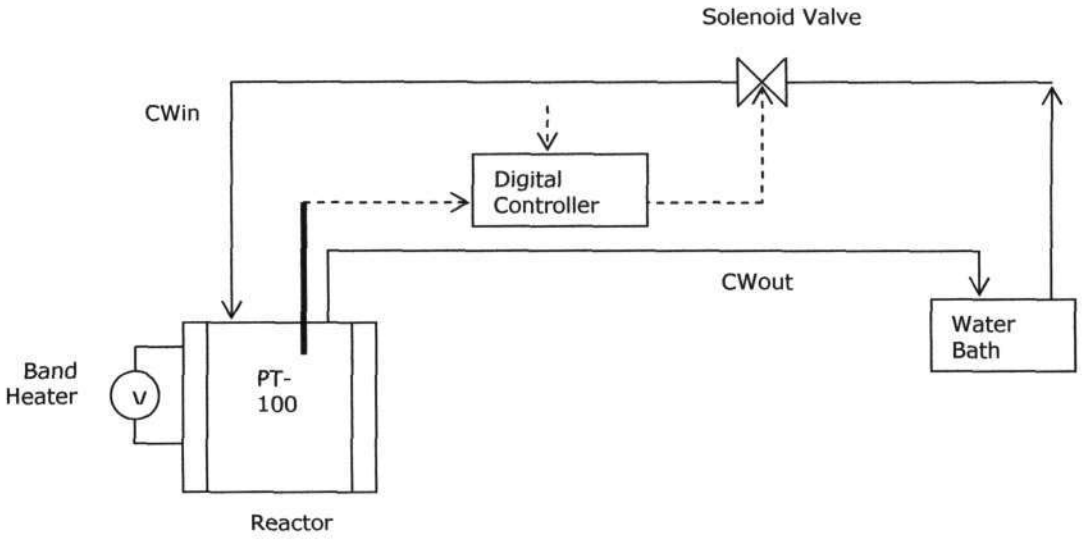

Figure 3-16 Schematic of the PID Feedback Control used to maintain the Reactor Temperature at Set-point

3.6 Reactor pressure control system

A ¼" Baumann valve, type 51000, complete with Type 3661 electro-pneumatic positioner and 67 CFR regulator (Figure 3-17) is used to control the reactor pressure at the set-point by controlling the flow-rate of ethylene gas into the reactor. The reactor pressure is measured by a pressure transmitter having a range of 0-10 bar and this pressure was recorded every second onto a spreadsheet. An example of the reactor pressure control is shown in Figure 3-19.

Figure 3-17 Pressure Control Valve

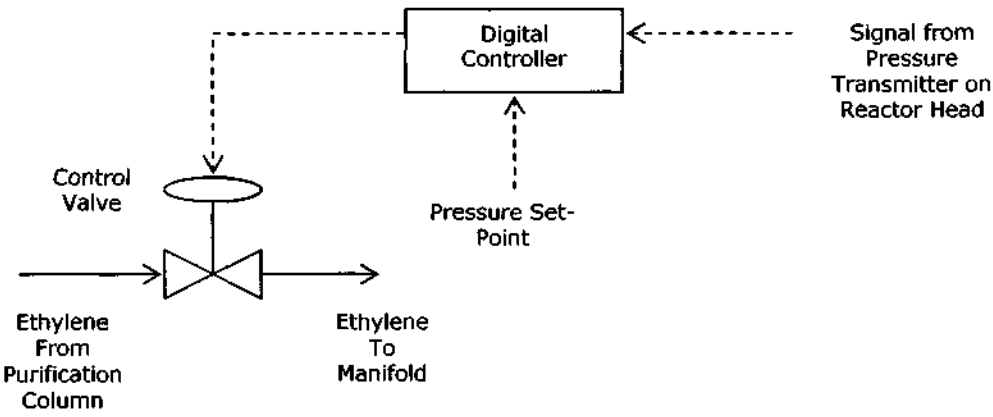

Figure 3-18 Schematic of the Reactor Pressure Control System

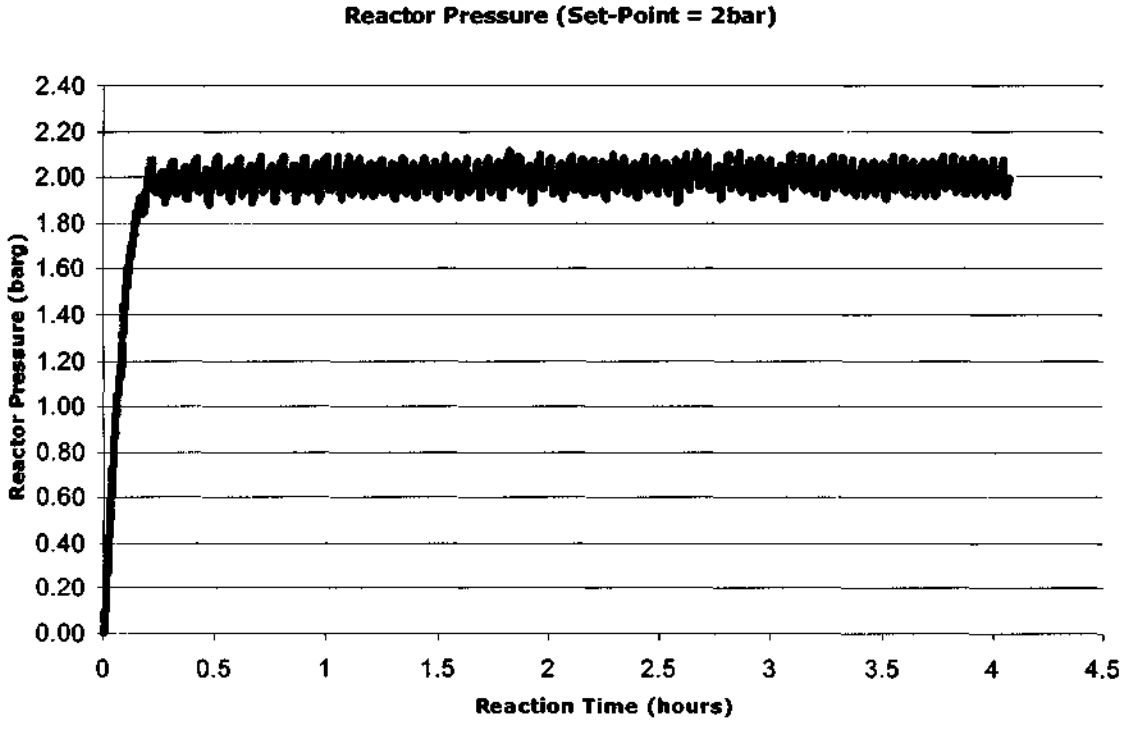

Figure 3-19 Example of Reactor Pressure Control (Set-Point = 2barg)

3.7 Overall Schematic of Experimental Setup

A schematic of the reactor system is shown in Figure 3-20. The reactor is operated under semi-batch mode with a feedback pressure control system.

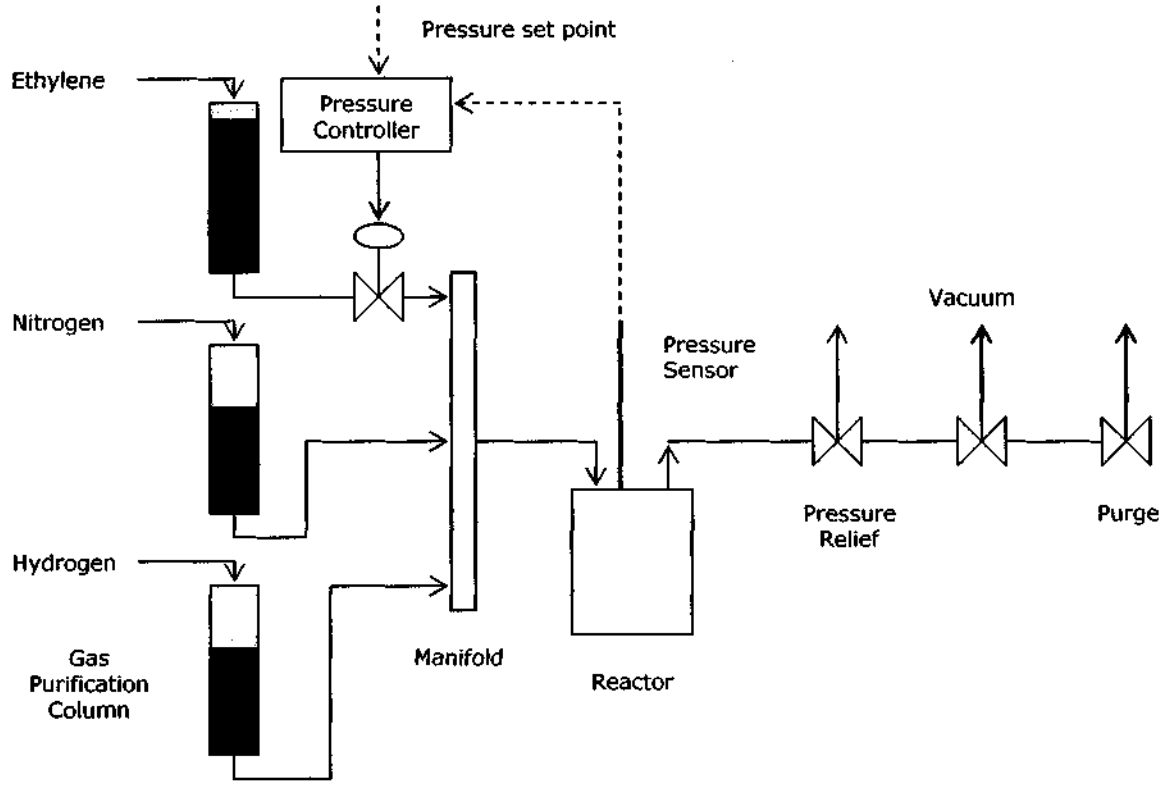

Figure 3-20 Overall Schematic of Reactor System

Chapter 4

Synthesis of a $MgCl_2$-Supported Ziegler-Natta Catalyst

In this chapter the procedures used to prepare the $MgCl_2$ support and the Ziegler-Natta catalyst are described. The spherical particles of $MgCl_2$ support were prepared by the re-crystallization (precipitation) method of solvent evaporation. The method essentially consists of reacting crystalline anhydrous $MgCl_2$ with ethanol, a protonic electron donor which readily dissolves the $MgCl_2$, and forming an emulsion of the liquid adduct with silicon oil, used as a dispersant. This is followed by precipitation of the active support, $MgCl_2.n$EtOH. Two different $MgCl_2$ supports were prepared, one with an ethanol/$MgCl_2$ molar ratio of 76.3 (S1) and the other with a ratio of 51.1 (S2). The Ziegler-Natta catalysts were then prepared by impregnating $TiCl_4$ and dibutyl phthalate (DBP), used as an internal electron donor (ID), onto the active supports. Scanning electron microscopy (SEM) analysis showed that both the support and catalyst particles were essentially spherical. The catalysts prepared from S1 (C1) and S2 (C2) were found to contain 3.687 wt% Ti and 6.477 wt% Ti respectively. These amounts were determined by inductively coupled plasma (ICP) analysis. Both the catalysts and the supports were then analyzed using infrared (IR) spectroscopy to determine if they still contained ethanol. Finally, experiments were carried out to determine if the catalysts, when activated with triethylaluminium (TEA), the co-catalyst, were capable of polymerizing ethylene. The final polymerization products were analyzed using IR spectroscopy and the products proved to be polyethylene.

4.1 Introduction

Highly active Ziegler-Natta catalysts for olefin polymerization prepared by impregnating $TiCl_4$ on a $MgCl_2$ support have been reported on extensively in the literature, particularly in recent years. One of the first examples however, dates back to 1955 and was an invention by Petrochemicals Ltd. (British Patent, 1955). They reasoned that since it is the "surface layer of each catalyst particle which is effective in promoting the polymerization reaction" it followed that a greater or more accessible catalyst surface area would result in a higher catalytic activity. They proposed that this could be achieved by supporting $TiCl_4$ on various carriers such as $MgCl_2$ and $MgCO_3$. The dimensions of a $MgCl_2$ crystal lattice, where Mg^{2+} has an ionic radius of 0.066 nm, makes it an optimum support for $TiCl_4$, where Ti^{4+} has a ionic radius of 0.068 nm (van der Ven, 1990).

In order to be successfully used as a catalyst support $MgCl_2$ must first be converted to a form which can efficiently incorporate $TiCl_4$, a process referred to as activation. The prevailing preparation method of active $MgCl_2$ is the ball-milling of anhydrous $MgCl_2$ with $TiCl_4$ or the treatment of a $MgCl_2$–electron donor complex, obtained by ball milling, with $TiCl_4$. This method, however, has only limited control over the texture of the catalysts since $MgCl_2$ prepared in this way still has a crystal structure which is too regular for loading $TiCl_4$. Also, since polymer morphology has a tendency to duplicate that of the catalyst, catalysts produced in this way result in undesirable morphology of the polymer particles. This phenomenon, known as the replication phenomenon, has been exploited industrially for some time and occurs when the polymer begins to grow not only on the active centers on the external surface of the catalyst but also on those inside the porous catalyst particle. The size and shape of the catalyst particles therefore control the size and shape of the resulting polymer particles. Other methods of catalyst preparation such as the re-crystallization (precipitation) method have as a result also been studied in order to overcome the disadvantages of the ball-milling method.

Therefore, in order to improve catalytic activity and to control polymer morphology the Ziegler-Natta catalyst preparation for olefin polymerization through $TiCl_4$ impregnation on re-crystallized $MgCl_2$ has been one of the most studied methods in recent years. The method involves dissolving crystalline anhydrous $MgCl_2$ in various media followed by the re-crystallization of the $MgCl_2$ from solution. The newly generated porous $MgCl_2$ has a crystal structure which is much better at supporting $TiCl_4$. Various types of chemical reagents have been used for the generation of highly disordered $MgCl_2$ with protonic electron donors, such as alcohols, often being preferred since they readily dissolve the $MgCl_2$ crystals. The support, which is essentially obtained through the formation of $MgCl_2.n$ROH liquid adducts followed by the controlled regeneration of the active support, can be prepared by various precipitation methods such as quick cooling, solvent evaporation, or precipitation by addition of either $SiCl_4$ or $TiCl_4$ to the liquid adducts. The method of solvent evaporation has been used to prepare the supports in this work. Finally, in order to obtain a catalyst for the polymerization of ethylene, $TiCl_4$ and an internal electron donor, most commonly dibutyl phthalate (DBP), are impregnated onto the active spherical support particles.

4.2 Preparation of the $MgCl_2$ support and Ziegler-Natta catalyst

4.2.1 Chemical reagents

Anhydrous magnesium dichloride ($MgCl_2$, >98%), anhydrous n-hexane (>99%, SeccoSolve®), dibutyl phthalate (DBP, >99%) and anhydrous ethyl alcohol (99.8%) were purchased from Merck. The ethyl alcohol was stored over molecular sieve 3A (Merck) while the other reagents were used without further purification. Anhydrous heptane (99%), triethylaluminium (TEA, 1M solution in heptane), titanium tetrachloride ($TiCl_4$, 99%) and mineral oil (white, light) were obtained from Aldrich and were used without further purification. Silicon oil was obtained from a local company, Laboratory Consumables and Chemical Suppliers.

4.2.2 Experimental equipment

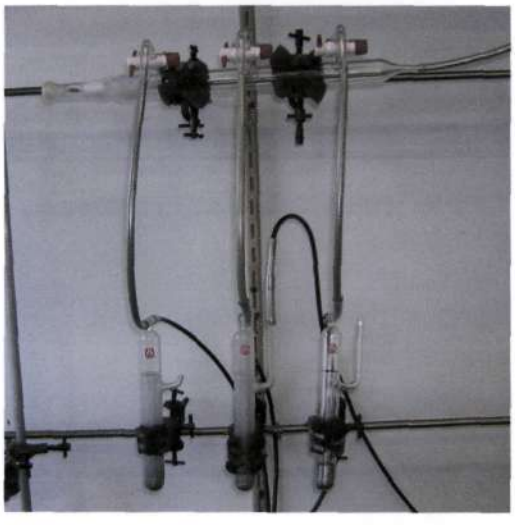

Figure 4-1 Nitrogen Manifold Supplying Three Mercury Bubblers

Figure 4-2 Reaction Flask used for Support Preparation

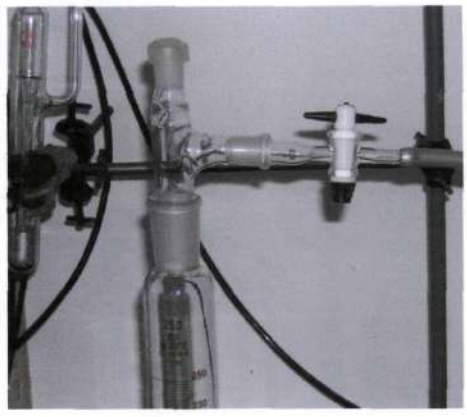

Figure 4-3 Measuring Cylinder Fitted with a Special Adapter for the Measurement and Transfer of Air Sensitive and Anhydrous Liquids

Figure 4-4 Frit Funnel and Vacuum Flask for Vacuum Drying the Support and Catalyst

All manipulations of the catalyst, the support, and of the anhydrous and air-sensitive chemicals used in their preparation were carried out under an inert atmosphere of ultra high purity nitrogen (UHP, Afrox) using standard Schlenk techniques, double tipped needle transfer techniques, syringe transfer techniques, and a glove bag (AtmosBag, Aldrich). Special Schlenk type glassware (Figure 4-1 to Figure 4-4) has been specifically designed and created to make manipulations involving air sensitive and anhydrous chemicals both simple and reliable. Although other inert gases are available, nitrogen was preferred because it has a density almost equal to that of air (relative density = 0.97). It therefore does not rapidly diffuse out of a system which makes it easier to maintain an inert atmosphere in cases where a flask needs to be momentarily opened.

Figure 4-1 shows the nitrogen manifold with three outlet ports, each fitted with a Teflon stopcock and feeding a mercury bubbler. Nitrogen was fed to the manifold from a gas cylinder via plastic tubing. The other end of the manifold was fitted with a silicon septum and was used together with the double tipped needles to pressurize air and moisture sensitive reagents out of their septum sealed bottles and into reaction vessels and the measuring cylinder. For these transfers one end of a needle was inserted into the septum on the manifold and the other was inserted into the septum on the reagent storage bottle but was kept above the liquid level. A second needle was then also inserted into the septum of the reagent bottle and the other end was inserted into the septum of a reaction vessel or measuring cylinder into which the liquid reagent was intended to be transferred into. Once a nitrogen pressure was applied to first needle, the tip of the second was pushed below the surface of the liquid and the desired amount was pressurized out. This method of reagent transfer is referred to as the 'double tipped needle transfer technique'. All needles and syringes were thoroughly purged with nitrogen before use. The mercury bubblers were used to maintain an air tight reaction system and to provide pressure relief in reaction vessels. Nitrogen was fed to all reaction vessels via the mercury bubblers so as to prevent nitrogen over-pressure in the vessels while at the same time maintaining a pressure slightly above atmospheric so ensure that no air was sucked in. During reactions excess reaction pressure was released through these bubblers.

The reaction flask used for the preparation of the support is shown in Figure 4-2. The flask is fitted with an inlet for nitrogen, to which a Teflon stopcock is fitted, and a septum inlet for the introduction of reagents by means of a syringe or double tipped needle (cannula transfer). Figure 4-3 shows the measuring cylinder which has been fitted with a specially modified adapter for the transfer of specific volumes of moisture and air sensitive reagents. To transfer reagents out of the measuring cylinder, a double tipped needle was inserted into the top septum and the reagents were pressurized out through the needle by supplying a nitrogen pressure by means of the stopcock on the side. Figure 4-4 shows the frit tube used for the catalyst preparation and a vacuum flask. The frit tube, like the reaction flask, is fitted with a nitrogen inlet Teflon stopcock and a septum inlet. The set-up illustrated here was used for vacuum drying both the support and the catalyst particles. All the nitrogen inlet tubes fitted onto the glassware have an olive at the end with ridges around which the nitrogen tubing snugly fits. Five nitrogen/vacuum cycles were carried out on all reaction vessels to remove air before reagents were introduced into them. An air driven vacuum pump (PIAB LVX20L) was used for vacuum operations.

4.2.3 $MgCl_2$ support preparation procedure

The first step in the synthesis of the catalyst consisted of the preparation of the catalyst support by the re-crystallization method involving solvent evaporation. Silicon oil was heated to 80°C and placed together with the ethyl alcohol, anhydrous $MgCl_2$, a weighing scale and the 500 mL three neck glass flask (Figure 4-2) into the AtmosBag. The bag was then sealed and five nitrogen/vacuum cycles were carried out to ensure that the space inside the bag was air and moisture free. To the reaction flask was added 100g of the silicon oil (which cooled to

approximately 50°C during the nitrogen/vacuum cycles), $MgCl_2$ and ethyl alcohol (for specific quantities see Table 4-1). The reagents were added in that specific order. The ethanol was used as a solvent to dissolve the $MgCl_2$ and the silicon oil was used to prevent the re-crystallized $MgCl_2$ from aggregating during the re-crystallization process. Most of the $MgCl_2$ dissolved in the ethanol at this point but separate ethanol, silicon oil and $MgCl_2$ phases could still be distinctly seen. All necks of the flask were then sealed, i.e. the nitrogen stopcock was closed, a rubber bung was inserted into the large center neck and a Suba Seal® (Aldrich) silicon septum was inserted into the third neck.

The flask was then removed from the AtmosBag and placed in a silicon oil bath preheated to 70°C and with a high stream of nitrogen applied through the nitrogen inlet tube of the flask the top bung was removed and one that accommodated a mechanical stirrer was inserted in its place. The mixture was then vigorously stirred at 1030 rpm for emulsification and the temperature was increased to 120°C in about 50 minutes. Within a few minutes of heating, the $MgCl_2$ completely dissolved in the ethanol and a perfect emulsion was formed with the $MgCl_2$-ethanol liquid adducts and the silicon oil. On continuing heating the emulsion, the ethanol slowly evaporated and within 50 minutes $MgCl_2$-ethanol solid particles began to precipitate.

The mixture in the reaction flask was then transferred via an adapter, connected to where the septum was fitted, to a 2 L flask containing approximately 300 mL of heptane at room temperature to wash the support by removing the silicon oil and any residual ethanol. The liquid was then removed via a stopcock fitted on the 2 L flask and another 200 mL of heptane (transferred using the double tipped needle technique) was added to further wash the re-crystallized particles. The precipitated support was then transferred to the glass Schlenk tube having a fritted disk at the bottom (Figure 4-4) where a wash with 50 mL heptane was repeated 5 times. After all the oil was washed away the white powder (Figure 4-5) of the $MgCl_2$-ethanol complex was dried under vacuum for 30 minutes to remove any residual heptane and then thermally treated to partially dealcoholate the re-crystallized particles. The temperature of the oil bath used for the thermal treatment was increased steadily from room temperature to about 120°C in 2 hours.

Table 4-1 Quantities of $MgCl_2$ and Ethanol used in Support Preparation

Support	$MgCl_2$ g	Ethanol g	EtOH/$MgCl_2$ molar ratio
S1	1.3	48	76.32
S2	1.7	42	51.07

4.2.4 Ziegler-Natta catalyst preparation procedure

The second step in the synthesis of the catalyst consisted of treating the partially dealcoholated $MgCl_2$-ethanol complex with $TiCl_4$ and dibutyl phthalate, the internal electron donor. To the glass Schlenk tube with a fritted disk at the bottom was added 1g of the $MgCl_2$ support and 15 mL of

heptane, used as a hydrocarbon diluent. The $MgCl_2$ support/heptane mixture was then cooled to -8°C in a bath consisting of a mixture of ethylene glycol and water (60:40 V/V) and dry ice. 20 mL of $TiCl_4$ was then slowly added to the flask, using the double tipped needle transfer technique, to remove ethanol in the $MgCl_2$-ethanol complex by reaction with $TiCl_4$ and to fix additional $TiCl_4$ onto the $MgCl_2$ support. The reaction temperature was then increased from -8°C to 60°C in 3 hours. The reaction flask was transferred to a silicon oil bath once the ethylene glycol/water bath warmed up to 15°C. In order to avoid the breakup of the support particles and to therefore ensure that the catalyst particles maintained the morphology of the support no stirrers were used in the catalyst preparation. The glass tube was therefore swirled occasionally to assist with mixing.

When the reaction temperature reached 60°C, 0.3 mL of dibutyl phthalate, an organic diester used as an internal electron donor, was added. The temperature was then increased to 110°C in 3 hours and thereafter maintained at this temperature for another hour. The liquid was then removed by filtration at reaction temperature and an additional 20 mL of $TiCl_4$ was added to the solid particles remaining in the reaction vessel. The temperature was then maintained at 110°C for another hour. The suspension was thereafter cooled to 50°C and washed with 30 mL of heptane to remove the last traces of un-reacted $TiCl_4$. The wash was repeated 10 times and hexane was used for the final wash. The light yellow/brown catalyst particles (see Figure 4-5) obtained were then dried under vacuum at room temperature for 30 minutes. The catalyst prepared from S1 is referred to as C1 while that prepared from S2 is referred to as C2. Both catalysts were prepared using the same procedures and reagent quantities.

Figure 4-5 White $MgCl_2$-Support Particles (Left) compared with the Yellow/Brown Catalyst Particles (Right)

4.2.5 Characterization results

X-ray powder diffraction (XRD) patterns were recorded on a Philips 1729 X-ray diffractometer with Co Kα radiation in the range $16° < 2\theta < 60°$. The diffractometer was operated at 40 kV and 40 mA with λ = 1.7901970Å and a chart speed = 2 cm/min. XRD peaks for crystalline anhydrous $MgCl_2$ were observed at 2θ = 17.56°, 35.45°, 40.85°, 45.80°, 54°, 59.10°, and

59.30°. When these peak intensities were compared with those of the re-crystallized $MgCl_2$-ethanol adducts it was found that all corresponding peaks were much weaker, suggesting that $MgCl_2.nC_2H_5OH$ was in fact formed. XRD diffraction analyses were carried out at the Department of Geology at the University of KwaZulu-Natal, Westville campus.

The morphology of the prepared $MgCl_2$-support and Ziegler-Natta catalyst were examined using a scanning electron microscope (LEO 1450 SEM). The samples were gold coated prior to being analyzed. The approximate spherical shape of the support and catalyst particles can be seen in Figure 4-6 and Figure 4-7 respectively. Since it was not possible to analyze the particles under a nitrogen atmosphere and since both the catalyst and support particles melt when in an environment containing air, it was not possible to attain better micrographs. The SEM micrographs were taken at the Department of Biology at the University of KwaZulu-Natal, Howard College.

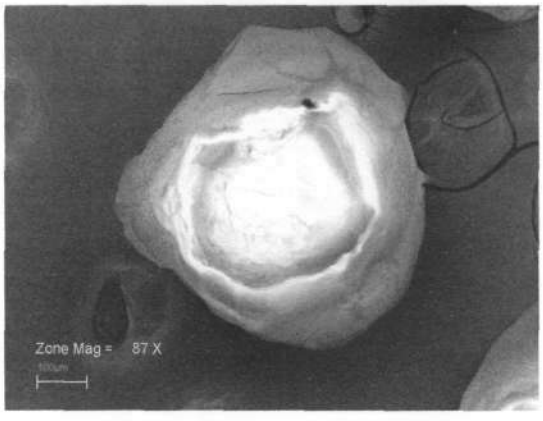

Figure 4-6 SEM Micrograph of a $MgCl_2$ Support Particle

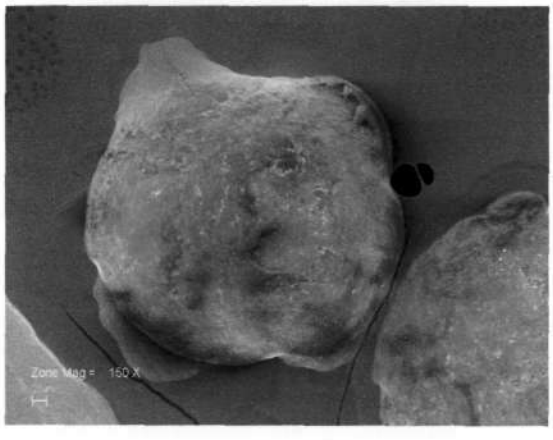

Figure 4-7 SEM Micrograph of a Catalyst Particle

The particle size distribution (PSD) of the catalyst (C2) was measured in the glove bag using sieve screens. It was found that approximately 70% of the particles had a diameter between 125 and 250 μm (Figure 4-8).

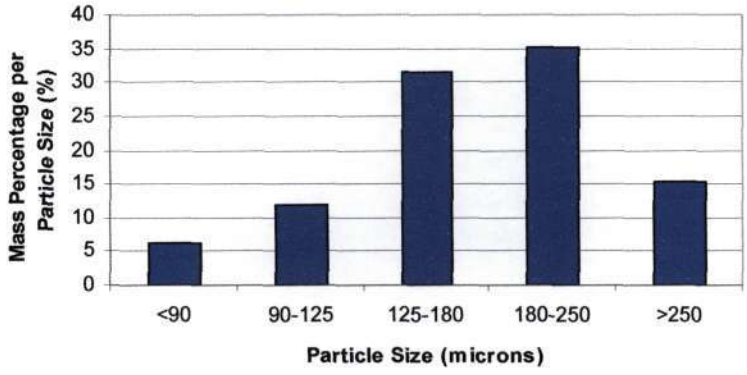

Figure 4-8 Particle Size Distribution of Catalyst Particles

Results of the Inductively Coupled Plasma (ICP) analysis on the final catalysts are as follows:

Table 4-2 Quantities of Mg and Ti Found in Catalysts C1 and C2

Catalyst	Mg wt%	Ti wt%
C1	17.19	3.687
C2	10.1	6.477

Both the support and catalyst particles were analyzed by Infrared Spectroscopy, using a Nicolet Impact 400D FTIR. The aim of the IR analysis was to determine if the support and catalyst contained large amounts of ethanol in spite of the fact that the support was thermally treated to remove ethanol prior to titanium impregnation and that the first titanium treatment was also meant for this purpose. FTIR analyses were carried out at the Department of Chemistry, at the University of KwaZulu-Natal, Howard College.

The method used for the FTIR analysis is described below. The powder samples to be examined were prepared by grinding together with potassium bromide (KBr) powder while aiming at a particle size small enough to cause scatter (theoretically < 2 μm). The samples were then pressed into a disk while attempting to keep the powder as homogenously dispersed as possible.

Method used for FTIR analysis

1. A small amount of sample, ~2mg, and KBr powder, ~200mg, were placed onto an agate mortar on a stand below a heating lamp. The KBr was of spectroscopic grade and was previously stored in a furnace to keep it moisture free.

2. The powders were ground together, with an agate pestle, until the sample was well dispersed and the mixture has the consistency of fine flour.
3. The die was then assembled. The ground mixture was transferred into the cylinder bore ensuring that it was evenly distributed across the polished face of the lower pellet. A plunger was then inserted to achieve a flat, even surface.
4. The second pellet was then inserted, polished face towards the mixture, into the bore. The plunger was inserted above this pellet and an O-ring placed in position to ensure a tight seal.
5. The die assembly was then securely placed in a hydraulic press, between the ram and the piston.
6. A vacuum was applied to the die assembly for approximately 2 minutes to remove air from the disk.
7. Thereafter the pressure in the press was increased to 10 tons.
8. The pressure was slowly released after approximately 3 minutes.
9. The vacuum was shut of and the die removed from the press.
10. The die was then dismantled using a hand press.
11. After observing that the disk was translucent and that the sample was homogeneously distributed in the disk, the disk was mounted on a disk holder and transferred to the spectrometer.

The infrared spectra of S2 and of C1 and C2 can be seen in Figure 4-12, Figure 4-13 and Figure 4-14 respectively and that of the KBR, pure $MgCl_2$ and ethanol can be seen in Figure 4-9, Figure 4-10 and Figure 4-11 respectively.

The presence of ethanol in a sample can be identified by both an -O-H- group, represented by a broad stretch between $3600cm^{-1}$ and $3200cm^{-1}$, and by a -C-O- group, represented by strong peaks between $1260cm^{-1}$ and $1000cm^{-1}$. These peaks can be seen in Figure 4-11. The IR spectra of both the KBR and the $MgCl_2$ also consisted of a broad stretch between $3600cm^{-1}$ and $3200cm^{-1}$. The stretch observed for $MgCl_2$ is most probably a result of absorbed moisture during the disk preparation. The other two peaks of the $MgCl_2$ spectrum, one at $2258cm^{-1}$ and the other at $1642cm^{-1}$ are characteristic of $MgCl_2$.

The spectra for S2 and for C1 and C2 all contain very broad peaks between $3600cm^{-1}$ and $3200cm^{-1}$. These could be a result of hydrogen bonding in ethanol, but also as a result of moisture absorbed during disk preparation and from the KBR. The peaks representing the -C-O- group in the support and the two catalyst samples are however extremely small and given that it is essential for an alcohol to contain both an -O-H- and a -C-O- group it was concluded that the thermal and $TiCl_4$ treatments were effective in removing most of the ethanol from the respective particles.

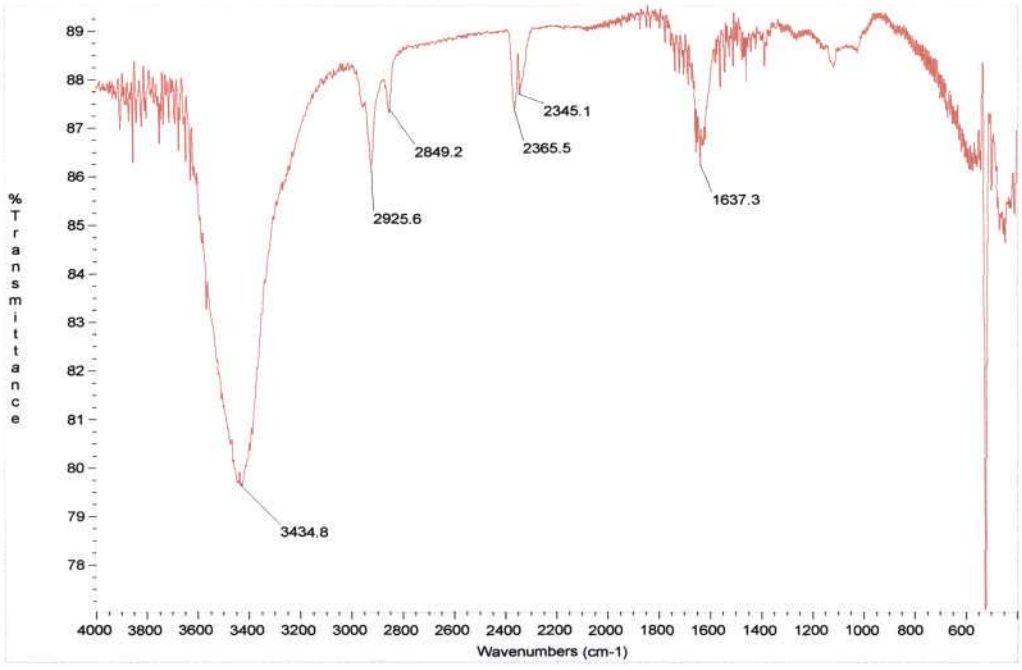

Figure 4-9 IR Spectrum of KBR

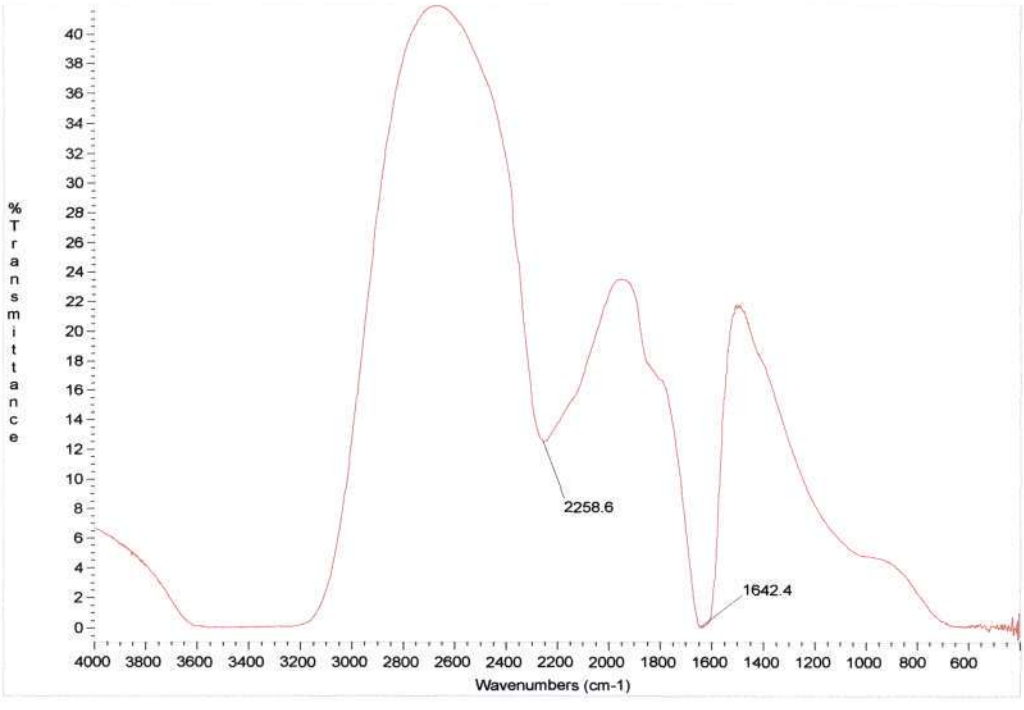

Figure 4-10 IR Spectrum of $MgCl_2$

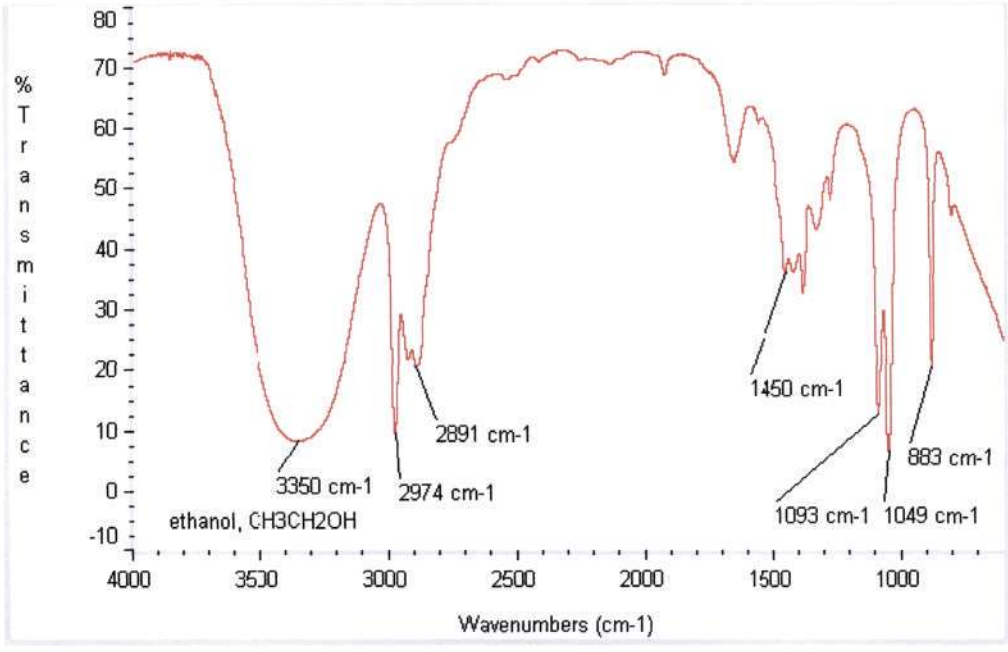

Figure 4-11 IR Spectrum of Ethanol

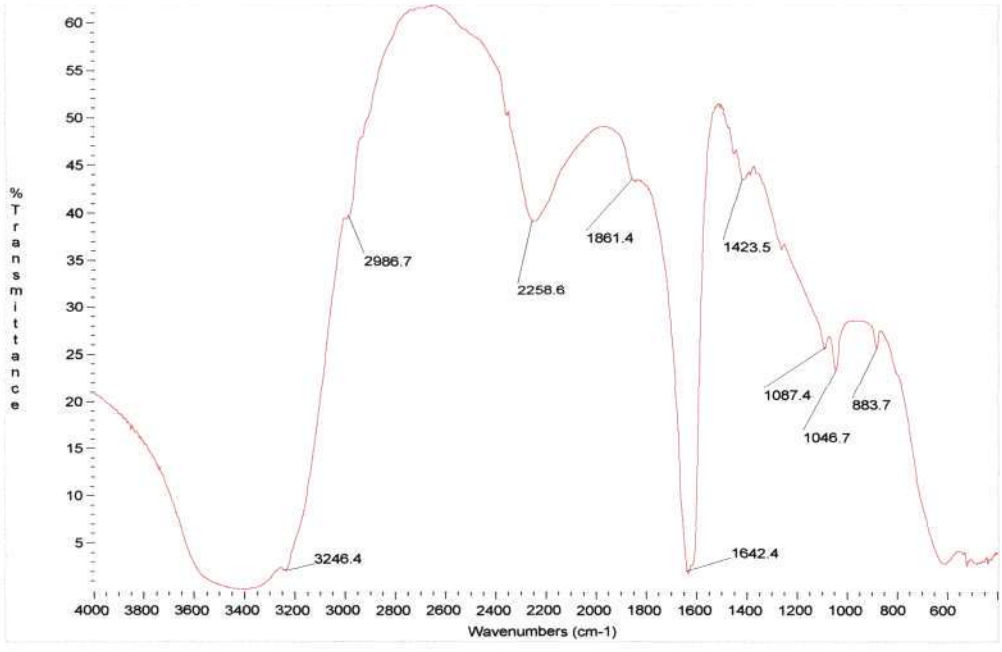

Figure 4-12 IR Spectrum of $MgCl_2$ Support S2

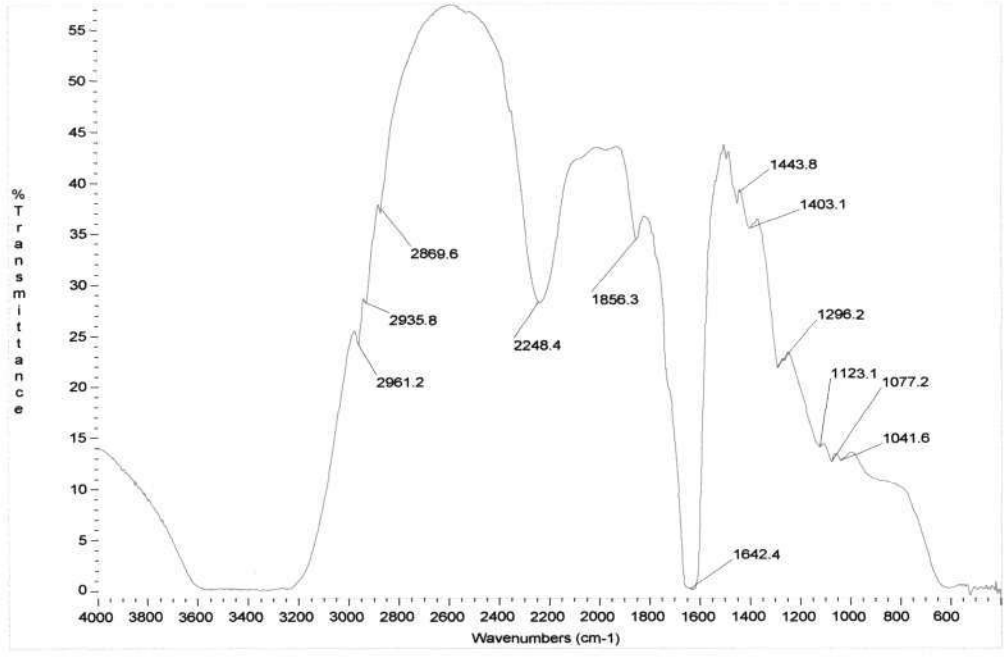

Figure 4-13 IR Spectrum of Catalyst C1

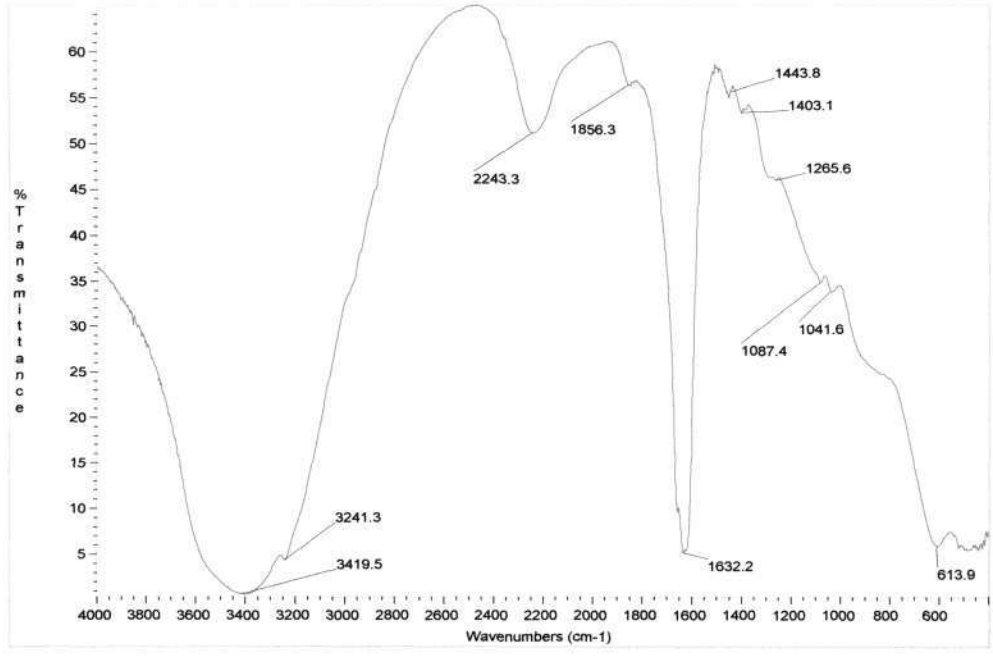

Figure 4-14 IR Spectrum of Catalyst C2

4.2.6 Discussion

The method used to prepare the $MgCl_2$ support essentially consisted of firstly forming an emulsion of anhydrous $MgCl_2$ and ethanol with a liquid that is immiscible with and does not react with the $MgCl_2$-ethanol adducts. This was followed by re-crystallizing the $MgCl_2$ from solution. The liquid is referred to as the dispersant and its purpose is to prevent the $MgCl_2$ from aggregating during the re-crystallization process. The formation of the $MgCl_2$-ethanol liquid adducts is represented by the following equation:

$$\mathbf{MgCl_2 + CH_3CH_2OH \rightarrow MgCl_2.}n\mathbf{CH_3CH_2OH}$$

The mixture of $MgCl_2$, ethanol and the dispersant (silicon oil) was mechanically stirred at a speed of 1030 rpm to form an emulsion. After the $MgCl_2$-ethanol liquid adducts were perfectly emulsified with the dispersant the emulsion was further heated and stirred in order to eliminate the ethanol by evaporation and in that way cause the $MgCl_2$ in solution to re-crystallize (precipitate). Due to the difference in the boiling points of the ethanol and the silicon oil, only ethanol was eliminated during this step. The effect of the dispersion speed has not been investigated in this work, but from research undertaken by Ye *et al.* (2002) it is known that the dispersion speed is a critical factor in controlling the particle size and the particle size distribution of the precipitated support particles and more specifically these researches found that the particle size of the adducts increased when the stirring speed of the emulsion was increased.

The method of support re-crystallization used in this work is referred to as the method of solvent evaporation and essentially consists of precipitating the $MgCl_2$-ethanol adducts out of solution by evaporating off the solvent (ethanol) in which it is dissolved. This method has also been used by Chung *et al.* (1995), Choi *et al.* (1996) and Parada *et al.* (2002), with the only difference being that these researchers used a magnetic stirrer to form the emulsion and evaporated off the ethanol under vacuum.

The method of using a vacuum to evaporate off the ethanol has been tested in this work. A solid bung was used to seal the centre neck of the reaction flask and a vacuum was applied to the side arm once an emulsion of the $MgCl_2$, ethanol and silicon oil had been formed. As in the works mentioned above, a magnetic stirrer was used to emulsify the mixture. $MgCl_2$ adducts however failed to re-crystallize under vacuum, even for times of up to 4 hours. An alternate method of solvent evaporation has therefore been proposed and it is the method that has been successfully used in this work. A mechanical stirrer was used to stir the emulsion at higher speeds than the magnetic stirrer was capable of and a bung with a hole to accommodate the stirrer was used to seal the centre neck. As it is essential that no air comes in contact with the emulsion, the emulsion was stirred under a constant stream of high purity nitrogen which entered through the nitrogen inlet tube on the reaction flask and exited through the annular space between the bung and the stirrer shaft. Air was therefore prevented from entering through this opening. Once the emulsion was formed, it was further stirred and heated until the

ethanol evaporated off and also exited through the annular space between the bung and stirrer shaft. With this method the $MgCl_2$ was found to re-crystallize in a period of approximately 50 minutes.

Another method of support precipitation is that of quick cooling, and involves the quick quenching of the emulsion in a hydrocarbon solvent which is generally at temperatures below -20 °C. The emulsion is normally transferred to the cold solvent by pressuring it through a thin pipe which most commonly has a diameter of approximately 3mm. This method has been used by Forte and Coutinho (1996), Wu *et al.* (1999), Ye *et al.* (2002) and Parada *et al.* (2002). It has also been tested in this work. Once the emulsion had been formed, a special adapter was used to connect the reaction flask to a 2L flask containing heptane at -30 °C. The adapter allowed for the reaction emulsion to be quickly poured out through a 4 mm tube and into the cold heptane. The reaction mixture was not pressurized out of the reaction flask due to the obvious safety hazards involved in pressurizing glass reaction vessels. This method however, only served to solidify the emulsion once it came into contact with cold heptane and no re-crystallized support particles were formed.

A further method of precipitating the support is by the introduction of the emulsion to either $SiCl_4$ or $TiCl_4$. Hu and Chien (1988) precipitated the support using $TiCl_4$, while Kothandaraman and Devi (1994) used $SiCl_4$. Parada *et al.* (2002) investigated the effects of both $TiCl_4$ and $SiCl_4$ as precipitating agents. This method has however not been tested in this work.

Of the three methods of support re-crystallization mentioned, only one has been used to prepare the support so a comparative study to investigate the performance of $TiCl_4$ catalysts supported on $MgCl_2$ re-crystallized by each of the different techniques could not be made. Such a study was however undertaken by Parada *et al.* (2002). They found that the variations of the dealcoholation levels due to the different re-crystallization techniques were found to highly influence the catalytic activity and the catalysts obtained by re-crystallization as a result of addition to $SiCl_4$ were found to be the most active, essentially due to almost all the ethanol being eliminated from the $MgCl_2$ during precipitation. They further found that the alcohol was not completely eliminated from the support when it was precipitated by the methods of quick cooling and solvent evaporation and it was for this reason that the supports particles synthesized in this work were thermally treated and that the $TiCl_4$ impregnation step was repeated.

The liquids most commonly used as a dispersant are aliphatic, aromatic or cycloaliphatic hydrocarbons and silicon oils. The effects of two types of such dispersants, mineral oil and silicon oil, were tested in this work. Although it was possible to form a perfect emulsion with the mineral oil and the $MgCl_2$-ethanol adducts it was not possible to obtain re-crystallized $MgCl_2$ adducts as separate particles. Instead, a completely agglomerated solid mass resulted after approximately 20 minutes of forming the emulsion. Silicon oil was found to be more appropriate and was as a result used for the support preparation. The one disadvantage of using silicon oil,

however, was that for reaction times longer than 60 minutes, the re-crystallized adducts were also found to be in the form of an agglomerated solid mass so only certain ratios of $MgCl_2$ and ethanol could be used so as to ensure that the $MgCl_2$ completely dissolved and that the adducts completely re-crystallized in a period shorter than 60 minutes. The agglomerated solid masses were attributed to changes in the oils due to the long heating times under vigorous stirring.

It was also found in this work that for ethanol/$MgCl_2$ molar ratios lower than 20 it was not possible to obtain the adducts in a totally dissolved form. Even for mixing times as long as 3 hours, the $MgCl_2$ did not completely dissolve in the ethanol. The optimum ethanol/$MgCl_2$ molar ratios were found to be between 50 and 80. For these ratios it was possible to obtain perfectly melted adducts which re-crystallized within 50 minutes. When a larger ratio than this was used the $MgCl_2$ dissolved completely but the time for the ethanol to evaporate was long and the final result was either the formation of an agglomerated solid mass or the $MgCl_2$ did not re-crystallize at all. Also, when the $MgCl_2$ was added to silicon oil which was at room temperature, the time required for the crystals to dissolve and for the adducts to re-crystallize was too long and the result was again an agglomerated solid mass rather than the preferred solid individual particles. The $MgCl_2$ was therefore added to silicon oil heated to a temperature of approximately 50°C.

The effects that the quantity of ethanol used has on the properties of the support have not been examined in detail in this work but have been reported on extensively in the literature. The quantity of ethanol used in the support preparation and more specifically the amount incorporated onto the re-crystallized $MgCl_2$-ethanol adducts has been reported to have a significant effect on the porosity, surface area and particle size of both the support and the final catalyst. The amount of ethanol incorporated has also been reported to be related to the activity of the final catalyst. Chung *et al.* (1995) prepared two different supports and found that the support prepared using a larger quantity of ethanol had a larger surface area and a smaller particle size (Table 4-3). They concluded that the smaller particle size was due to the decreased $MgCl_2$ concentration in the ethanol droplets in the dispersant.

Table 4-3 Characterization of Supports and Catalysts (Chung *et al.*, 1995)

	Surface area m^2/g	**Ethanol** wt%	**Avg. size** μm
$MgCl_2$/DNBP/EtOH (30mL)	8.1	62.3	35.6
$MgCl_2$/DNBP/EtOH (30mL)/TEA	101.5	19.7	17.6
$MgCl_2$/DNBP/EtOH (30mL)/TEA/$TiCl_4$	112.6	5.57	14.1
$MgCl_2$/DNBP/EtOH (100mL)	12.1		25.2
$MgCl_2$/DNBP/EtOH (100mL)/TEA/$TiCl_4$	180.6		13.8

Ethanol, which is the solvent used in this work, has been the alcohol most often used in the preparation of the support in the literature. It has been used by Chung *et al.* (1995), Choi *et al.* (1996), Forte and Coutinho (1996), Wu et al. (1999) and Ye *et al.* (2002). Other alcohols have however been reported to be more efficient. Kothandaraman and Devi (1994) for example

investigated the effects of seven different alcohols (*p*-cresol, *n*-butanol, *n*-pentanol, *n*-hexanol, *n*-octanol, *t*-butanol and *2*-ethylhexanol) and concluded that alcohols with higher carbon numbers and branching were more efficient in increasing the surface area of the catalysts, i.e. *2*-ethylhexanol was found to be most suitable.

Choi *et al.* (1996) compared the effects of propanol to that of ethanol (Table 4-4) and found that the surface area of the catalyst prepared with propanol was larger than that prepared with ethanol. The propanol treated catalyst also showed a lower alcohol content and a higher dibutyl phthalate (internal electron donor) and Ti content than the ethanol treated catalyst. Smaller amounts of alcohol remained in the propanol-treated catalysts after treatment with $TiCl_4$ implying that propanol was more readily removed from the adducts than ethanol. Since $MgCl_2$ forms a $MgCl_2$-alcohol complex by activation with alcohols it is likely that ethanol, a stronger Lewis base than propanol, interacted more strongly with $MgCl_2$ than the propanol did. Also, the $MgCl_2$-ethanol complex formed was thought to retard the Ti impregnation on the support. This was concluded as a result of the higher Ti content found in the catalyst prepared with propanol than in the catalyst prepared with ethanol.

Table 4-4 Characterization of Supports and Catalysts (Choi *et al.*, 1996)

	Alcohol wt%	**Ti wt%**	**Surface area m^2/g**	**Avg. size µm**
$MgCl_2$/DNBP/EtOH (30mL)	62.3			
$MgCl_2$/DNBP/1-Propanol (40mL)	61.1			
$MgCl_2$/DNBP/EtOH (30mL)/$TiCl_4$	13.9	3.6	122.53	13.6
$MgCl_2$/DNBP/1-Propanol (40mL)/$TiCl_4$	9.3	4.88	182.24	12.1

The preparation conditions strongly affect the performance and morphology of the $MgCl_2$ support. The various affects have been studied by Ye *et al.* (2002) and are shown in Table 4-5. They found that poor purity of the reagents led to poor morphology of the adducts. When anhydrous $MgCl_2$ had absorbed some humidity they found that the surfaces of the support particles were irregularly spiny. This was concluded to be due to the complexes between H_2O and $MgCl_2$ which had a negative effect on the $MgCl_2$ dissolving in the ethanol and also dramatically influenced the crystallization process by affecting the velocity of crystallization in certain directions and therefore resulting in the formation of irregular, non-spherical particles. The quality of the reagents used in this work is extremely high, and their high purities were maintained by never exposing them to the atmosphere. The ethanol was stored over molecular sieve 3A to keep it moisture free and the opened bottles of the $MgCl_2$ were stored in a desiccator. All other reagent bottles were fitted with septum caps through which the reagents were pressurized out using double tippled needle transfer techniques which ensured that the reagents were never exposed to the atmosphere.

Table 4-5 Important Conditions for Supported Catalyst Preparation (Ye *et al.*, 2002)

Factor	Affected Aspect
Reagent purity	Catalyst performance
Agitation speed	Particle size and particle size distribution
Time-temperature profile	Performance and composition
Reagent ratios	Particle shape and stereospecificity
Order of reagent addition	Morphology and performance

Prior to the impregnation of dibutyl phthalate (DBP) and $TiCl_4$, the support was subjected to a thermal treatment aimed at lowering the alcohol content and as a result increase the porosity of the support. Findings by Cho and Lee (2003), Forte and Coutinho (1996) and those presented in Brazilian Patent (1990) are discussed here to illustrate the necessity of the dealcoholation step in the preparation procedure.

Cho and Lee (2003) investigated the effects of the thermal treatment on the final alcohol content of the support and on the resulting surface area. It can be seen from their results (Table 4-6) that the alcohol content in the thermally treated support drastically decreased with an increase in the treatment temperature. Also, a decrease in the alcohol content was found to correspond to an increase in the surface area of the support.

Table 4-6 Effect of Thermal Treatment on Final Alcohol Content in Support (Cho and Lee, 2003)

Supports	Alcohol content wt%	Surface area m^2/g
Anhydrous $MgCl_2$	-	1.7
$MgCl_2.4CH_3OH$	56.5	14.1
$MgCl_2.3.33C_2H_5OH$	61.3	12.3
$MgCl_2.4CH_3OH$ at 100°C	13.4	16.8
$MgCl_2.4CH_3OH$ at 200°C	7.21	20.5

Forte and Coutinho (1996) also suggested that support dealcoholation is an important factor which should be considered for good morphology to be attained in the catalyst and hence in the polymer. They found that the amount of Ti incorporated in the catalyst was dependent on both the internal donor used and on the amount of alcohol incorporated into the support. The degree of dealcoholation was found to have a strong influence on both the porosity and surface area of the supports and catalysts.

In Table 4-7 the influence of the degree of dealcoholation on the physical properties of both the support and the catalyst is shown. It can be seen that the degree of dealcoholation has a strong influence on both the porosity and the surface area of the support particles.

It is for the reasons presented above that the support particles in this work were thermally treated prior to $TiCl_4$ impregnation and the FTIR analysis results of S2 shown above indicate that

the thermal treatment was efficient in removing most of the ethanol used in the support preparation.

Table 4-7 Effect of the Degree of Dealcoholation on the Support and Catalyst Properties (Brazilian Patent, 1990)

Dealcoholated support mol EtOH	**1.7**	**1.5**	**1**	**0.4**	**0.15**
Bulk density (g/cm^3)	0.607	0.564	0.535	0.41	nd
Porosity (cm^3/g)	0.904	0.946	1.208	1.602	1.613
Surface area (m^2/g)	9.2	9.1	11.5	36.3	22.2
Catalyst					
%Ti/%DBP	2.5/8.2	2.5/6.8	2.2/6.8	nd	nd
Bulk density (g/cm^3)	0.554	0.555	0.44	nd	nd
Porosity (cm^3/g)	0.405	0.389	0.261	0.427	nd
Surface area (m^2/g)	249	221	66.5	66.5	nd

nd: not determined

The titanium impregnation methods presented in United States Patent (1981) and by Wu *et al.* (1999) were used in the synthesis of the catalyst for this work. The titanation step basically consisted of reacting the $MgCl_2$ support particles with a Ti compound, $TiCl_4$, the active catalyst entity. While the methods proposed in United States Patent (1981) were used as a general guideline in terms of quantities, reaction temperatures and reaction times, the exact preparation procedure more closely resembled that proposed by Wu and co-workers.

In United States Patent (1981) it has been recommended that the reaction with $TiCl_4$ be carried out either by adding the $MgCl_2$ support to undiluted $TiCl_4$ maintained at a temperature between 0 °C and 100 °C or by operating in a hydrocarbon diluent, at temperatures preferably lower than 40 °C. The solid reaction product separated from the reaction mixture should then be further reacted with a second quantity of $TiCl_4$ at a temperature between 110 °C and 135 °C. It has also been suggested that the solid reaction product be separated from the excess of the $TiCl_4$ compound at a temperature at which the undesirable Ti compounds (titanium ethoxides) remain dissolved in the reaction medium so that they can be filtered out simultaneously. They have further recommended that the treatment with $TiCl_4$ be carried out more than once.

The initial treatment of the support with $TiCl_4$ is aimed at removing the ethanol from the $MgCl_2$-ethanol complex by reaction with $TiCl_4$ and to fix additional $TiCl_4$ onto the support. Hu and Chien (1988) found that after the first treatment of the support with $TiCl_4$, both $TiCl_4$ and Cl_3TiOR were found on the $MgCl_2$ support and although the support was found to contain a large percentage of Ti, 30% existed as part of Cl_3TiOR, which was inactive for polymerization. According to Kothandaraman and Devi (1994), the first $TiCl_4$ treatment is expected to almost completely remove the ethanol from the support resulting in an increase in the specific surface area of the

supported catalyst. Chung *et al.* (1995) also showed that the decrease in the amount of ethanol in the support after $TiCl_4$ addition corresponded to an increase in the surface area (Table 4-3). They suggested that the ethanol was removed in the form of titanium ethoxide which was formed by reaction of the $TiCl_4$ with the ethanol in $MgCl_2.n$EtOH. In the present work, two treatments with $TiCl_4$ have also been carried out. Although the thermal treatment of the support was aimed at removing the majority of the ethanol incorporated into the support, the first $TiCl_4$ treatment was taken as an extra measure.

In United States Patent (1981) it has been reported that although the product of the $TiCl_4$ and the support maintained the spherical morphology of the support, the surface area and the porosity were found to decrease. Choi *et al.* (1996) also noticed that the size of the catalyst particles was much smaller than that of the support, implying that the size of the support particles was reduced as a result of $TiCl_4$ addition. The occurrence of this size reduction has also been observed in this work.

In the preparation of the catalyst the first treatment of the $MgCl_2$-ethanol complex with $TiCl_4$ was carried out in the presence of an electron donor compound (internal donor) and as a result of this contact the electron donor remained deposited on the catalyst. Esters are most commonly selected for this purpose and specific examples of such esters are n-butyl phthalate, di-isobutyl phthalate, di-n-octyl phthalate, ethyl benzoate and p-ethoxy ethyl benzoate. In the literature, the diester, dibutyl phthalate, has been shown to be the most efficient and was as a result used in this work.

Hu and Chien (1988) compared the effects of using a monoester (ethyl benzoate, EB) or a diester (dibutyl phthalate, DBP) in the catalyst preparation and found that the diester modified catalysts differed from the monoester modified catalysts in every respect. By comparison the diester modified catalysts had more than 10 times the pore volume, more than 100-fold the surface area and about 50% higher productivity than the monoester modified catalysts.

Kothandaraman and Devi (1994) also tested the effects of these esters as internal electron donors and showed that dibutyl phthalate contributed to a higher surface area and consequently a higher productivity, i.e. diesters were found to be more efficient than monoesters. Forte and Coutinho (1996) investigated the performance of di-isoctyl phthalate (DIOP) and di-isobutyl phthalate (DIBP) as internal electron donors and found that for the catalyst prepared with DIBP no particle breaking was observed during support titanation or during polymerization, contrary to what was observed with the DIOP catalysts.

The importance of using an internal donor in the catalyst preparation has been reported on by Hu and Chien (1988) who noticed an 80% lower content of ethanol in the catalyst when the first treatment with $TiCl_4$ was done in the presence of an ester. They suggested that this was due to an exchange and replacement of Cl_3TiOR by the ester in the $MgCl_2$ complexes. As a result of this they found that the catalysts prepared with only one treatment of $TiCl_4$, with no further ester or

$TiCl_4$ addition, showed the highest Ti contents. The amount of Ti was however lower if an ester was added during catalyst preparation. A second treatment of the catalyst with $TiCl_4$ was found to greatly increase both the surface area and porosity, while further decreasing the Ti content of the catalyst. From this they suggested that there may exist $TiCl_4$-ester complexes adsorbed on the surface which could be extracted by $TiCl_4$. Forte and Coutinho (1996) further found that catalysts prepared without an internal electron donor usually presented poorer morphologies and lower activities than those prepared with the donors.

The scheme below shows the chemical equations that have been postulated to describe reactions between the catalyst components during support titanation (Hu and Chien, 1988). There is a general agreement in the literature that these equations correctly predict the reactions.

$MgCl_2.EtOH$	+	$TiCl_4$	→	$MgCl_2$	+	$EtOTiCl_3$	+	HCl	(4-1)
$MgCl_2$	+	$MgCl_2$	→	$MgCl_2$(solid)					(4-2)
$MgCl_2.EtOH$	+	ID	→	$MgCl_2.EtOH.ID$					(4-3)
$MgCl_2.EtOH.ID$	+	$TiCl_4$	→	$MgCl_2.EtOTiCl_3.ID$	+	HCl			(4-4)
$MgCl_2.EtOTiCl_3.ID$	+	$TiCl_4$	→	$MgCl_2$	+	$MgCl_2.ID$	+	$TiCl_4.ID$	(4-5)
							+	$TiCl_4.EtOTiCl_3$	
$MgCl_2.ID$	+	$TiCl_4$	→	$MgCl_2.TiCl_4.ID$					(4-6)
$MgCl_2$(solid)	+	$TiCl_4$	→	$MgCl_2$(solid).$TiCl_4$					(4-7)

Chemical Equations Postulated to Describe Reactions between the Catalyst Components: $MgCl_2$.*n*EtOH, Internal Donor (ID) and $TiCl_4$ during the Titanium Impregnation Step

The by-product titanium ethoxide, $EtOTiCl_3$, is soluble in hot $TiCl_4$ and can therefore be removed from the catalyst by filtering at high temperatures. It is essential that this product be removed since the catalytic performance largely depends on chemical factors such as the formation of such inert complexes which do not participate in the formation of active sites. Parada *et al.* (2002) found that when $TiCl_4$ was added to $MgCl_2$.*n*ROH adducts, the $TiCl_4$ reacted with the alcohol to form titanium alkoxides and this formation was found to be the reason for the low catalytic activity since titanium alkoxides are inactive for polymerization. The Cl_3TiOR formed not only increased the catalyst weight but also blocked the remaining active centers in the activated support material. Although the support is often washed several times after ethanol evaporation, there is often still alcohol bonded to the support which reacts with $TiCl_4$ during impregnation resulting in the corresponding titanium alkoxide formation. In this work, after the first treatment of the support with $TiCl_4$, the liquid was removed by filtering at 110°C so that the by-product titanium ethoxide remained dissolved and was as a result removed. The reaction between $TiCl_4$ and ethanol is highly exothermic and the addition of $TiCl_4$ to the support during the catalyst preparation was therefore carried out at a low temperature of -8 °C.

The intermediary products in the reaction scheme containing an ID in their structures result in a high surface area and catalyst activity when treated with an additional amount of $TiCl_4$. It seems that the main functions of the internal donor (ID) (equations 3 to 6) are to protect the catalyst particles against breakage, and to control the fixation of $TiCl_4$ on the $MgCl_2$ faces. It has also been proposed that ID mainly prevents $TiCl_4$ from co-ordination on those $MgCl_2$ crystal faces where mostly non-stereospecific active sites would be formed. For the stereospecific polymerization of α-olefins both an ID and an external electron donor (ED) such as ethyl benzoate (EB) should be used (Forte and Coutinho, 1996). The purpose of the ED, often added during polymerization, is to selectively inhibit the non-stereospecific centers and to decrease the reaction of the co-catalyst (TEA) with the ID.

In this work, both catalysts C1 and C2 were prepared using the same reagent quantities and preparation procedures. The supports were however prepared using different ethanol/$MgCl_2$ molar ratios. S1 was prepared with a molar ratio of 76.2 while S2 was prepared with a ratio of 51.1. The consequence of this was that S1 was found to contain 3.687 wt% Ti and S2 was found to contain 6.477 wt% Ti. The higher Ti content was therefore found in the catalyst prepared from the support synthesized with less alcohol. Since the supports were extensively treated to remove the ethanol prior to the final $TiCl_4$ impregnation, it can be concluded that the quantity of Ti measured does not partly belong to titanium ethoxide complexes.

4.3 Polymerization tests

The catalysts C1 and C2 were tested in slurry polymerization experiments to determine if they were capable of producing polyethylene. TEA was used as the catalyst activator.

4.3.1 Experimental equipment setup

The experimental equipment essentially consisted of a 3 neck, 500 mL flat bottom glass Schlenk reactor (Figure 4-2), two mercury bubblers and a plate heater with a magnetic stirrer option. The ethylene was fed from a gas cylinder through the gas purification column described in Chapter 3, and thereafter through the first mercury bubbler. The outlet of the first bubbler was connected to the inlet of the reactor. A continuous flow of ethylene through the reactor was observed by connecting the reactor exit line to a second bubbler. The two bubblers were used to observe a continuous monomer flow entering and leaving the reactor, to provide and air tight system and to provide pressure relief.

4.3.2 Polymerization experiments

Three polymerization experiments were carried out. The first consisted of producing polyethylene using pure $TiCl_4$ and TEA in hexane. This was done in order to obtain a polyethylene sample to be used as a standard for FTIR analysis comparisons. The other two

reactions made use of catalysts C1 and C2. These catalysts were both activated by TEA and the reactions were also carried out in hexane.

Experiment 1

The glass reactor was first dried overnight in an oven to remove moisture adsorbed onto the glass surface. In the glove bag, under a nitrogen atmosphere, 1.5 mL of $TiCl_4$, 1 mL of TEA solution and 40 mL of hexane were transferred into the glass reactor. The openings of the reactor were then sealed and the reactor was removed from the glove bag and placed on the heater. Under a high flow of ethylene the inlet and outlet tubes were connected. The reaction mixture was then stirred at a temperature of approximately 50 °C for 30 minutes. The reaction was terminated by stopping the ethylene gas flow to the reactor and injecting several aliquots of ethanol into the reactor. The product was then filtered, further washed with ethanol and dried under vacuum for 30 minutes.

Experiment 2

The reactor was prepared as for Experiment 1. In the glove bag, under a nitrogen atmosphere, 0.0917g of the supported catalyst C1, 1 mL of TEA solution, and 40 mL of hexane were transferred into the reactor. The reactor was then connected as for Experiment 1 and the reaction mixture was stirred at a temperature of approximately 50 °C for 60 minutes.

Experiment 3

The reactor was prepared as for Experiment 1. In the glove bag, under a nitrogen atmosphere, 0.0719g of the supported catalyst C2, 1 mL of TEA solution, and 40 mL of hexane were transferred to the reactor. The reactor was then connected as for Experiment 1 and the reaction mixture was stirred at a temperature of approximately 50 °C for 60 minutes.

4.3.3 Experimental Results

The products of the three experiments were analysed using infrared spectroscopy (FTIR). The first experiment was undertaken so as to obtain a standard spectrum for polyethylene, this spectrum is shown in Figure 4-15. The second and third experiments were carried out to determine if the products produced were indeed polyethylene. The spectrums obtained for the products of these experiments are shown in Figure 4-16 and Figure 4-17 respectively.

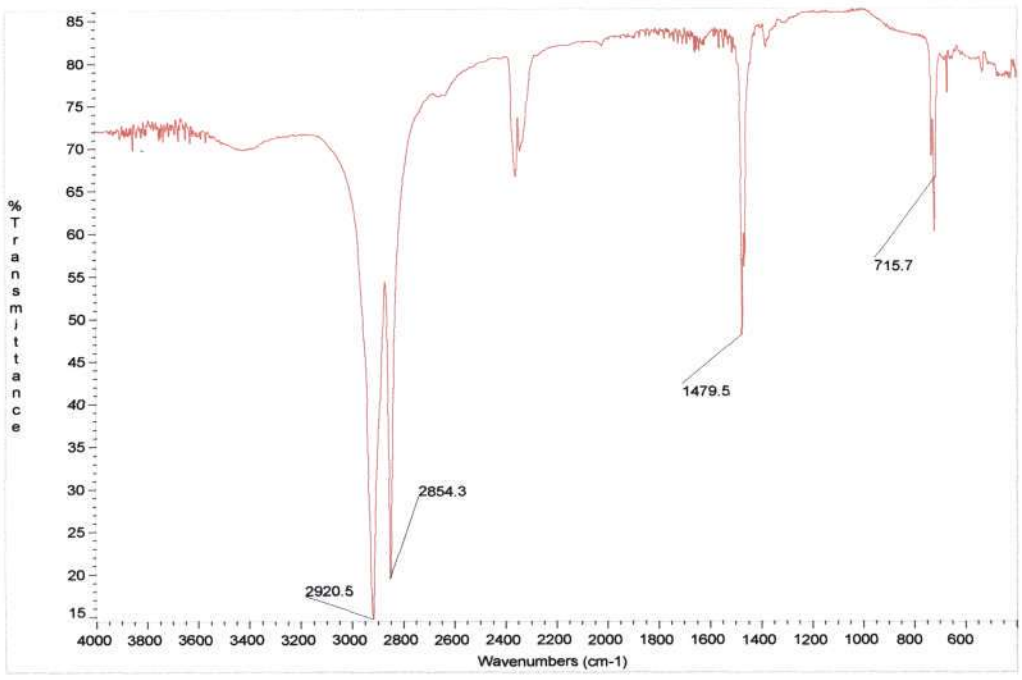

Figure 4-15 IR Spectrum of Polyethylene Produced with $TiCl_4$/TEA in Hexane

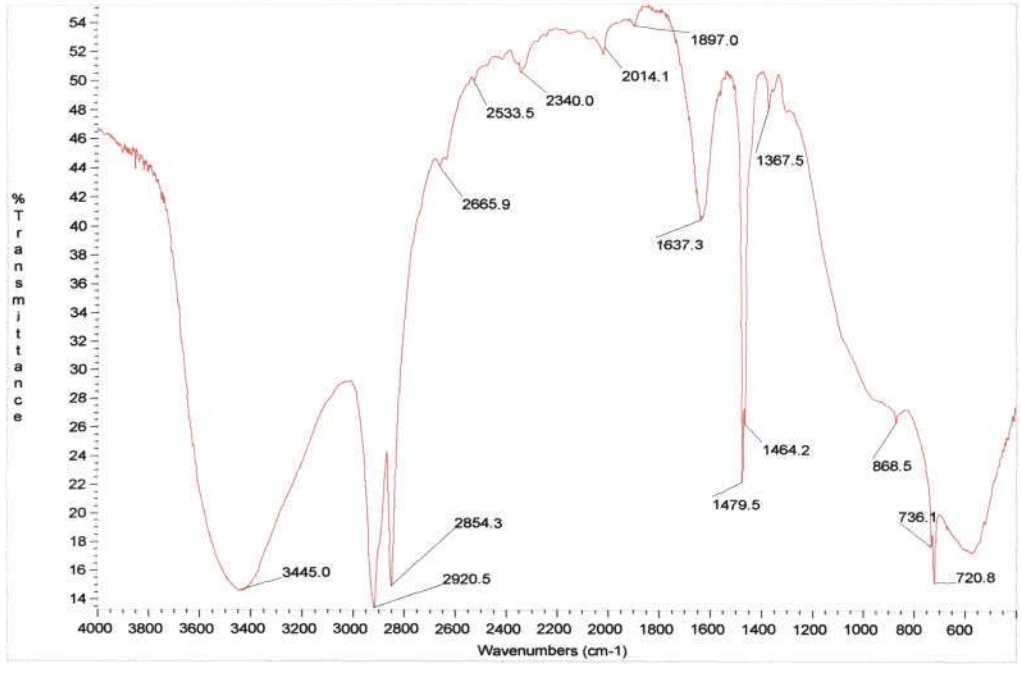

Figure 4-16 IR Spectrum of Polyethylene Produced with Catalyst C1 in Hexane

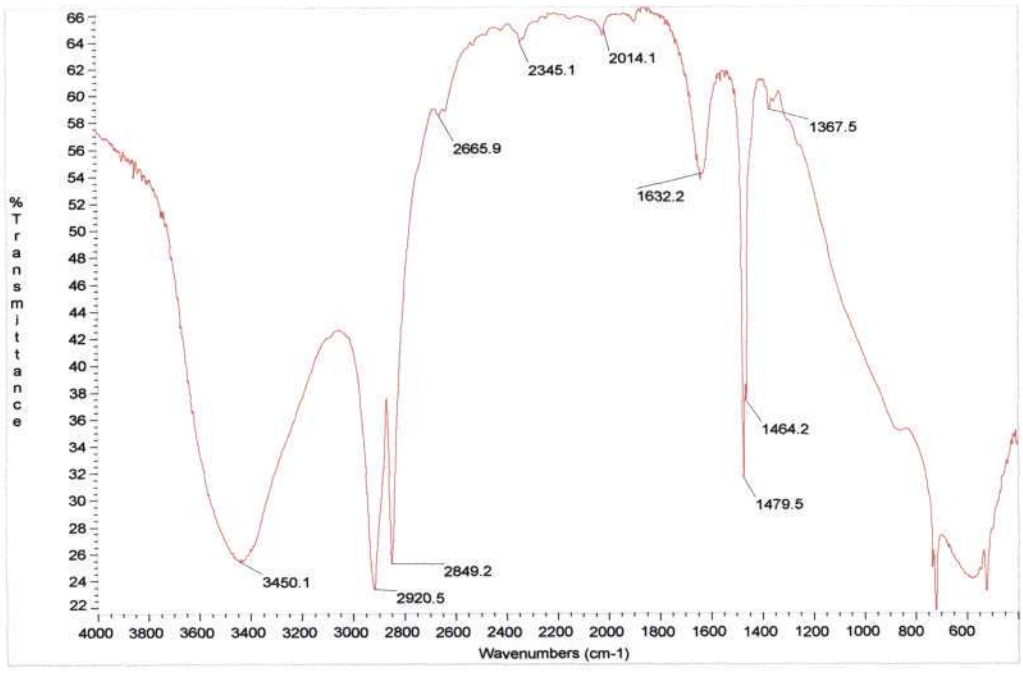

Figure 4-17 IR Spectrum of Polyethylene Produced with Catalyst C2 in Hexane

4.3.4 Discussion

The first confirmation that the products produced in Experiments 2 and 3 are in fact polyethylene is that the spectrum of Experiment 1, which shows strong bands at 2920, 2854, and 1480cm^{-1}, is almost identical to that of the spectra of experiments 2 and 3. The only difference is that the second and third experiments show a broad peak at 3450cm^{-1}. If this peak represented the presence of ethanol, the peak would also show in Figure 4-15 and would be as a result of residual ethanol from washing of the products. The peak however does not appear in Figure 4-15 and is therefore probably as a result of $MgCl_2$ present in the polymer matrix. It is probably detected here because product quantities were very small, making the ratio of polymer to catalyst also small, and the fraction of catalyst components were as a result large enough to be detected.

Principal transmittance bands that can be used to identify a spectrum as that of polyethylene are shown in Table 4-8. The strong bands in the region between 3000cm^{-1} and 2800cm^{-1} and between 1480 cm^{-1} and 1460 cm^{-1} in Figure 4-15, Figure 4-16 and Figure 4-17indicate the presence of CH_3 and CH_2 groups. The presence of these functional groups further confirms that all three samples analyzed are polyethylene. The strong and intense bands at approximately 2920cm^{-1} *and* 2850cm^{-1} *are due to C-H stretching vibrations of the methyl and methylene* groups, respectively. The C-H bending vibrations of the methyl and methylene groups are seen at approximately 1460cm^{-1} and 1370cm^{-1} respectively.

Although the quantities of products for these experimental runs were not recorded, and as a result activity and yields were not determined, it was visually observed that C2 was much more active than C1. In experiment 3, polyethylene was formed instantaneously upon ethylene addition and a much greater quantity of product was produced. From this it was concluded that the larger quantity of Ti in C2 was indeed as a result of the presence of $TiCl_4$ and not as part of inactive Cl_3TiOR. C2 was therefore used for the kinetic investigations undertaken in Chapter 5.

Table 4-8 Table of IR Absorptions to Identify Polyethylene

Group	Principal Transmittance Bands (cm^{-1})			
$-CH_3$	2962	2872	1460	1375
$-CH_2-$	2926	2863	1455	

Chapter 5

Gas Phase Ethylene Polymerization

A series of experimental studies on gas-phase ethylene polymerization has been carried out in a semi-batch reactor system using a heterogeneous Ziegler-Natta catalyst. Both the synthesis of the catalyst and the design of the reactor system have been fully discussed in previous chapters. Triethylaluminium (TEA) has been used as the co-catalyst for the experiments, all of which were run for a duration of 4 hours. The polymerization experiments were aimed at examining the effect of the Al/Ti molar ratio, the reaction temperature, and the reaction pressure on ethylene homo-polymerization yields and activities. In this chapter the reactor pre-treatment, catalyst and co-catalyst injection method, and the polymerization experimental procedure are described. The results of the polymerization experiments are then presented and a discussion of these follows.

5.1 Introduction

Kinetic studies on Ziegler-Natta catalyst systems are of fundamental importance, especially for those systems based on $MgCl_2$-supported Ti complexes. In fact, such studies make it possible to obtain essential data with regard to the formulation of reaction models as well as to the optimization of catalyst performance and process engineering.

Other α-olefins differ inherently from ethylene in several ways, including their considerable double bond polarity, high dipole moments, and Lewis base nature. Consequently, it is not surprising to observe that under the same operating conditions, ethylene polymerization exhibits kinetic behaviour significantly different from that of other olefins. It has also been observed that ethylene polymerization sites are much more stable than those of propylene and that for ethylene polymerization, reaction orders greater than one are common.

Ethylene polymerization with $MgCl_2$-supported $TiCl_4$ catalysts show various types of activity curves depending on their nature, titanium content, the type and concentration of the co-catalyst, reaction temperature, etc. In general, the curves show a short period of acceleration followed by a prolonged steady period. However, in the presence of electron donors they may show the typical decay rate kinetics observed during propylene polymerization. Rate decay is mainly ascribed to a chemical deactivation of active centres, however, in the case of ethylene it appears that diffusive phenomena may also play a role in the drop of the polymerization rate. Also, for the polymerization of ethylene with supported Ziegler-Natta catalysts, more complicated activity profiles, for example profiles with two maxima, have been reported by Han-Adebekun *et al.* (1997c) and Wu *et al.* (1999).

Comparative studies of ethylene polymerizations in gas- and slurry-phase reactors show differences in the rate-time profiles (Wu *et al.*, 1991). Higher activities in the early stages and declining kinetics were observed for the gas-phase polymerizations and were considered to be due to the higher macro-particle diffusivity and to fast deactivation of the active centres.

The most comprehensive kinetic scheme for ethylene polymerization was provided by Bohm in 1978. This model, of the Rideal type, is of general applicability and includes and explains the most relevant phenomena involved in Ziegler-Natta polymerization. Mathematical formulation of the proposed reaction scheme led to the following equation for the polymerization rate R_p and the number average molecular weight of polymer (M_n) in the absence of hydrogen:

$$R_p = \frac{1}{M_m}\frac{dY}{dt} = \frac{k_p k_a [M]_o}{k_p + k_d + k_a [M]_o}\frac{C_p^*}{1+(b/a)+(c/a)} \qquad (5\text{-}1)$$

$$\frac{Y}{M_n} = C_p^* + \frac{Y}{M_{n,\infty}} \qquad (5\text{-}2)$$

where $[M]_0$ is the monomer concentration at the catalyst surface, M_m is the monomer molecular mass, C_p^* the quantity of all active centres referred to the quantity of transition metal used, and Y refers to the catalyst yield. Equation (5-2) provides a method for determining the number of active centres by measuring M_n as a function of the catalyst yield, Y.

Even though supported catalysts provide a much higher activity and polymer yield, they do not maintain this high activity for long periods. The reduction of activity with time has been viewed by some researchers as being a result of diffusional effects. However, the results obtained by Giannini (1981), Doi *et al.* (1982), Keii *et al.* (1982),Chien *et al.* (1985), and Wu *et al.* (1999) to name a few, have convincingly shown that the rate reduction is due to the deactivation of sites rather than diffusion limitations.

It is generally believed that the catalyst surface is heterogeneous in nature and that the rate of deactivation of sites is proportional to its activity (Cunningham *et al.*, 1988). This multiplicity of sites leads to the production of polymer with a large polydispersity, where polydispersity is a ratio used to represent the broadness of a molecular weight distribution. Many researches have however demonstrated that a simple two-site model can be used to predict the broad molecular weight distribution produced with supported catalysts.

Polymerization of ethylene with many heterogeneous Ti-based Ziegler-Natta catalysts exhibit several peculiar features compared to polymerization reactions of α-olefins such as propylene, 1-butene, etc. They have been summarized by Kissin *et al.* (1999) and are as follows:

1. Ethylene is the most active compound among all olefins, as follows from the values of its activity ratios in co-polymerization reactions. For example, ethylene is at least three to five times more active than propylene and over 50 times more active than 1-hexene or 4-methyl-1-pentene. However when direct comparisons of polymer yields and catalyst activities are made, ethylene never exhibits a level of activity expected from its relative activity in co-polymerization reactions.

2. Comparisons of ethylene homo-polymerization and co-polymerization with other α-olefins show another unusual feature. Based on the co-polymerization kinetics theory, introduction of any α-olefin to an ethylene polymerization reaction should bring about a rate reduction due to the lower activity of the α-olefin. However, investigations of these co-polymerization reactions catalyzed by numerous heterogeneous Ziegler-Natta catalysts showed that, instead, the reaction rate becomes markedly higher in the presence of α-olefins. This co-monomer effect has been researched thoroughly, and was confirmed for ethylene co-polymerization reactions with propylene, 1-butene, 1-pentene, 1-hexene, 1-decene, 3-methyl-1-butene, 4-methyl-1-pentene, etc. The nature of this activation effect has been the subject of many hypotheses ranging from diffusion effects to purely kinetic explanations. The α-olefins activation effect was observed even when

the co-polymerization reactions were carried out at high temperatures and when the co-polymers were completely dissolved in the reaction medium. This fact undermines an often-proposed hypothesis that the α-olefin activation effect is primarily caused by diffusion phenomena and that ethylene/α-olefin copolymers present a lower diffusion barrier for ethylene due to a lower crystallinity.

3. Studies of ethylene ter-polymerization reactions (reactions involving ethylene and two different α-olefins) showed that the presence of one α-olefin increases the activity of another. For example, 1-butene significantly increases the co-polymerization activity of such linear α-olefins as 1-decene, 1-dococene, etc.

4. The overall rate of ethylene homo-polymerization with heterogeneous Ti-based Ziegler-Natta catalysts has a reaction order *n* with respect to the ethylene concentration in solution, C_E, ($R_{pol} = k_{eff} C_E^n$), significantly exceeding 1. Several earlier measurements gave the *n* value in the range 1.7 to 1.9, whereas ethylene co-polymerization reactions at high α-olefin concentrations have a reaction order close to 1.0.

5. Introduction of hydrogen causes a significant depression of the ethylene polymerization rate, an effect opposite to that observed in the polymerization of propylene with similar catalysts. The rate-depression effect is completely reversible, suggesting the chemical nature of the deactivation.

In the literature there is a limited quantity of research available on gas-phase ethylene polymerizations using $MgCl_2$-supported Ziegler-Natta catalysts. Han-Adebekun *et al.* (1997a, b, c), Lynch and Wanke (1991), Wu *et al.* (1999), and Kissin *et al.* (1999) are among the few to have conducted gas-phase ethylene polymerization experiments.

Han-Adebekun *et al.* (1997a) modified the gas-phase reactor designed by Choi and Ray (1985) for their work. The reactor had been used by Choi and Ray for propylene polymerization experimentation using unsupported catalysts. They gave a detailed description of their reactor system and this system together with that designed by Choi and Ray are fully described in Chapter 2 of this work. For their kinetic investigations, Han-Adebekun and co-workers used a high activity $MgCl_2$-supported catalyst with no external electron donor. TEA was used as the co-catalyst and hydrogen as the chain transfer agent. They investigated the effects of temperature, hydrogen, and the Al/Ti molar ratio, on the polymerization rate and their findings are discussed later in this chapter.

Lynch and Wanke (1991) gave a detailed description of the reactor pre-treatment method that they developed. This procedure, which is highly important due to the extreme sensitivity of the catalyst and co-catalyst to air/moisture, has been used in this work and has proved to be highly efficient. A detailed description of the gas-phase reactor system designed by Lynch and Wanke

and which was later used by Wu *et al.* (1999) is given is Chapter 2 of this work. Wu and co-workers used a pre-polymerized $MgCl_2$-supported Ziegler-Natta catalyst to study the effect of temperature on the ethylene reaction rate and their results will also be discussed later in this chapter.

As mentioned above, the procedure for the overnight pre-treatment of the reactor developed by Lynch and Wanke (1991) has been used in this work prior to each experiment being performed. This method of reactor pre-treatment has also been used by Wu *et al.* (2005) for slurry and solution polymerization experiments. Reactor pre-treatment began by heating the sealed, leak tested reactor to 85°C and evacuating it overnight. The reactor was then filled with nitrogen, at the same temperature, to a pressure of approximately 0.15 MPa and an amount of co-catalyst (DEAC) was injected into the reactor. Lynch and Wanke (1991) found that even after the prolonged evacuation period there was still a significant amount of water adsorbed on the walls of the reactor, making the treatment with the co-catalyst necessary.

They found that ethane was produced in the reactor if 2 mL of co-catalyst (DEAC) was injected after the reactor had been heated to 85°C and evacuated overnight. According to Kissin (1985), one molecule of water can produce two molecules of ethane when contacted with aluminium alkyls such as TEA. From this it evident that ethane production is an indication of the presence of water in the reactor even after the long evacuation. Lynch and Wanke (1991) observed ethane production for a few hours following DEAC injection, and recommended that at least 2 to 3 and preferably 8 to 10 hours be allowed following co-catalyst injection to ensure a moisture free environment prior to catalyst injection.

5.2 Experimental Procedure

5.2.1 Reactor pre-treatment

1. The reactor was sealed by bringing the flanges of the reactor head and cylinder together and tightening the cap bolts in place. The catalyst holder was then attached to the rest of the catalyst injection line.
2. The reactor was thereafter leak tested at a pressure of 3 bar by closing all valves leading into and out of it and observing the reactor pressure reading from the pressure transmitter. If it was found that the pressure decreased, the leak was found using Snoop (Swagelok) and necessary adjustments were made.
3. Once it was certain that no leaks existed, the set-point on the reactor temperature controller was set to 100°C and the reactor was evacuated overnight at this temperature.
4. The reactor was then filled with nitrogen to a pressure of approximately 0.5 bar and 1 mL of the co-catalyst (TEA, 1M solution in heptane, Aldrich) was injected into the reactor via the septum on the catalyst injection line. This was followed by a continuous nitrogen purge for 4 hours.

5. The temperature on the digital controller was then set to the desired reaction temperature.

5.2.2 Catalyst and co-catalyst injection

1. Under a high flow of nitrogen, the catalyst holder was detached from the reactor head and was replaced by a septum cap. The holder was then placed in the glove bag. The catalyst, the co-catalyst (TEA), and two gas-tight syringes were also placed in the glove bag.
2. The bag was sealed and 5 nitrogen/vacuum cycles were carried out to ensure that the environment inside the bag was air and moisture free.
3. The desired quantities of solid catalyst and liquid co-catalyst were then transferred from their respective air-tight containers to the body of the catalyst holder. The accurate volume of the co-catalyst was measured using a Hamilton gas-tight syringe. The stem of the catalyst holder was then inserted into the body and the valves on either side were closed. The catalyst was thereby transferred to the reactor without contaminating the catalyst. 10 mL of heptane was also measured in a gas-tight syringe and the end was sealed with a rubber stopper.
4. Under a high flow of nitrogen the septum cap was removed and the catalyst holder was reattached to the rest of the catalyst injection line.
5. The reactor was then evacuated for 2 minutes to remove any air that may have been introduced and to remove the nitrogen from the reactor.
6. The valves on either side of the catalyst holder were then opened and the catalyst and co-catalyst slurry was allowed to fall into the catalyst basket. Any catalyst and co-catalyst residue on the walls of the injection line were then washed into the catalyst basket with the 10 mL of heptane previously measured.

5.2.3 Polymerization procedure

1. The pressure set-point was set on the pressure controller and a voltage was supplied to the stirrer motor.
2. Polymerization was initiated by introducing the monomer into the reactor and starting the data logging system which recorded the reactor pressure. All reactions were carried out at a constant temperature and pressure, and with the reactor in semi-batch mode.
3. After 4 hours, the feed gas flow-rate and the data logger were stopped, ethanol was injected into the catalyst basket to terminate the polymerization reaction, and the reactor was purged with nitrogen for a few minutes.
4. The reactor was then cooled and the cap bolts removed so that the polymer contained in the catalyst basket could be removed.
5. The polymer was then transferred to a frit funnel where it was washed several times with ethanol and thereafter dried overnight at 60°C.
6. The dry product was then weighed to determine the yield of the reaction.

5.3 Experimental results and discussion

The catalyst and co-catalyst were injected into the catalyst holder in the glove bag and then transferred to the reactor where the mixture was injected into the catalyst basket. Heptane was then injected to wash the catalyst and co-catalyst residue on the walls of the injection line into the basket. Pre-mixing the catalyst and co-catalyst prior to injection into the reactor can result in catalyst deactivation due to the over-reduction of the catalyst. In this work however, the pre-contact was necessary since the catalyst basket was porous and if the co-catalyst was injected after catalyst injection, the contact time in the basket may be insufficient for activation. Also, over-reduction in the case of ethylene polymerization is not a major concern since ethylene also polymerizes on Ti^{2+}. Another factor is that the catalyst and co-catalyst contact time before catalyst injection never exceeded 5 minutes, whereas aging times of up to 25 minutes have been used by Han-Adebekun *et al.* (1997b) for the same catalyst system and for gas-phase ethylene polymerization.

The introduction of the heptane also presents no serious problems in this work since the basket is porous and none of the heptane will be held in the basket. This means that there isn't a possibility of a catalyst slurry being present in the basket, thereby ensuring that the reaction will be strictly gas phase. For experiments carried out in a stirred bed reactor, the heptane injected to wash the catalyst into the basket has to be vapourized out to prevent the presence of a slurry mixture in the reactor.

To avoid the problem of grinding of the growing polymer particles by the stirrer, a spinning catalyst basket was used to contain the catalyst for the duration of the reaction and as a means of gas and solid phase agitation. Although this method of agitation may have been efficient in preventing temperature and concentration gradients in the gas phase, it was however difficult to maintain a well mixed state in the basket, especially as the basket filled with polyethylene product. Growing polymer particles tended to agglomerate and although these were easily broken down once left overnight in ethanol, it did mean that melting of the polymer had occurred which probably led to catalyst deactivation, which obviously affected polymer yield, and affected polymer properties. The particles that did not agglomerate were analyzed by scanning electron microscopy and the results are discussed later in the Chapter.

The yields obtained in the polymerization reactions were generally low and this could be due to two possible reasons. Firstly, the low yields could be the result of low catalytic surface areas. Secondly, melting of the growing polymer particles in the basket led to agglomeration and deactivation of active catalytic sites and therefore also to a decrease in the yield.

5.3.1 Effect of pressure on ethylene homo-polymerization reactions

The effect of monomer concentration (partial pressure) on the ethylene homo-polymerization yield was investigated by conducting polymerization experiments at two different pressures (1 and 2 bar); the experimental results are shown in Table 5-1.

The effect of increasing the pressure by 1 bar at 50 °C was determined at two different Al/Ti ratios. At Al/Ti = 33, a change in the pressure from 1 to 2 bar resulted in an increase in the yield by 1.4 times and at Al/Ti = 50, the same increase in the pressure resulted in an increase in the yield by 1.2 times. Although an increase in the pressure did increase the yield, the increase was not substantial.

Table 5-1 Influence of Ethylene Pressure on Polymerization Yield

Pressure bar	Temperature °C	Al/Ti molar ratio	Time hours	Activity* g PE/g Ti. h	Yield g PE/g cat. h
1.0	50	33	4	130.78	8.47
2.0	50	33	4	185.51	12.02
1.0	50	50	4	218.70	14.16
2.0	50	50	4	261.88	16.96

*wt% Ti = 6.5

The effect of the monomer concentration on the olefin polymerization rate is generally investigated during a single reaction run. Reaction orders are determined by varying the reactor pressure and observing the corresponding change in the monomer consumption rate at a fixed reaction temperature. Calculating the reaction order with data from a single run ensures highly accurate results since the same charge of catalyst is used. As it was not possible to determine the instantaneous reaction rate in this work, it was also not possible to determine the reaction order. Han-Adebekun *et al.* (1997b) and Kissin *et al.* (1999) were able to undertake these investigations using supported $MgCl_2$ catalysts and for ethylene polymerization and have reported reaction orders of 1.68 and 1.8 respectively.

5.3.2 Effect of temperature of ethylene polymerization reactions

The effect of temperature on the ethylene polymerization yield was determined at 1 bar and with Al/Ti = 33. The experimental results are shown in Table 5-2 and in Figure 5-1. It was found that the yield increased when the temperature was increased from 50 to 60°C and that it thereafter decreased as the temperature was further increased to 70°C. The decrease in the activity at higher temperatures has been widely recognised in the literature and is believed to be due to the deactivation of active sites at higher temperatures.

Table 5-2 Effect of Temperature on Ethylene Homo-Polymerization Reaction Yields

Pressure bar	Temperature °C	Al/Ti molar ratio	Time hours	Activity* g PE/g Ti. h	Yield g PE/g cat. h
1	50	33	4	130.78	8.5
1	60	33	4	377.15	24.43
1	70	33	4	122.66	7.9

*wt% Ti = 6.5

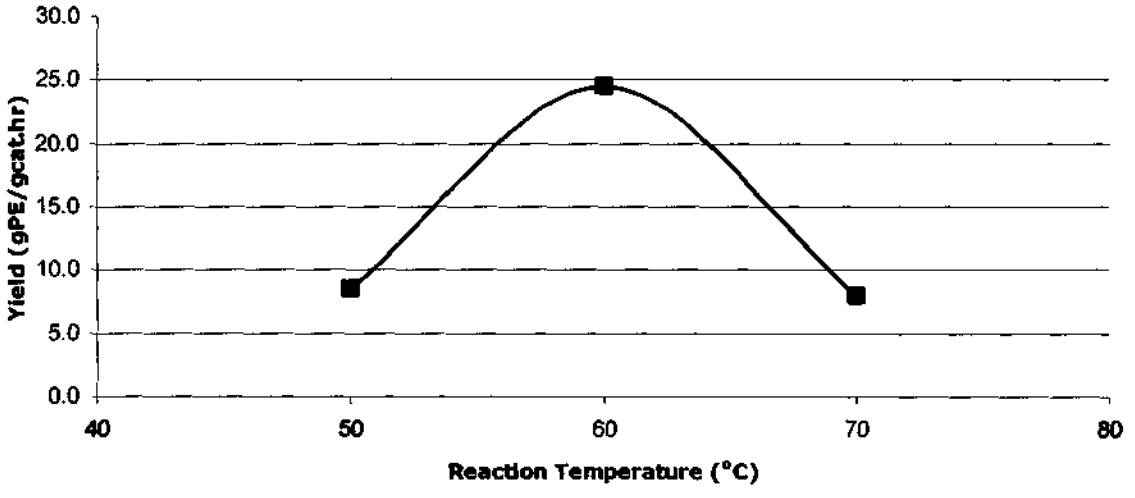

Figure 5-1 Effect of Temperature of Ethylene Homo-Polymerization Reaction Yields

The decrease in the polymerization rate at high temperatures was also noticed by Han-Adebekun *et al.* (1997c) who studied the effect of the reaction temperature on the gas-phase polymerization rate of ethylene using a high activity $MgCl_2/TiCl_4/AlEt_3$ catalyst and with Al/Ti = 86. They found that the rate initially increased from 50 to 90°C and then decreased as the temperature was further raised to 120°C. Their reactor system allowed them to measure the instantaneous ethylene consumption rate and they observed that the time in which the second peak in the rate curve emerged appeared to be correlated with the reaction temperature. They found the second peak to occur earlier as the temperature was increased.

Wu *et al.* (1999) also undertook a study in which the effect of temperature on the rate of gas-phase polymerization of ethylene was investigated. These authors also used a $MgCl_2$-supported $TiCl_4$ catalyst. Their results are shown in Figure 5-2.

The following observations were made from the results presented in Figure 5-2:

1. All the activity profiles show deactivation at longer times.
2. For low reaction temperatures (≤40°C), there is a single maximum in the activity profiles.

3. For higher reaction temperatures (≥50°C), the activity profiles have two maxima (referred to as the first peak and the second peak, respectively).
4. The first peak occurs sooner and the second peak becomes more pronounced with increasing polymerization temperature.
5. The second peak is broader than the first peak and the second peak is not observed for polymerization times less than 2 hours.
6. The overall polymerization rate increases with increasing temperature up to 60°C and then decreases at higher temperature.

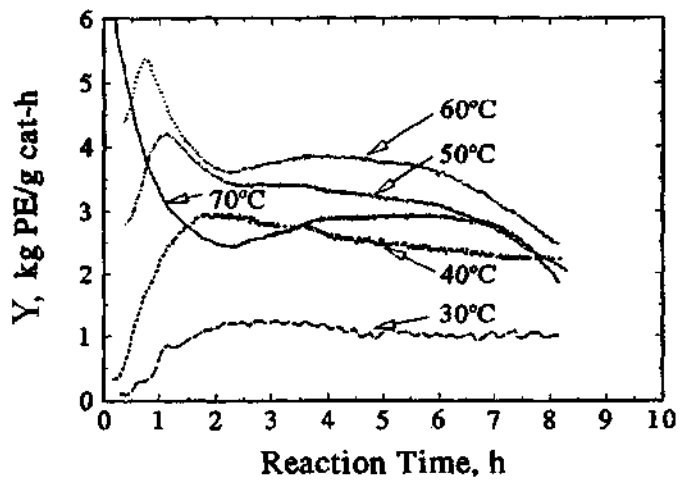

Figure 5-2 Polymerization Rate Profiles as a Function of Polymerization Temperature at Ethylene Pressure of 680 kPa (Wu *et al.*, 1999)

Wu *et al.* (1999) explained that the reason for the first peak occurring sooner with increasing temperature was due to the existence of an initiation step of catalytic sites by ethylene before chain propagation. If the initiation rate is sensitive to temperature, the initiation rate constant would increase with the increase of polymerization temperature. At low temperatures, the low initiation rate constant would give a long accelerating period and at high temperatures, the accelerating period would be shorter. In Figure 5-2, the appearance of the second peak implies the presence of a second type of catalytic site in the catalyst (site 1 for the first peak and site 2 for the second peak). The nature of these sites is, however, unknown.

The temperature effect on the polymerization rate in Figure 5-2 also shows that the overall polymerization rate increases with increasing temperature up to 60°C and then decreases at higher temperatures. Similar temperature effects over a range of 30 to 70°C were observed by Dusseault and Hsu (1993) with a maximum productivity at 55°C for the gas-phase polymerization of ethylene using a $MgCl_2$/ethyl benzoate/$TiCl_4$/TEA catalyst at a high Al/Ti ratio.

5.3.3 Effect of Al/Ti on ethylene homo-polymerization reactions

There are two major functions of the aluminium alkyl in olefin polymerization with transition metal catalysts: (1) it acts as a key agent for transition metal oxidation state reduction, and (2) it acts as an aid in bimetallic active site formation. Various studies have shown that Ti^{3+} is active for both ethylene and α-olefins while Ti^{2+} is only active for ethylene.

The effect of Al/Ti on the ethylene homo-polymerization yield was determined at three different ratios at 50°C and 1 bar. An increase in Al/Ti was found to result in an increase in the reaction yield. Generally, in the literature, an optimum ratio is observed. This optimum was however not observed in this work and is probably a result of the highest Al/Ti ratio (60) being too low to observe such an optimum. The experimental results are presented in Table 5-3.

Table 5-3 Effect of Al/Ti Molar Ratios on Ethylene Homo-Polymerization Yields

Pressure bar	Temperature °C	Al/Ti molar ratio	Time hours	Activity* g PE/g Ti. h	Yield g PE/g cat. h
1	50	60	4	218.70	14.16
1	50	33	4	130.78	8.47
1	50	10	4	12.54	0.81

*wt% Ti = 6.5

When low levels of alkyl are used, a much larger fraction is used for scavenging trace quantities of O_2 and H_2O and less is available for site activation. This is a possible reason for errors in the yield at very low Al/Ti ratios.

Here again the effect of Al/Ti on the instantaneous reaction rate curves for gas-phase ethylene polymerization could not be determined due to the limitations of the reactor system. These investigations were however carried out by Han-Adebekun *et al.* (1997b) and their results are discussed below. They used a reaction temperature of 50°C, a pressure of 2 atm, and an aging time of 25 minutes. By aging time is meant the contact time between the catalyst and the co-catalyst prior to initiating the polymerization reaction by introducing monomer into the reactor. Their results are presented in Figure 5-3. For ethylene homo-polymerization, optimum activity behaviour is generally observed and in general, ethylene polymerization has a much higher optimum Al/Ti ratio compared with that of propylene. For ethylene polymerization, if the Al/Ti ratio continues to increase, a rate decrease can be observed and this is probably due to the over-reduction of Ti^{2+} to Ti^{+}; where the latter is inactive for polymerization.

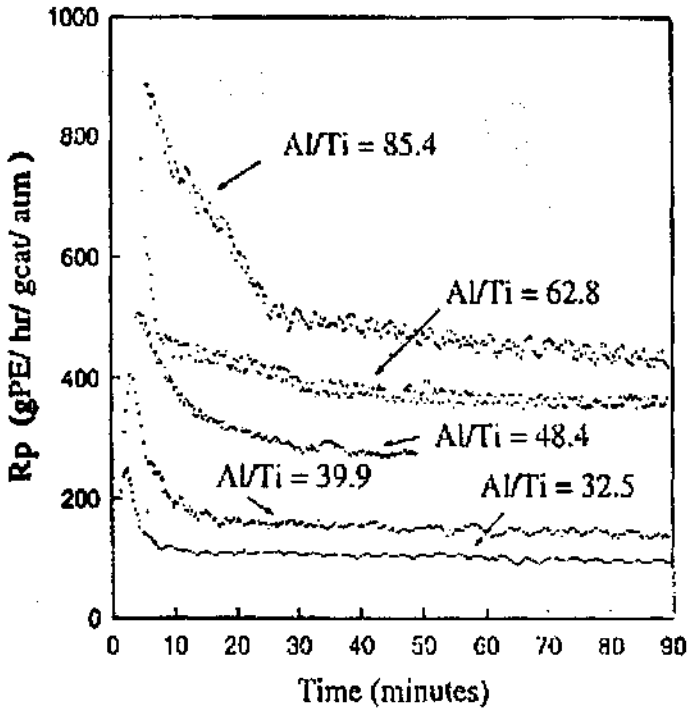

Figure 5-3 Effect of Al/Ti ratios on Ethylene Homo-Polymerization Reaction Rates (Han-Adebekun *et al.*, 1997b)

Han-Adebekun *et al.* (1997c) also investigated the influence of the Al/Ti molar ratio on the ethylene polymerization rate at 50°C. They tested three different ratios, Al/Ti = 85, 110, and 170, and found that the higher the Al/Ti molar ratios were, the earlier the second peak occurred. There is overwhelming evidence in the literature supporting the idea that the titanium oxidation state affects catalyst activity. It appears that the co-catalyst, TEA, plays the role of reducing agent to the titanium catalyst, which is in the 4+ oxidation state. All olefins polymerize on the 3+ oxidation state, and only ethylene polymerizes on the 2+. The reason for ethylene's behaviour is not fully understood. While the monomers appear to participate in the site transformation reactions, their specific role as reductants or oxidants is unknown.

Fregonese *et al.* (2001) found that Ti^{4+} undergoes reduction to lower oxidation states owing to treatment with TEA and the process is dependent on activation temperature, aging time (Table 5-5), and Al/Ti molar ratio (Table 5-4). They also found that the Ti^{4+} reduction appeared to be incomplete even by using excess of the co-catalyst or long aging times. Thus, a catalyst activated for 2 hours at 70°C with Al/Ti = 200 showed the following distribution: $Ti^{4+}:Ti^{3+}:Ti^{2+}$=9:31:60. The activity of ethylene was also found to be a function of the aging time and a practically steady activity in the ethylene polymerization with increasing aging times was observed. They further confirmed that the polymerization of ethylene is catalyzed by both Ti^{3+} and Ti^{2+} while that of propylene polymerizes only on Ti^{3+}.

Table 5-4 Al/Ti molar ratio effect at 70°C on both Titanium Oxidation State Distribution and Activity* (Fregonese *et al.*, 2001)

Al/Ti	Ti (IV)%	Ti(III)%	Ti(II)%	Activity (kg PE/g Ti. h)
15	36	36	28	28
50	10	**34**	**56**	34
100	12	**33**	**55**	31.8
200	9	31	60	31.4

*Polymerization conditions: P = 2 atm; aging time = 2 hours

Table 5-5 Aging Time Effect at 70°C on both Titanium Oxidation State Distribution and Activity* (Fregonese *et al.*, 2001)

Aging time (min)	Ti (IV)%	Ti(III)%	Ti(II)%	Activity (kg PE/g Ti. h)
10	30	**56**	14	25
20	19	**59**	**22**	31.4
30	15	**40**	**45**	32
60	12	**30**	**58**	33.2
120	**10**	34	56	34

*Polymerization conditions: P = 2 atm; Al/Ti = 50

5.3.4 Molecular weight and distribution

The effect of a change in Al/Ti on the molecular weights in ethylene homo-polymerization reactions were investigated at Al/Ti = 26 and 60. Hydrogen was not used to control the molar masses in these investigations. The results are shown in Table 5-6 and it can be seen that a larger width of the distribution was obtained at a lower Al/Ti.

Table 5-6 Effect of Al/Ti on the Molar Masses in Ethylene Homo-Polymerization Reactions

Run	Al/Ti molar ratio	Activity* g PE/g Ti. h	Yield g PE/g cat. h	M_n	M_w	PDI
1	26	196.94	12.76	227 000	1 260 600	5.6
2	60	218.70	14.16	330 400	1 516 400	4.6

*wt% Ti = 6.5

Physical properties such as molecular weight strongly influence the polymer's strength and flexibility and therefore determine the application in which the polymer can be used. These properties, which refer to the micro-scale arrangements of the constituent monomers, are measured using gel permeation techniques. Gel permeation chromatography (GPC) also known as size exclusion chromatography (SEC) is used for providing both the molecular weight averages and distribution and has been used to determine the molar mass quantities shown in Table 5-6. These quantities were determined at the University of Stellenbosch, at the Department of Chemistry and Polymer Science. Although it was required that more samples

be analyzed, it was not possible to dissolve the other polymer samples in the necessary solvents using standard sample preparation methods.

The polydispersity index (PDI) is an indication of the width of the molecular weight distribution (PDI = M_w/M_n). Flory (1953) demonstrated that for a single catalytic site, the maximum value of the polydispersity index is 2. For the Ziegler-Natta catalyst, however, the experimentally observed PDI is always found to have a value greater than 2, with indices in the 4 to 40 range being observed. Polydispersity indices higher than 2 have also been measured in this work.

Two explanations for the observed broad molecular weight distributions have been proposed in the literature thus far. The encapsulation theory proposes that growth of polymer leads to monomer concentration gradients in the catalyst, resulting in a variation in the propagation rate, and is therefore responsible for the broad MWD's. All catalytic sites are assumed to be equally active. In the presence of severe diffusion resistance, the outer regions of the growing polymer particle experience a higher concentration of monomer than do the inner regions and polymer of sufficiently different molecular weight might be produced to give a broad MWD. To quantify intraparticle diffusion resistance in solid-catalyzed polymerization, a physically reasonable particle model is required. The multigrain model (MGM), a well-defined transport resistance model, has often been used to estimate the impact of diffusion resistance on polydispersity but even though this model predicts higher polydispersities than those without mass transfer limitations, it consistently under-predicts the experimental results.

The second explanation proposes the existence of multiple active catalyst sites (catalytic site heterogeneity), each polymerizing at different rates, which results in the wide distributions observed. This requires the existence of catalyst sites of sufficiently varied activities and/or transfer rates in order to produce polymers with a broad MWD. As a consequence, the MWD of the overall polymerization is represented as a weighed sum of the MWDs of polymer made on each site type. The multiplicity of types of active sites offers a convincing explanation of both the polydispersity and the shape of the MWD curves observed by GPC and it is now generally accepted that the broad distributions are caused by the presence of these several types of active sites, although heat and mass transfer resistances can broaden the distribution under certain polymerization conditions.

As is mentioned above, there is now a general agreement that heterogeneous Ziegler-Natta catalysts have more than one type of active site, each one with distinct ratios of chain transfer to propagation rates, co-monomer reactivity ratios, and stereoselectivities. Since polymer chains made by each site type have different average chain lengths the whole polymer made with heterogeneous Ziegler-Natta catalysts is in reality a mixture, at the molecular level, of polymer chains having very dissimilar average properties. These dissimilar average properties are reflected in the broad MWDs that are frequently observed in polymers made with heterogeneous Ziegler-Natta catalysts.

The molecular weight distributions affect the final mechanical and rheological properties of polyolefins, and ultimately determine their applications. Polyethylene with broad MWDs are easier to process, because of greater flowability in the molten state at high shear rate, while polyethylene with narrow MWDs have greater dimensional stability, higher impact resistance, greater toughness at low temperatures, and higher resistance to environmental stress cracking.

There is no single trend in how polydispersity depends on reaction conditions. This is as expected because varying the monomer concentration, the aluminium alkyl type and concentration, the hydrogen concentration and temperature, and so on lead to changes in the relative populations of active sites through deactivation and/or new site formation. The generally broader polydispersities observed in polyethylene as compared to polypropylene, however, may result from the participation of more types of active sites as well as from greater diffusion limitations in ethylene polymerization. Ethylene polymerization rates are at least an order of magnitude higher than propylene polymerization rates over similar catalysts.

It is useful to interpret the broad MWD of polymers obtained with Ziegler-Natta catalysts as a resulting from the superposition of individual MWDs of polymer chains produced on each type of active site. It is generally accepted that, under most polymerization conditions, the effect of multiple site types is far more important than heat and mass transfer resistances. Under these conditions, each site type instantaneously produces polymer that is assumed to have Flory's most probably MWD. Therefore, the instantaneous MWD of accumulated polymer made with heterogeneous Ziegler-Natta catalysts can be considered an average of that produced by individual site types, weighted by the weight fraction of polymer produced by each site type (Figure 5-4).

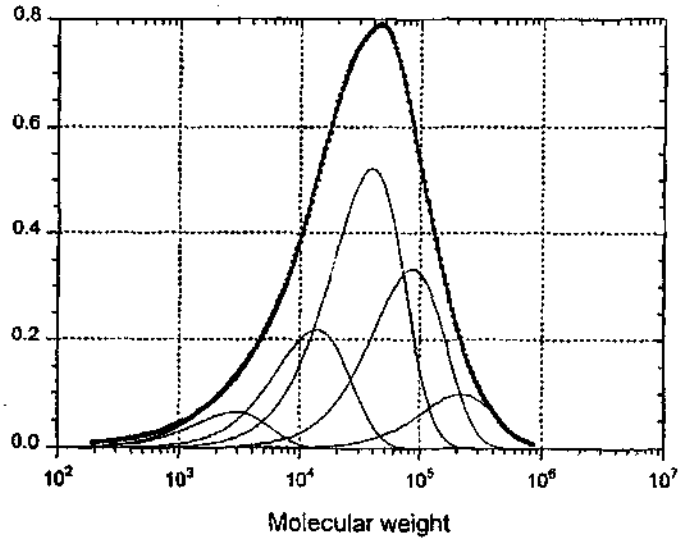

Figure 5-4 GPC Curves of a Polypropylene Sample and its Resolution into Flory Components (Kissin, 2003)

5.3.5 Polymer morphology

SEM micrographs of a catalyst and polymer are shown below. Figure 5-5 is a micrograph of a catalyst particle and Figure 5-6 and Figure 5-7 are micrographs of a polymer particle. The latter two micrographs clearly show the polymer surface to be an assembly of smaller, spherical structures. Micrographs of the polymers produced by van der Ven (1990) are shown in Figure 5-8 and it can be seen that those for polyethylene are very similar to that shown in Figure 5-6 and Figure 5-7.

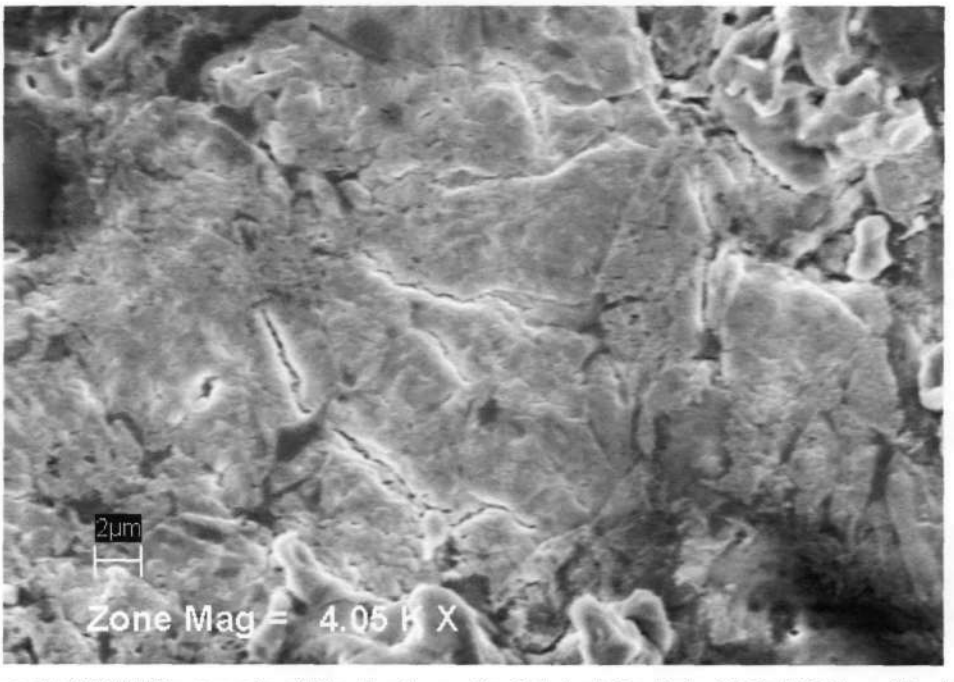

Figure 5-5 SEM Micrograph of the Surface of a Catalyst Particle (4.05 KX Magnification)

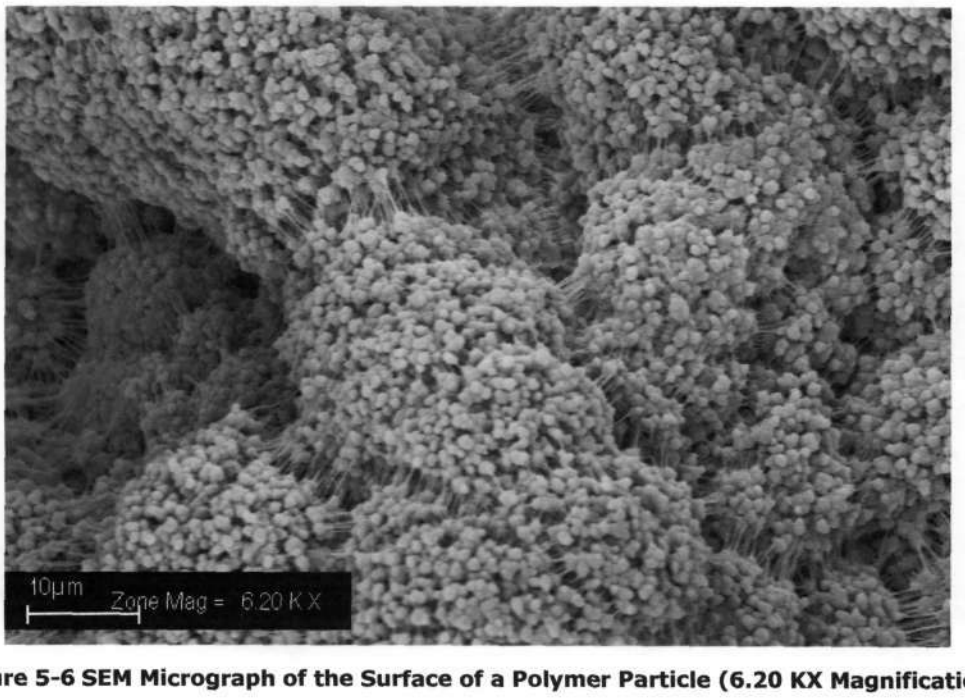

Figure 5-6 SEM Micrograph of the Surface of a Polymer Particle (6.20 KX Magnification)

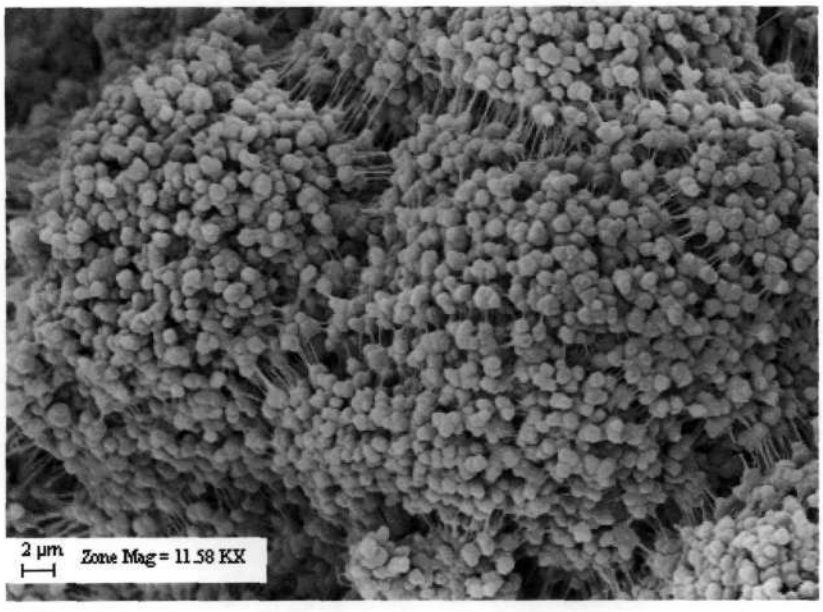

Figure 5-7 SEM Micrograph of the Surface of a Polymer Particle (11.58 KX Magnification)

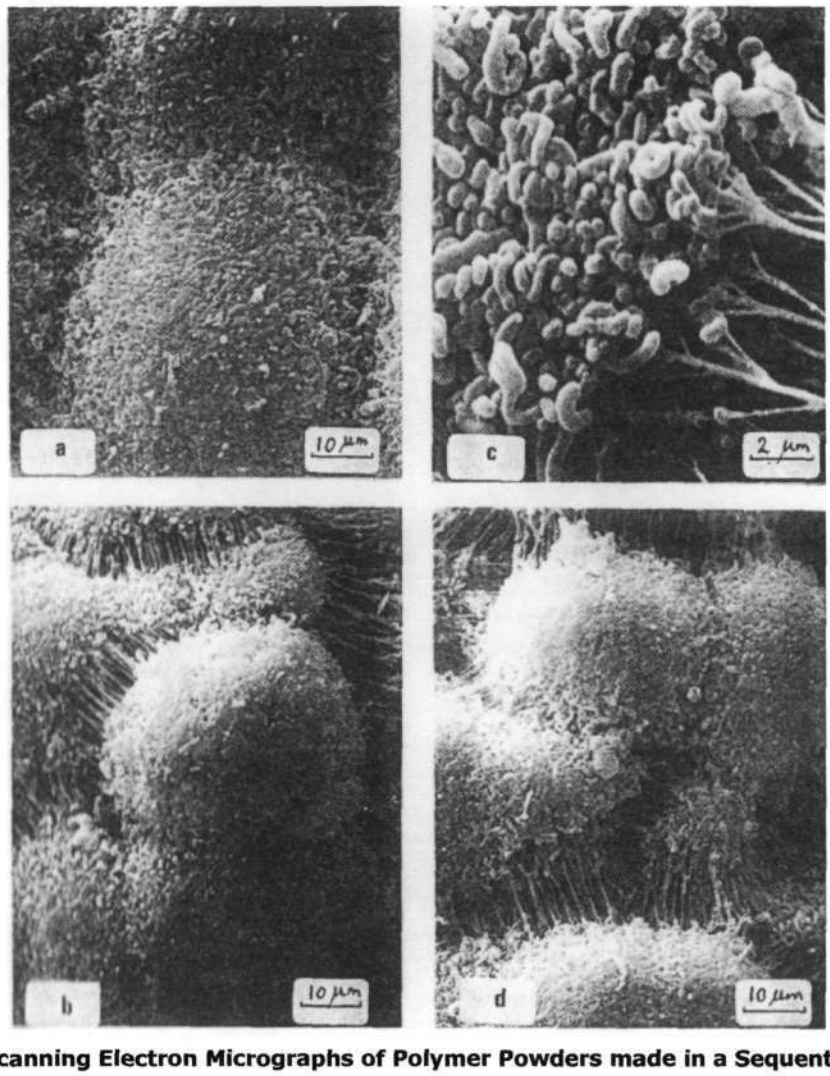

Figure 5-8 Scanning Electron Micrographs of Polymer Powders made in a Sequential Ethylene-Propylene Polymerization: (a) Homo-polymer Polypropylene; (b) Sequential Polymer; (c and d) Polyethylene (van der Ven, p 285, 1990)

Heterogeneous Ziegler-Natta catalysts are able to replicate their morphology into the morphology of the polymer particles. This is commonly known as the replication phenomenon. The basic requirements for the catalyst to be replicated are: high porosity, high mechanical resistance during manipulation and polymerization, but capability of breaking down into particles during polymer growth, and homogeneous distribution of active centres having equal reactivity and access to monomer. Under these conditions, the elementary morphology of the polymer generally consists of micro-globules covering catalyst particles. The micro-globules usually form globular aggregates which can be interconnected by fibres originated as a result of the expansion of the polymer particle.

It was observed that the morphology of the polymer particles replicated that of the catalyst and the ultimate objective of preparing the supported catalyst was therefore realized. A micrograph of whole polymer particles is shown in Figure 5-9.

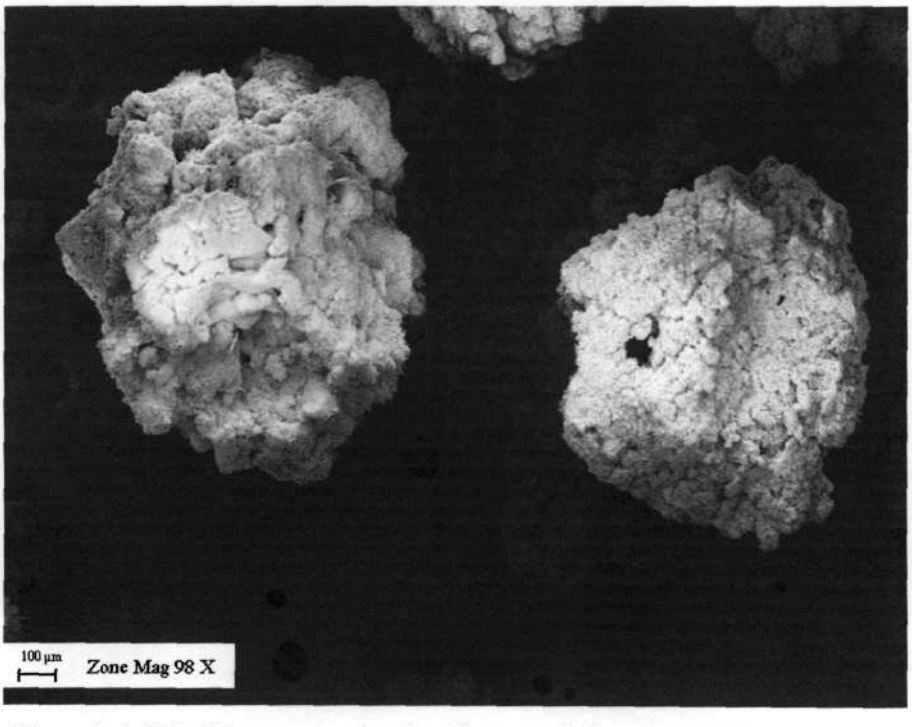

Figure 5-9 SEM Micrograph showing the morphology of a Polymer Particle

Chapter 6

Conclusions and Recommendations

A third generation $MgCl_2$-supported Ziegler-Natta catalyst was synthesized for ethylene polymerization investigations. This generation of catalyst is reported to be 50 times more reactive than the previous generations and is the most widely used in industry. The catalyst has a further benefit in that it has the ability to replicate its morphology into the morphology of the polymer. Morphology-controlled polyolefins having a spherical shape, high bulk density, narrow particle size distribution and low content of fines, have advantages in terms of energy savings in both polymerization processes and product processing.

In order to be successfully used as a catalyst support, $MgCl_2$ must first be converted to a form which can efficiently incorporate $TiCl_4$, a process referred to as activation. The prevailing method of active $MgCl_2$ preparation is the ball-milling of anhydrous $MgCl_2$ with $TiCl_4$, or the treatment of a $MgCl_2$–electron donor complex, obtained by ball milling, with $TiCl_4$. However, this method has only limited control over the texture of the catalyst since $MgCl_2$ activated in this way still has a crystal structure which is too regular for loading $TiCl_4$. It is also difficult to control the morphology of the resulting polymer particles when using ball-milled $MgCl_2$ as the catalyst support. The more recently developed re-crystallization (precipitation) method for active support preparation is therefore preferred for synthesizing high activity catalysts with controlled morphology and one of the implementations of this method was employed in this work.

The method used consisted of reacting crystalline, anhydrous $MgCl_2$ with ethanol and then forming an emulsion of the liquid adduct with silicon oil. This was followed by re-crystallization of the active support, $MgCl_2.n$EtOH. Two of the three support re-crystallization methods presented in the literature were tested but both the quick quenching and the solvent evaporation methods proved to be unsuccessful and a variation of the latter was therefore

proposed. The solvent evaporation method involves re-crystallizing the $MgCl_2$ support by evaporating the ethanol in which it is dissolved. In the literature a magnetic stirrer was used to mix the emulsion and the ethanol was evaporated under vacuum. In the method proposed for this work the emulsion was more vigorously stirred with a mechanical stirrer and a vacuum was not required. Instead, the reaction emulsion was stirred under a high, continuous flow of nitrogen which together with the evaporated ethanol passed through an opening in the reaction flask. This method was successfully used to produce spherical, active $MgCl_2$ which was subsequently used for the synthesis of a spherical Ziegler-Natta catalyst. For polymerization reactions the final catalyst system was $MgCl_2/TiCl_4$/dibutyl phthalate (DBP), activated by the co-catalyst triethylaluminium (TEA).

A special experimental system was set-up for the synthesis of the support and catalyst since these and the reagents from which they were synthesized are extremely air and/or moisture sensitive. The set-up consisted of Schlenk type glassware, vacuum and nitrogen lines and manifolds, mercury bubblers, a glove bag, double tipped needles, and gas-tight syringes. All manipulations of the catalyst components and precursors were carried out under an inert atmosphere of nitrogen and special Schlenk type glassware was designed and created to make manipulations involving air sensitive and anhydrous chemicals both simple and reliable.

Various analysis methods were used to characterize the support and catalyst. X-ray diffraction analysis proved that the synthesized support particles were in fact $MgCl_2.n$EtOH adducts. The morphology of the support and catalyst were examined by scanning electron microscopy and were found to be approximately spherical. The titanium content of the two catalysts prepared was determined by inductively coupled plasma analysis and they were found to contain 3.69 wt% Ti and 6.48 wt% Ti, respectively. Infrared spectroscopy (FTIR) was used to analyze both the support and catalyst to determine if they still contained ethanol after both a thermal treatment of the support and a repeated treatment of the catalyst with $TiCl_4$ were carried out. The FTIR analysis showed that these treatments were successful.

Gas-phase ethylene polymerization experiments were carried out in a laboratory polymerization reactor system which has been designed and constructed as part of this work. These experiments were aimed at determining the effect of the co-catalyst/catalyst (Al/Ti) molar ratio, the reaction pressure and the reaction temperature on the product yield. TEA was used as the co-catalyst and the experiments were run for 4 hours. To determine the effect of pressure, experiments were conducted at 1 and 2 bar, at 50°C and with Al/Ti = 33 and 50. At Al/Ti = 33, an increase in the pressure from 1 to 2 bar led to an increase in the yield from 11.3 to 12 g PE/g cat. h. while at Al/Ti = 50, the same increase in the pressure led to an increase in the yield from 14.2 to 17 g PE/g cat. h. The effect of Al/Ti was determined at ratios of 10, 33, and 60, and the yields obtained were 0.8, 8.5, and 14.2 g PE/g cat. h., respectively. These runs were carried out at 1 bar and 50°C. It was found that an increase in Al/Ti resulted in a systematic increase in the yield. In the literature, however, an optimum Al/Ti ratio between 60 and 100, resulting in a maximum yield, is generally observed. The effect of temperature was assessed at 50, 60 and

70°C and the yields obtained were 8.5, 24.4 and 8 g PE/g cat. h., respectively. These runs were carried out at 1 bar and with Al/Ti = 33. The yield was found to increase as the temperature was increased from 50 to 60°C, but decreased when the temperature was further increased to 70°C. An optimum temperature is generally observed in the literature, but is different for different types of catalyst systems.

The molar masses of the products of two experiments, carried out at 1 bar and 50°C, were determined by gel permeation chromatography. For Al/Ti = 26 and 60, the number average molecular weight (M_n) was found to be 227 000 and 330 400, respectively, and the weight average molecular weight (M_w) was found to be 1 260 600 and 1 516 400, respectively. The polymer produced with the Al/Ti = 26 had a polydispersity index (PDI) of 5.6 while that produced with Al/Ti = 60 had an index of 4.6. These are within the expected range for supported catalysts. The PDI is an indication of the width of the molecular weight distribution (PDI = M_w/M_n) and it has been demonstrated in the literature that for a single catalytic site, the maximum value is 2. For the Ziegler-Natta catalyst, however, the experimentally observed PDI is always found to have a value greater than 2, with indices in the 4 to 40 range being observed. The generally accepted explanation for the wide distribution is the existence of multiple active catalyst sites (catalytic site heterogeneity), each polymerizing at different rates.

The basic results obtained from the polymerization experiments were the product yields which were measured at the end of each run. For modelling studies, however, it is essential that instantaneous rate data is obtained. A gas flow-meter is therefore required to continuously measure the flow-rate of ethylene into the reactor operated in semi-batch mode and from this the instantaneous ethylene consumption rates can be calculated and rate versus time profiles can be obtained. Therefore, a recommendation for future work is to continuously measure the ethylene flow-rate required to keep the reactor at a constant pressure. More detailed information on the effects that changes in the catalyst system and process conditions have on the rate/time profiles will therefore be obtainable.

As was mentioned above, the polymerization experiments were carried out in a gas-phase semi-batch reactor system which has been specifically designed and constructed as part of this work. A 28cm^3 spinning catalyst basket was used for holding the supported catalyst, and hence the growing polymer, so that they would not be mechanically damaged by the stirring action of an impeller. Scanning electron micrographs showed that the polymer particles had the same spherical shape as the catalyst particles and one of the objectives of preparing the supported catalyst was therefore realized. The rotating basket was also meant to serve as an impeller for stirring the reactants. Although it was efficient in preventing the formation of temperature and concentration gradients in the gas phase outside the basket, polymer agglomeration due to the initially high reaction rates was observed indicating that the gas surrounding the growing polymer particles was not sufficiently mixed and that temperature hot spots existed within the basket. Efficiency in mixing and heat removal is essential since phenomena such as particle

melting and agglomeration lead to catalyst deactivation. The design of the spinning basket was therefore found to be unsuitable for the experimental investigations undertaken.

In the literature, stirred bed reactors are most commonly used primarily because they facilitate isothermal operation. However, particle morphology is destroyed by the action of the stirrer and a catalyst basket reactor is therefore preferred. Future work on this reactor system should therefore focus on modifying the basket agitation. With enough mixing energy the contents of the catalyst basket, which initially consists of 40mg of catalyst and thereafter with growing polymer, can be sufficiently mixed and isothermal. It is therefore recommended that a higher horse power motor and magnetic drive should replace the motor used in this work to ensure that sufficient stirrer torque and speeds are available for proper operation. Furthermore, coaxial impellers can be used to ensure better reactant circulation over the contained catalyst.

With the exception of the inadequate mixing, the rest of the reactor system has proved to be efficient. The temperature control system, which consisted of a band heater and stainless steel cooling coils, was capable of controlling the reaction temperature of the exothermic polymerization reaction. With this control system, the gas-phase temperature was maintained to within ±0.5°C of the set-point for the duration of the reaction. Also, the PID feedback pressure control system was efficient in controlling the reactor pressure and the catalyst injection system was successfully used to inject the catalyst and co-catalyst without contamination.

The polymer product yields obtained in this work were found to be lower than those presented in the literature. There are two reasons for this and the first and most obvious is the inefficient agitation of the growing polymer particles. A second reason for the low yields could be that the synthesized catalyst has a much lower specific surface area than those used in the literature. Future work on the catalyst system should therefore focus on increasing the specific surface areas of the support and catalyst. In order to be able to determine which preparation steps need to be modified it is essential that detailed analyses of both the support and catalyst be carried out after each step of the synthesis process. These analyses should include determining organic and inorganic compositions, particle size distributions, the effects of varying reagent quantities, temperatures and reaction times on porosity and surface areas, and the effects of various internal donors.

In this work the many difficulties in producing the air-sensitive Ziegler-Natta catalyst have been overcome and although the catalytic activity was not optimised, the catalyst was capable of polymerizing ethylene. Also, favourable support, catalyst and polymer morphologies were attained and the designed catalyst experimental system has proved to be efficient.

References

Albizzati, E., U. Giannini, G. Balbontin, I. Camurati, J.C. Chadwick, T. Dall'Occo, Y. Dubitsky, M. Galimberti, G. Morini, and A. Maldotti, "Propylene polymerization with catalysts containing divalent titanium", *J. Polym. Sci.*, **35**, 2645-2652 (1997)

Barbe, P.C., L. Noristi, G. Baruzzi, and E. Marchetti, "Microscopic Analysis of Polyolefin Initial Formation on $TiCl_4/MgCl_2$ Supported Catalysts", *Makromol. Chem. Rap. Commun.*, **4**, 249-254 (1983)

Barbe, P.C., G. Cecchin, and L. Noristi, "The Catalytic System Ti-Complex/$MgCl_2$", *Adv. Polym. Sci.*, **81**, 1-8 (1987)

Bohm, L.L, "Reaction model for Ziegler-Natta polymerization processes", *Polymer.*, **19**, 545-552 (1978a)

Bohm, L.L., "Ethylene polymerization process with a highly active Ziegler-Natta catalyst: 1. Kinetics", *Polymer.*, **19**, 553-561 (1978b)

British Patent 841 822 to Petrochemicals Ltd. (1955)

Brazilian Patent 9001991 to Himont Inc. (1990)

de Carvalho, A.B.M. and A.E. Hamielec, "A kinetic model for heterogeneous Ziegler-Natta co-polymerization. Part 2: Stereochemical sequence length distributions", *Polymer.*, **31**, 1294-1311 (1990)

Carter J.W. and H. Husain, "The simultaneous adsorption of carbon dioxide and water vapour by fixed beds of molecular sieves", *Chem. Eng. Sci.*, **29**, 267-273 (1974)

Chien, J.C.W. and J.C. Wu, "Magnesium chloride supported high mileage catalysts for olefin polymerization. II. Reactions between aluminium alkyls and promoters", *J. Polym. Sci.: Polym. Chem. Ed.*, **20**, 2445-2460 (1982)

Chien, J.C.W., J.C. Wu and C.I. Kuo, "Magnesium chloride supported high-Mileage catalysts for olefin polymerization V. BET, Porosimetry and X-Ray Diffraction Studies", *J. Polym. Sci. Polym. Chem. Ed.*, **21**, 737-742 (1983)

Chien, J.W.C., C. Kuo, and T.J. Ang, "Magnesium chloride supported high mileage catalyst for olefin polymerization. VI. Definitive evidence against diffusion limitation", *J. Polym. Sci.: Polym. Chem. Ed.*, **23**, 723-729 (1985)

Chien, J.C.W., S. Weber, and Y. Hu, "Magnesium chloride supported catalysts for olefin polymerization. XIX. Titanium oxidation states, catalyst deactivation, and active site structure", *Polym. Sci. Part A: Polym. Chem.*, **27**, 1499-1514 (1989)

Chien, J.C.W. and T. Nozaki, "High activity magnesium chloride supported catalysts for olefin polymerization. XXIX. Molecular basis of hydrogen activation of magnesium chloride supported Ziegler-Natta catalysts", *Polym. Sci. Part A: Polym. Chem.*, **29**, 505-514 (1991)

Cho, H.S. and W.Y. Lee, "Synthesis of inorganic $MgCl_2$-alcohol adduct via re-crystallization method and it application in supported organometallic catalysts for the polymerization of ethylene with 1-hexene", *J. Mol. Catal. A: Chem.*, **191**, 155-165 (2003)

Choi, K.Y. and W.H. Ray, "Polymerization of olefins through heterogeneous catalysis. II. Kinetics of gas phase propylene polymerization with Ziegler-Natta catalysts", *J. Appl. Polym. Sci.*, **30**, 1065-1081 (1985)

Choi, K.Y. and W.H. Ray, "The dynamic behaviour of continuous stirred-bed reactors for the solid catalyzed gas phase polymerization of propylene", *Chem. Eng. Sci.*, **43(10)**, 2587-2604 (1988)

Choi, J.H., J.S. Chung, H.W. Shin, I.K. Song and W.Y. Lee, "The effect of alcohol treatment in the preparation of $MgCl_2$ support by a re-crystallization method on the catalytic activity and isotactic index for propylene polymerization", *Eur. Polym. J.*, **32**, 405-410 (1996)

Chung, J.S., J.H. Choi, I.K. Song and W.Y. Lee, "Effect of ethanol treatment in the preparation of $MgCl_2$ support for the propylene polymerization catalyst", *Macromol.*, **28**, 1717-1718 (1995)

Cossee, P., "Ziegler-Natta catalysts 1. Mechanisms of polymerization of α-olefins with Ziegler-Natta catalysts", *J. Catal.*, **3**, 80-89 (1964)

Doi, Y., M. Murata, K. Yano, and T. Keii, "Gas-phase polymerization of propene with the supported Ziegler catalyst: $TiCl_4/MgCl_2/C_6H_5COOC_2H_5/Al(C_2H_5)_3$", *Ind. Eng. Chem. Prod. Res. Dev.*, **21**, 580-585 (1982)

Dusseault, J.J.A. and C.C. Hsu, "$MgCl_2$-supported Ziegler-Natta catalysts for olefin polymerization: basic structure, mechanism, and kinetic behaviour", *J.M.S.-Rev. Macromol. Chem. Phys.*, **C33 (2)**, 103-145 (1993)

Floyd, S., T. Heiskanen, and W.H. Ray, "Solid catalyzed olefin polymerization", *Chem. Eng. Prog.*, **84**, 56-62 (1988)

Forte, M.C. and F.M.B. Coutinho, "Highly active magnesium chloride supported Ziegler-Natta catalysts with controlled morphology", *Eur. Polym. J.*, **32**, 223-231 (1996)

Fregonese, D. and S. Bresadola, "Catalytic systems supported on $MgCl_2$ doped with $ZnCl_2$ for olefin polymerization", *J. Mol. Cat. A: Chem.*, **145**, 265-271 (1999)

Fregonese D., S. Mortara, and S. Bresadola, "Ziegler-Natta $MgCl_2$-supported catalysts: relationship between titanium oxidation states distribution and activity in olefin polymerization", *J. Mol. Catal. A: Chem.*, **172**, 89-95 (2001)

Galli, P., P. Barbe, G. Guidetti, R. Zannetti, A. Martorana, A. Marigo, M. Bergozza, and A. Fichera, "The activation of $MgCl_2$-supported Ziegler-Natta catalysts: A structural investigation", *Eur. Polym. J.*, **19**, 19-24 (1983)

Gorbach, A.B., S.D. Naik, and W.H. Ray, "Dynamics and stability analysis of solid catalyzed gas-phase polymerization of olefins in continuous stirred bed reactors", *Chem. Eng. Sci.*, **55**, 4461-4479 (2000)

Han-Adebekun, G.C., J.A. Debling, and W.H. Ray, "Polymerization of olefins through heterogeneous catalysis. XVI. Design and control of a laboratory stirred bed copolymerization reactor", *J. Appl. Polym. Sci.*, **64**, 373-382 (1997a)

Han-Adebekun, G.C. and W.H. Ray, "Polymerization of olefins through heterogeneous catalysis. XVII. Experimental study and model interpretation of some aspects of olefin polymerization over a $TiCl_4/MgCl_2$ catalyst", *J. Appl. Polym. Sci.*, **65**, 1037-1052 (1997b)

Han-Adebekun, G.C., M. Hamba and W.H. Ray, "Kinetic study of gas phase olefin polymerization with $TiCl_4/MgCl_2$ catalyst I. Effect of polymerization conditions", *J. Polym. Sci. Part A: Polym. Chem.*, **35**, 2063-2075 (1997c)

Hu, Y. and J.C.W. Chien, "Superactive and stereospecific catalysts. 1. Structures and productivity", *J. Polym. Sci. Part A: Polym. Chem.*, **26**, 2003-2018 (1988)

Huang, J.C.K., Y. Lacombe, D.T. Lynch, and S.E. Wanke, "Effects of hydrogen and 1-butene concentrations on the molecular properties of polyethylene produced by catalytic gas-phase polymerization", *Ind. Eng. Chem. Res.*, **36**, 1136-1143 (1997)

Hutchinson, R.A., C.M. Chen, and W.H. Ray, "Polymerization of olefins through heterogeneous catalysis X: Modeling of particle growth and morphology", *J. Appl. Polym. Sci.*, **44**, 1389-1414 (1992)

Karol, F.J., "Studies with high activity catalysts for olefin polymerization", *Catal. Rev.-Sci. Eng.*, **26**, 557 (1984)

Kashiwa, N. and A. Toyota, "$MgCl_2$ supported titanium catalyst prepared by mechanical pulverization", *Polym. Bull.*, **11(5)**, 471-477 (1984)

Kashiwa, N. and J. Yoshitake, "Kinetic study on propylene polymerization by a high activity catalyst system: $MgCl_2/TiCl_4/PhCO_2Et$-$AlEt_3/PhCO_2Et$", *Polym. Bull.*, **11(5)**, 479-484 (1984)

Keii, T., E. Suzuki, M. Tamura, M. Murata, and Y. Doi, "Propene polymerization with a magnesium chloride supported Ziegler-Natta catalyst. 1. Principle kinetics", *Makromol. Chem.*, **183**, 2285 (1982)

Keii, T., Y. Doi, E. Suzuki, M. Tamura, M. Murata, and K. Soga, "Propene polymerization with a magnesium chloride supported Ziegler catalyst, 2. Molecular weight distribution", *Makromol. Chem.*, **185 (8)**, 1537-1557 (1984)

Keii, T., "Mechanistic studies on Ziegler-Natta catalysis: A methodical reconsideration", *Stud. Surf. Sci. Catal.*, **25**, 1-7 (1986)

Kim, I., J.H. Kim, and S.I. Woo, "Kinetic study of ethylene polymerization by highly active silica supported $TiCl_4/MgCl_2$ catalysts", *J. Appl. Polym. Sci.*, **39**, 837-854 (1990)

Kissin, Y.V., "*Isospecific polymerization of olefins with heterogeneous Ziegler-Natta catalysts*", Springer-Verlag, NewYork (1985)

Kissin, Y.V., "Kinetics of olefin co-polymerization with heterogeneous Ziegler-Natta catalysts", *Macromol. Symp.*, **89**, 113-123 (1995)

Kissin, Y.V., R.I.Mink, and T.E. Nowlin, "Ethylene polymerization reactions with Ziegler-Natta catalysts. 1. Ethylene polymerization kinetics and kinetic mechanism", *J. Polym. Sci. Part A: Polym. Chem.*, **37**, 4255-4272 (1999)

Kissin, Y.V., R.I. Mink, T.E. Nowlan, and A.J. Brandolini, "Ethylene polymerization reactions with Ziegler-Natta catalysts. 3. Chain-end structures and polymerization mechanism", *J. Polym. Sci. Part A: Polym. Chem.*, **37**, 4281-4294 (1999)

Kissin, Y.V., "Main kinetic features of ethylene polymerization reactions with heterogeneous Ziegler-Natta catalysts in the light of a multicentre reaction mechanism", *J. Polym. Sci. Part A: Polym. Chem.*, **39**, 1681-1695 (2001)

Kissin, Y.V., "Multicentre nature of titanium based Ziegler-Natta catalysts: comparison of ethylene and propylene polymerization reactions", *J. Polym. Sci. Part A: Polym. Chem.*, **41**, 1745-1758 (2003)

Kohl, A.L., "*Gas Purification*", Huston, Texas, Gulf (1979)

Kojoh, S, M. Kioka, N. Kashiwa, M. Itoh, and A. Mizuno, "A study of chain-end structures of propylene prepared with a $MgCl_2$-supported titanium catalyst", *Polymer.*, **36**, 5015-5018 (1995)

Kothandaraman H. and M.S. Devi, "Kinetics of Polymerization of 1-Octene with $MgCl_2$-Supported $TiCl_4$ Catalysts", *J. Polym. Sci., Polym. Chem.*, **32**, 1283-1294 (1994)

Liu, B., K. Fukuda, H. Nakatain, I. Nishiyama, M. Yamahiro, and M. Terano, "27Al MAS solid state NMR study on coordinative nature of alkyl-al co-catalysts on a novel SiO_2-supported Ziegler-Natta catalyst for controlled multiplicity of molecular weight distribution", *J. Mol. Catal. A: Chem.*, **219**, 363-370 (2004)

Lorenzini, P., P. Bertrand, and J. Vilermaux, "Modelling ethylene and α-olefin co-polymerization using Ziegler-Natta catalyst", *Can. J. Chem. Eng.*, **69**, 682 (1991)

Lynch, D.T. and S.E. Wanke, "Reactor design and operation for gas-phase ethylene polymerization using Ziegler-Natta catalysts", *Can. J. Chem. Eng.*, **69**, 332-339 (1991)

Mannan, T.M., H. Hammawa, D.T. Lynch, and S.E. Wanke, "A laboratory reactor for gas-phase olefin polymerization", *Can. J. Polym. Sci.*, **82**, 371-381 (2004)

McKenna, T.F. and J.B.P. Soares, "Single Particle Modeling for Olefin Polymerization on Supported Catalysts: A Review and Proposals for Future Developments", *Chem. Eng. Sci.*, **56**, 3931-3949 (2001)

McAuley, K.B., J.F. MacGregor, and A.E. Hamielec, "A kinetic model for industrial gas-phase ethylene co-polymerization", *AIChE J.*, **36 (6)**, 837-850 (1990)

McAuley, K.B., D.A. Macdonald, and P.J. McLellan, "Effects of operating conditions on stability of gas-phase polyethylene reactors", *AIChE J.*, **41(4)**, 868-878 (1995)

Mori, H., M. Endo, and M. Terano, "Deviation of hydrogen response during propylene polymerization with various Ziegler-Natta catalysts", *J. Mol. Catal. A: Chem.*, **145**, 211-220 (1999)

Nagel, E.J., V.A. Kirillov, and W.H. Ray, "Prediction of molecular weight distributions of high-density polyolefins", *Ind. Eng. Chem. Res. Dev.*, **19**, 372-379 (1980)

Parada, A., T. Rajmankina, J.J. Chirinos and A. Morillo, "Influence of support re-crystallization Techniques on Catalyst Performance in Olefin Polymerization", *Eur. Polym. J.*, **38**, 2093-2099 (2002)

Rawatlal, R., Unsteady state modeling of Ziegler-Natta catalyzed olefin polymerization reactor systems, PhD thesis, University of KwaZulu-Natal (2004)

Ray, W.H., and C.M. Villa, "Nonlinear Dynamics found in Polymerization Processes - A Review", *Chem. Eng. Sci.*, **55**, 275-290 (2000)

Rishina, L.A., E.I. Vizen, L.N. Sosnovskaya, and I.L. Dubnikova, "Propylene polymerization on a titanium-magnesium catalyst in the presence of various organoaluminium compounds", *Kinet. Catal.*, **37**, 396-401 (1996)

Samson, J.J.A., G. Weickert, A.E. Heerze, and K.R. Westerterp, "Liquid-phase polymerization of propylene with a highly active catalyst", *AIChE J.*, **44**(6), 1424-1437 (1998)

Samson, J.J.C., B. Middelkoop, G. Weickert, and K.R. Westerterp, "Gas-phase polymerization of propylene with a highly active Ziegler-Natta catalyst", *AIChE J.*, **45** (7), 1548-1558 (1999)

Skomorokhov, V.B., V.A. Zakharov, and V.A. Kirillov, "Determination of the activation energies of ethylene polymerization on titanium-magnesium catalysts: experiment and mathematical modelling", *Kinet. Catal.*, **39(5)**, 696-701 (1998)

Soares, J.B.P and A.E. Hamielec, "Kinetics of propylene polymerization with a non-supported heterogeneous Ziegler-Natta catalyst - effect of hydrogen on rate of polymerization, stereoregularity, and molecular weight distribution", *Polymer.*, **37 (20)**, 4607-4614 (1996)

Soares, J.B.P., J.D. Kim, and G.L. Rempel, "Analysis and control of the molecular weight and chemical composition distributions of polyolefins made with metallocene and Ziegler-Natta catalysts", *Ind. Eng. Chem. Res.*, **36**, 1144-1150 (1997)

Soga, K., T. Sano, and R. Ohnishi, "Co-polymerization of ethylene with propylene over the thermally reduced γ-Al_2O_3-supported $TiCl_4$ catalyst", *Polym. Bull.*, **4**, 157-164 (1981)

Soga, K., S. Chen, and R. Ohnishi, "Correlation between oxidation states of titanium and the polymerization activities for higher α-olefins and diene compounds", *Polym. Bull.*, **8**, 473-478 (1982)

Townsend, E.J., "Pilot plants for polyolefin research and development", Presentation at Ecorep Conference on Polyolefins, France (2000)

Triebe R.W. and F.H. Tezel, "Adsorption of nitrogen, carbon monoxide, carbon dioxide and nitric oxide on molecular sieves", *Gas. Sep. Purif,*. **9(4)**, 223-230 (1995)

Triebe R.W., F.W. Tezel and K.C. Khulbe, "Adsorption of methane, ethane and ethylene on molecular sieve zeolites", *Gas. Sep. Purif.*, **10 (1)**, 81-84 (1996)

United States Patent 4399054, to Montedison S.p.A. (1983)

van der Ven, S., "*Polypropylene and other Polyolefins, Polymerization and Characterization*", Billiton Research, Arnhem, The Netherlands (1990)

Weekman, V.W., "Laboratory reactors and their limitations", *AIChE J.*, **20(5)**, 833-840 (1974)

Weist, E.L., A.H. Ali, and W.C. Conner, "Morphological study of supported chromium polymerization catalysts 2. Initial stages of polymerization", *Macromol.* **22**, 3244-3252 (1989)

Wester, T.S. and M. Ystenes, "Kinetic studies of the injection of co-monomers during polymerization of ethane and propene with $MgCl_2$-supported Ziegler-Natta catalysts", *Macromol. Chem. Phys*, **198**, 1623-1648 (1997)

Wu, Q., H. Wang, and S. Lin, "Gas-phase versus slurry copolymerization of ethylene with 1-butene over $MgCl_2$-supported titanium catalysts after pre-polymerization", *Macromol. Chem. Phys.*, **197(1)**, 155-163 (1995)

Wu, L., D.T. Lynch, and S.E. Wanke, "Kinetics of gas-phase ethylene polymerization with morphology-controlled $MgCl_2$-supported $TiCl_4$ catalyst", *Macromol.*, **32**, 7990-7998 (1999)

Wu, L., N. Bu, and S.E. Wanke, "Kinetic behaviour of ethylene/1-hexene co-polymerization in slurry and solution reactors", *J. Polym. Sci. Part A: Polym. Chem.*, **43**, 2248-2257 (2005)

Xie, T., K.B. McAulay, J.C.C. Chien, and D.W. Bacon, "Gas phase ethylene polymerization: production processes, polymer properties, and reactor modelling" *Ind. Eng. Chem. Res.*, **33**, 449-479 (1994)

Ye, Z-Y, L. Wang, L-F. Feng, X-P. Gu, H-H. Chen, P-Y. Zhang, J. Pan, S. Jiang and L-X. Feng, "Novel spherical Ziegler-Natta catalyst for polymerization and co-polymerization. 1. Spherical $MgCl_2$ support", *J. Polym. Sci. Polym. Chem.*, **40**, 3112-3119 (2002)

Yoon, J-S. and W.H. Ray, "Simple mechanistic model for the kinetics and catalyst activity decay of propylene polymerization over $TiCl_3$ catalyst with DEAC co-catalyst", *Ind. Eng. Chem. Res.*, **26**, 415-422 (1987)

Zakharov, V.I., N.B. Chumarvskii, Z.K. Bulatova, and Y.I. Yermakov, "Determination of the rate constants for chain transfer with the monomer and hydrogen in Ziegler-Natta polymerization", *React. Kinet. Catal. Lett.*, **5**, 429-434 (1976)

Zakhrov, V.A., S.I. Makhtarulin, V.A. Poluboyarov, and V.F. Anufrienko, "Study of the state of titanium ions and the composition of the active component in titanium-magnesium catalyst for ethylene polymerization", *Macromol. Chem.*, **185(9)**, 1781-1793 (1984)